Universidade de Évora - Escola de Ciências e Tecnologia

Mestrado em Biologia da Conservação

Dissertação

Influence of Environmental Variables on the Vertical Movement Patterns of Shortfin Mako Sharks in the South Atlantic

Rita Alexandra Brissos Cruz

Orientador(es) | Marisa Graziela Cerqueira Vedor

Pedro R. Almeida

Nuno Miguel Cabral Queiroz

Évora 2025

Universidade de Évora - Escola de Ciências e Tecnologia

Mestrado em Biologia da Conservação

Dissertação

Influence of Environmental Variables on the Vertical Movement Patterns of Shortfin Mako Sharks in the South Atlantic

Rita Alexandra Brissos Cruz

Orientador(es) | Marisa Graziela Cerqueira Vedor

Pedro R. Almeida

Nuno Miguel Cabral Queiroz

Évora 2025

A dissertação foi objeto de apreciação e discussão pública pelo seguinte júri nomeado pelo Diretor da Escola de Ciências e Tecnologia:

Presidente	|	Paulo Sá-Sousa (Universidade de Évora)
Vogais	|	Ana Mafalda Correia (Universidade do Porto) (Arguente) Marisa Graziela Cerqueira Vedor (Universidade do Porto) (Orientador)

Évora 2025

Acknowledgments

I would like to express my deepest gratitude to my supervisors, Professor Marisa Vedor and Professor Nuno Queiroz, for granting me the opportunity to join, even if only for a short period, a research team dedicated to the study of sharks. I am sincerely thankful for all the knowledge they have shared with me, for their constant guidance, and for all the support they have provided throughout this journey. I am also very grateful for the opportunity to spend some time in Porto, an experience that allowed me to meet extraordinary people and to grow both personally and academically.

I would like to extend my heartfelt thanks to my family for their unconditional moral and financial support throughout my academic journey. A very special thank you to my mother, who has always encouraged me to follow my dreams and supported me in every decision and to my grandmother for all the candles she lit in my name and for the unwavering faith she has always shown in me.

Finally, I wish to express my deepest appreciation to my partner, Rui Monteiro, for accompanying me over the years and for always being by my side through the highs and lows of my academic life. Your support, patience, and understanding have been invaluable and have played an essential role in helping me reach this milestone.

Influence of Environmental Variables on the Vertical Movement Patterns of Shortfin Mako Sharks in the South Atlantic

Abstract

Climate change is intensifying ocean warming and acidification, creating biological and habitat constraints for *Isurus oxyrinchus*. As apex predators, these sharks play a key role in oceanic dynamics and are essential for the health of marine ecosystems.

Ten individuals were monitored in the south-eastern Atlantic, a poorly studied region, using electronic tags. Vertical movements ranged from the surface to depths of 1,200 m, with a preference for waters shallower than 100 m, complemented by deep dives associated with elevated temperatures, weak thermal gradient and oxygen availability.

Horizontal movements occurred between the open ocean and areas near the Namibian continental shelf, with a preference for productive waters and temperatures between 21–23 °C. This preference increases the species vulnerability to fishing activities and, when combined with climate change, further constrains its habitat. These findings highlight the urgent need for integrated conservation measures.

Keywords: *Isurus oxyrinchus*; Satellite telemetry; South Atlantic; Vertical movements; Environmental variables; Marine conservation.

Influência das Variáveis Ambientais nos Padrões de Movimento Vertical de Tubarões-anequim no Atlântico Sul

Resumo

As alterações climáticas estão a intensificar o aquecimento e a acidificação dos oceanos, criando limites biológicos e no habitat da espécie *Isurus oxyrinchus*. Como predadores de topo, desempenham um papel-chave nas dinâmicas oceânicas e são cruciais para a saúde dos ecossistemas marinhos.

Dez indivíduos foram monitorizados no Atlântico Sudeste, uma região pouco estudada, utilizando marcadores eletrónicos. Movimentos verticais foram registados desde a superfície até aos 1200 m, com preferência por profundidades inferiores aos 100 m, complementadas por mergulhos profundos associados a temperaturas elevadas, termogradiente baixo e disponibilidade de oxigénio.

Os movimentos horizontais ocorreram entre o oceano aberto e áreas próximas da plataforma continental da Namíbia, preferindo águas produtivas e temperaturas entre 21–23 °C. Estas preferências expõe a espécie à pesca, combinada com alterações climáticas, limita o habitat, sublinhando a necessidade urgente de medidas de conservação integradas.

Palavras-chave: *Isurus oxyrinchus*; Telemetria por satélite; Atlântico Sul; Movimentos verticais; Variáveis ambientais; Conservação marinha.

Contents

List of figures

Figure 9: Distribution of mean depth (m) and temperature (°C) used by individuals throughout the monitoring period, stratified by year (A–B) and sex (C–D).

Figure 10: Daily variation in maximum recorded depth (MaxDepth) for individuals tagged in 2024 (C and D) and individuals tagged in 2021/22 (A and B). The points are coloured according to the bathymetry levels (m), illustrating the relationship between the maximum depth reached and the depth available at the site.

Figure 11: Relationship between maximum depth and maximum (MaxTemp) and minimum (MinTemp) temperature for ID S6 (A) and S10 (B). Points are coloured according to local bathymetry at the time of recording.

Figure 12: Relationship between thermal gradient and maximum diving depth of tagged mako sharks: (A) all dives combined (open-ocean and <200 m bathymetry), (B) dives in open-ocean environments, and (C) dives in regions with bathymetry <200 m. Each point represents an individual dive (triangles: 2021/22; circles: 2024).

Figure 13: Relationships between maximum diving depth and environmental variables: (A, B) chlorophyll concentration at the surface and at 100 m depth; (C, D) dissolved oxygen at the surface and at 100 m depth; (E, F) temperature at the surface and at 100 m depth; (G) thermal gradient; (H) depth of the thermocline onset; (I) lunar phase (percentage of illumination).

Figure 14: Distribution of the percentage of time spent by individuals across different depth intervals.

Figure 15: Distribution of daytime and nighttime occurrence percentages by depth stratum for individual S5 during weeks 5 (A) and 6 (B).

Figure 16: Distribution of daytime and nighttime occurrence percentages by depth stratum for individual S6 during weeks 4 (A) 5 (B) and 9 (C).

Figure 17: Spatial distribution of time spent above the thermocline, based on the trajectories of tagged individuals. The colour scale represents the percentage of time spent above the thermocline along individual trajectories.

Figure 18: Relationship between the percentage of time spent above the thermocline and the thermal gradient. (A) Data from the open ocean. (B) Data from coastal areas with bathymetry <200 m. Linear regressions with confidence intervals are shown.

Figure 19: Scatterplots of time above the thermocline versus initial thermocline depth and thermal gradient. (A) Open ocean. (B) Coastal areas <200 m; (C) Thermal gradient, points colour-coded by thermocline onset depth in the open ocean; (D) Thermal gradient, points colour-coded by thermocline onset depth in areas <200 m.

Figure 20: (A) Percentage of time spent above the thermocline in relation to surface water temperature, with fitted regression line; (B) bathymetry <200 m; (C) Open-ocean data showing the relationship between time above the thermocline, surface temperature (colour scale), and thermal gradient. (D) bathymetry <200 m data showing the relationship between time above the thermocline and surface temperature and thermal gradient.

Figure 21: Time spent above the thermocline in relation to environmental variables and the day/night period: (A, B) dissolved oxygen at the surface and at 100 m depth; (C, D) chlorophyll at 100 m depth and at the surface; (E, F) temperature at the surface and at 100 m depth; (G) thermal gradient of the thermocline; (H) lunar illumination.

Figure A 1: Depth and Temperature Profile Analysis recorded by *Isurus oxyrinchus* individuals during the tagging period. (A) S1; (B) S2; (C) S3; (D) S4; (E) S5; (F) S6;(G) S7. Lines represent depth over time, while colour shading indicates water temperature.

Figure A 2: Variation in the percentage of time spent by individuals (A) S1; (B) S2; (C) S3, (D)S4; (E) S5; (F)S6; (G) S7; (H) S8; (I) S9; (J) S10 at different depths and temperatures.

Figure A 3: Relationship between maximum depth and maximum (MaxTemp) and minimum (MinTemp) temperature for ID; (A) S1; (B) S2; (C) S3, (D)S4; (E) S5; (F)S7; (G) S8; (H) S9. Points are coloured according to local bathymetry at the time of recording.

Figure A 4: Distribution of daytime and nighttime occurrence percentages by depth stratum for individual S1 during all block of days.

Figure A 5: Distribution of daytime and nighttime occurrence percentages by depth stratum for individual S2 during all block of days; (A) block 1; (B) block 2; (C) block 3, (D) block 4; (E) block 5; (F) block 6; (G) block 7; (H) block 8; (I) block 9 and (J) block 10.

Figure A 6: Distribution of daytime and nighttime occurrence percentages by depth stratum for individual S3 during all block of day 1 (A); 2(B); 3(C).

Figure A 7: Distribution of daytime and nighttime occurrence percentages by depth stratum for individual S4 during all block of days (A) block 1; (B) block 2; (C) block 3, (D) block 4; (E) block 5; (F) block 6.

Figure A 8: Distribution of daytime and nighttime occurrence percentages by depth stratum for individual S5 during the block 1 (A); 2 (B); 3 (C); 4 (D); 7 (E); 8 (F); 9(G); 10 (H); 11 (I) and 12 (J).

Figure A 9: Distribution of daytime and nighttime occurrence percentages by depth stratum for individual S6 during the block of days 1 (A); 2 (B) ; 3 (C); 6(D); 7 (E); 8 (F); 9(G); 10(H); 11(I); 12 (J); 13(K).

Figure A 10: Distribution of daytime and nighttime occurrence percentages by depth stratum for individual S7 during the block of days 1 (A); 2 (B); 3 (C); 4(D); 5 (E) and 6 (F).

Figure A 11: Distribution of daytime and nighttime occurrence percentages by depth stratum for individual S8 during 1 (A); 2 (B); 3 (C); 4(D); 5 (E); 6 (F); 7 (G); 8 (H); 9 (I); 10 (J).

Figure A 12: Distribution of daytime and nighttime occurrence percentages by depth stratum for individual S9 during block of days 1 (A); 2 (B); 3 (C); 4(D); 5 (E); 6 (F); 7 (G).

Figure A 13: Distribution of daytime and nighttime occurrence percentages by depth stratum for individual S10 during block of days 1 (A); 2 (B); 3 (C); 4(D).

Figure A 14: Graphical analysis of the GLM and GLMM models. (A) Best model GLMM at day; (B) Best model GLMM at night; (C) Best model GLM at night; (D) Best model GLM at day.

List of tables

List of abbreviations and acronyms

CMS- Convention on Migratory Species

CPUE- Catch per unit effort

DO- Dissolved oxygen

DVM- Diel vertical migration

EEZ- Exclusive Economic Zones

ENSO- El Niño-Southern Oscillation

ETP- Eastern Tropical Pacific

FL- Fork length

GPS- Global Positioning System

MLD- Mixed layer depth

MPAs - Marine Protected Areas

OMZ- Oxygen minimum zones

PSAT- Pop-off satellite archival tag

SST- Sea surface temperature

TAD- Time-at-depth

TAT- Time-at-temperature

UTC- Coordinated Universal Time

WC- Wildlife Computers

1. Introduction

1.1 Impacts of climate change on the oceans

Climate change is generating significant impacts on the oceans, leading to profound transformations within marine ecosystems. As the planet warms due to the increase in greenhouse gas emissions, the oceans are undergoing a series of alterations. These changes are not only reshaping marine biodiversity but are also disrupting the balance of ecosystems that have existed for millennia, raising concerns about their future stability and resilience (Doney *et al*., 2012; Jewett & Romanou, 2017; Jorda *et al*., 2020; Worm & Lotze, 2021; Yao & Somero, 2014). One of the most pressing effects of global environmental change is the increase in ocean temperature, a phenomenon associated with substantial modifications and challenges for marine ecosystems, directly affecting the physiological and ecological functioning of numerous biological groups.

Algae represent one of the most sensitive groups to these changes. Thermal variations influence their physiology, productivity, and community structure, leading to shifts in the ecosystems where they play fundamental ecological roles (Richardson & Schoeman, 2004; Wernberg *et al*., 2011). The rise in sea surface temperature (SST) can alter the composition of algal communities, favouring heat-tolerant species and reducing the abundance of those adapted to cooler waters, with direct impacts on the base of marine food webs. Similarly, coral reefs have shown pronounced vulnerability to global warming. The increasing frequency and intensity of corals bleaching and mortality events observed in recent decades are strongly correlated with the acceleration of climate change (Carilli *et al*., 2012; Cantin *et al*., 2010; Pandolfi *et al*., 2011).

Among fish populations, rising SST has driven shifts in species distributions, with many moving to higher latitudes or deeper layers of the water column to avoid warmer surface waters and in search of more suitable thermal conditions (Dulvy *et al*., 2008a; Perry *et al*., 2005). In some tropical warm-water species, increases in abundance and community diversity have been observed following moderate

warming (MacNeil *et al.*, 2010; Simpson *et al.*, 2011). In contrast, the condition of cold-water species has declined (MacNeil *et al.*, 2010). Ocean warming has also facilitated the invasion of thermophilic species, thereby altering the ecological and competitive dynamics of marine ecosystems (MacNeil *et al.*, 2010).

Climate change likewise affects organisms at lower trophic levels. The decline in phytoplankton abundance due to rising SST may lead to subsequent decreases in copepods that feed on algae and, consequently, in carnivorous zooplankton species at higher trophic levels (Richardson & Schoeman, 2004). Such changes can modify the diversity and biogeographic distribution of marine copepods, with cascading effects throughout the trophic system (Rombouts *et al.*, 2009).

Beyond ecological alterations, climate change exerts significant physiological effects. In Norway, the proportion of one-year-old Atlantic salmon (*Salmo salar*) completing reproductive migration has decreased in parallel with rising SST (Otero *et al.*, 2012). Elevated temperatures have also proven detrimental to embryonic development and survival in invertebrates such as the squid *Loligo vulgaris*, causing premature hatching, due to reduced metabolic activity, and oxidative stress in eggs (Rosa *et al.*, 2012).

These effects, combined with ocean acidification resulting from the absorption of excess carbon dioxide, further exacerbate environmental challenges (Nagelkerken & Munday, 2016). Cao *et al.*, (2014) demonstrated that climate change reduces the average concentration of dissolved oxygen (DO) in the oceans, increasing the risk of hypoxic zones (areas with low oxygen levels). Each degree of climate sensitivity results in additional ocean warming of approximately 0.8 °C, reducing dissolved oxygen by about 5%. These hypoxic regions, known as oxygen minimum zones (OMZs), occur across all ocean basins and develop where dissolved oxygen reaches low (hypoxic) levels, between <0.45–1.00 ml O_2 l^{-1}, at depths of approximately 200–800 m (Keeling *et al.*, 2010; Gilly *et al.*, 2013). The vertical expansion of OMZs can affect crucial microbial processes involved in nutrient cycling and gas fluxes (Levin & Le Bris, 2015), alter predator–prey dynamics (Ekau *et al.*, 2010; Stewart *et al.*,

2013), and modify the distribution, abundance, and catch risk of ecologically significant species.

The need to address these changes has generated intense debate over policy measures and conservation strategies. Although approaches such as Marine Protected Areas (MPAs) and ecosystem-based management aim to mitigate certain effects, the effectiveness of these strategies in the face of rapid environmental change remains a central concern among scientists and policymakers (Bruno *et al.*, 2018; Duncanson *et al.*, 2023; Wilson *et al.*, 2020). As the oceans continue to change, understanding these environmental and ecological factors is essential for assessing not only habitat preferences but also the potential impacts of changing conditions on the dynamics of marine ecosystems. The main difficulty in understanding animal movement lies in identifying the external factors, physiological state and locomotion and navigation capabilities that influence them (Nathan *et al.*, 2008).

The selection of optimal thermal habitats, movements between productive foraging zones, and predatory and competitive interactions occur simultaneously in the vertical and horizontal planes. The three-dimensional habitat of marine ecosystems allows combinations of vertical and horizontal movements, being an essential parameter for understanding ecological interactions (de Perera *et al.*, 2013). The vertical behaviour of marine organisms, from microscopic phytoplankton to apex predators such as sharks, plays a crucial role in marine ecosystems, influencing ecological interactions, trophic dynamics, and conservation efforts. This behaviour encompasses a variety of migratory patterns, particularly diel vertical migration (DVM), which refers to the synchronised movement of zooplankton and fish ascending and descending through the water column over a 24-hour cycle. This phenomenon is widely observed in pelagic communities, both marine and freshwater, and involves a broad range of species. Typically, organisms migrate towards the surface at dusk and shortly before sunrise, this migration is reversed, and the animals return to their daytime residence in the mesopelagic zone (at depths of 200–1000 m) (Hays,2003; Lampert, 1989). This daily excursion is considered primarily an adaptation to avoid visual predators in the sunlit surface

layer and was first recorded nearly 200 years ago using ship-based net trawls (Bandara *et al.*, 2021). These animals may cover vertical distances of tens to hundreds of metres within just a few hours. These movements are significant not only for the organisms themselves but also for the overall health and stability of marine ecosystems, as they facilitate nutrient cycling and energy transfer within the food web.

The decline of apex predators disrupts the top–down trophic control that regulates prey populations and maintains the balanced structure of marine communities. In the absence of sharks, there is an increase in mesopredators, smaller predatory fish and invertebrates, which alters the overall dynamics of the ecosystem. This shift generates cascading effects, including the proliferation of certain species, the collapse of others, and a subsequent loss of productivity in habitats such as coral reefs, seagrass meadows, and coastal ecosystems, as demonstrated by several recent studies (Dedman *et al.*, 2024; Simpfendorfer *et al.*, 2023; Henderson *et al.*, 2024; Ferretti *et al.*, 2010).

Recent research, such as that by Simpfendorfer *et al.* (2023), reveals a global decline of between 60% and 73% in reef shark populations, accompanied by an increase in rays, which fundamentally alters community structure and function. This ecological substitution reduces biodiversity and degrades vital ecosystem services, including prey regulation and reef stability.

Despite their ecological importance, many shark species are experiencing severe population declines globally, making their conservation an urgent priority for marine ecosystem management. Studies highlight the severity of this situation. For instance, Roff *et al.* (2018) reported substantial declines, ranging from 74% to 92%, in the catch per unit effort (CPUE) of several apex shark species, including the scalloped hammerhead (*Sphyrnidae*), the bull shark (*Carcharhinidae*), the tiger shark (*Galeocerdo cuvier*), and the great white shark (*Carcharodon carcharias*). These declines were accompanied by reductions in the average size of captured individuals and a lower likelihood of encountering mature, reproductive adults,

indicating selective pressure on larger sharks, which are critical for maintaining the reproductive capacity of populations.

Consistently, Pacoureau *et al*. (2021) demonstrated that, since 1970, the global abundance of sharks and oceanic rays has declined by approximately 71%, a trend associated with an eighteen-fold increase in relative fishing pressure over the same period. Consequently, three-quarters of the assessed species are currently threatened with extinction, representing a global conservation crisis for a taxonomic group that is functionally essential to trophic stability and the ecological balance of marine ecosystems.

Beyond overfishing, climate change has caused significant shifts in the distribution and behaviour of sharks. Between 1982 and 2021, estuaries in the Gulf of Mexico recorded an average increase of 1.55 °C in autumn water temperatures and delays in cold fronts of approximately 0.5 days per year (Matich *et al*., 2024). These environmental changes influenced the migratory behaviour of juvenile bull sharks (*Carcharhinus leucas*), whose departures from more northern estuaries occurred 25 to 36 days later in 2021 compared to 1982. Although warming waters facilitated these behavioural changes, the most influential factor was the reduced availability of prey, a consequence of diminished reproductive success among forage species associated with climate change, which caused juveniles to remain longer in their natal estuaries.

Complementary experimental studies indicate that projected oceanic conditions by the end of the twenty-first century, both warmer and more acidic, severely compromise the physiology, condition, and survival of tropical juvenile sharks (Rosa *et al*., 2014). This research provides direct evidence that ocean acidification, in combination with global warming, represents a concrete and immediate threat to the viability of shark populations, emphasising the vulnerability of these predators to climatic alterations.

Furthermore, Osgood *et al*. (2021) demonstrated that elasmobranch responses to environmental changes vary according to species' mobility and ecology. For example, the scalloped hammerhead *(Sphyrna lewini*) exhibited a reduction of more

than 14% in counts and a 19.4% decrease in the occurrence of large schools for every 1 °C increase in sea surface temperature (SST).

Understanding such behaviours of these predators is therefore crucial to developing management and conservation strategies that ensure the sustainable use and protection of ocean resources.

1.2 Electronic Tags as a Tool for the Study of Shark Ecology and Conservation

For management plans to be implemented effectively, it is essential to obtain detailed information on the movements and behaviour of these species. The application of electronic tagging technologies, particularly satellite tags, has transformed the study of highly mobile marine species, such as pelagic fishes. Such data are typically collected via electronic devices attached to the animals, capable of transmitting or recording a wide range of information (Sims *et al.*, 2003; Weng *et al.*, 2005), thereby enhancing understanding of sharks ecological requirements and supporting more effective conservation strategies.

These species often travel thousands of kilometres across the oceans, making it impossible to monitor their movements using traditional approaches such as nets or direct observation, which, although capable of providing point information on presence, abundance, or morphological traits, are insufficient to document large-scale movement patterns or to capture continuous behavioural data. Importantly, these traditional methods are not entirely replaceable; rather, they serve as complementary tools to electronic tagging, since each approach offers distinct advantages and limitations. Satellite tags enable real-time or near-real-time tracking, providing a precise understanding of migratory routes and filling critical knowledge gaps that conventional methods cannot address.

Furthermore, many tags record depth, water temperature, and diving patterns, offering valuable information on vertical behaviour, feeding habits, and habitat preferences, data that would not be accessible through visual observation alone (Hammerschlag *et al.*, 2011) delivering crucial data for ecology, biology, and policy, particularly (Hussey *et al.*, 2015; Hays *et al.*, 2019).

One of the most used devices for satellite tagging, particularly in sharks, are Pop-up Satellite Archival Tags (PSATs), the same devices used in the present study. These devices are externally attached and allow monitoring of species that dive deeply or spend little time at the surface, as is the case for the species in this study, recording continuous depth and temperature data and covering long oceanic distances essential conditions for studying vertical behaviour and migrations of pelagic sharks, while enabling geolocation estimates (Block et al., 1998; Skubel et al., 2020; Horton et al., 2024; Musyl et al., 2001).

PSATs transmit data via the Argos system, eliminating the need for recapture, and include automatic release mechanisms in the event of failure, animal mortality, or reaching the programmed release date. Despite their advantages, they have limitations, such as premature release due to battery failure, mechanical damage, and lower spatial accuracy compared to other devices (Arnold & Dewar, 2001; Musyl et al., 2011). To improve the accuracy of location estimates derived from light levels recorded throughout the day, from which sunrise and sunset times are determined, allowing longitude to be estimated based on the timing of solar noon and latitude based on day length, several methods have been developed, including the removal of outlier values (Schaefer and Fuller, 2002), the application of smoothing techniques such as moving averages (Matsumoto *et al.*, 2005), the processing of location estimates using state-space movement models, namely Kalman filters (Sibert *et al.*, 2003) and particle filters (Royer *et al.*, 2005), and the comparison of sea surface temperatures recorded by the tags with remotely sensed data (Delong *et al.*, 1992).

SPOT (Smart Position and Temperature Transmitting), are other electronic tagging methods frequently used, allow near real-time tracking with higher spatial

resolution, but they depend on the frequency with which the animal comes to the surface, limiting their use for species that dive deeply or spend little time at the surface, even though they offer higher location accuracy in near real-time.

According to the scientific review conducted by Hammerschlag *et al*. (2011) on the use of satellite tagging technologies in sharks and their contribution to understanding the spatial ecology and behaviour of these marine predators, it was reported that, up to the time of publication, 17 shark species from seven families (*Alopiidae*, *Carcharhinidae*, *Cetorhinidae*, *Rhincodontidae*, *Dalatiidae*, *Somniosidae*, and *Sphyrnidae*), representing four orders (*Lamniformes*, *Carcharhiniformes*, *Orectolobiformes*, and *Squaliformes*), had been successfully satellite tagged using different types of satellite tags, including both PSAT and SPOT technologies. This total includes the shortfin mako shark (*Isurus oxyrinchus*).

1.3 Biology and ecology of Shortfin Mako (*Isurus oxyrinchus*), (Rafinesque, 1810)

The shortfin mako (*Isurus oxyrinchus*) belongs to the family *Lamnidae* which comprises only five species, including some of the most iconic predators: *Carcharodon carcharias* (white shark), *Isurus oxyrinchus* and *Isurus paucus* (makos), *Lamna nasus* (porbeagle), and *Lamna ditropis* (salmon shark). Members of this family are characterised by a morphology highly specialised for active and sustained locomotion. They display a robust body, capable of swimming at high speeds, with a fusiform and hydrodynamically efficient shape, a conical snout with large, blade-like teeth lacking cusps or serrations, large gill slits optimised for gas exchange, a second dorsal fin, and a heterocercal tail with lobes of similar size, providing powerful propulsion and as a species exhibiting regional endothermy (Compagno, 2001) .

This species is considered particularly well suited for the use of fin-mounted satellite tags, as it is a highly migratory species that travels long distances across

vast ocean basins, making it especially suitable for studies employing electronic tagging to track long-term movements (Block *et al.*, 2011; Nasby-Lucas *et al.*, 2019; Santos *et al.*, 2020; Santos *et al.*, 2021; Vaudo *et al.*, 2024). Moreover, the shortfin mako exhibits a wide geographical distribution, occurring in tropical, subtropical, and temperate seas worldwide (Rigby *et al.*, 2019).

Furthermore, this species is of both ecological and economic importance. As an apex predator, its movement patterns are crucial for understanding the dynamics and health of marine ecosystems. In addition, data derived from tagging studies support fisheries management by identifying areas and periods of increased vulnerability to capture (Campana *et al.*, 2005; Campana *et al.*, 2016; Queiroz *et al.*, 2019). The consistent use of satellite tagging across different regions of the world has clarified the distribution, behaviour, and migratory patterns of the shortfin mako shark throughout its range.

This species is widely distributed in oceanic waters of temperate and tropical regions worldwide (Abascal *et al.*, 2011). In the eastern Atlantic, it occurs from northern Europe to South Africa, in the western Atlantic, from the Gulf of Maine to Argentina, including the Gulf of Mexico and the Caribbean Sea. In the Indo-Pacific, its range extends from South Africa to Hawaii and from Russia to Australia, with some coastal exceptions and absence in New Zealand. In the eastern Pacific, it ranges from the Aleutian Islands to Chile (Rigby *et al.*, 2019) (Figure 1).

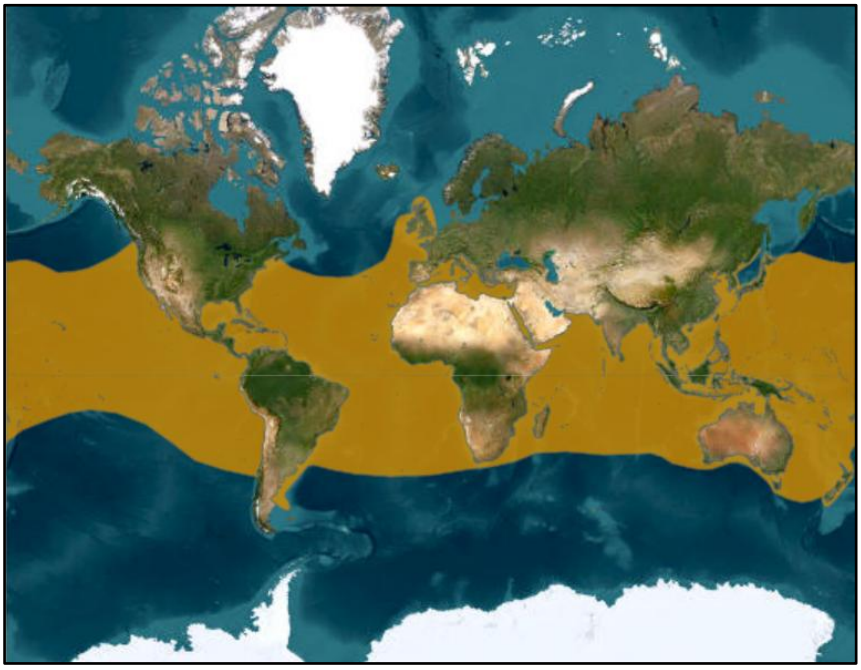

Figure 1: Geographical distribution of *I.oxyrinchus*. IUCN SSC Shark Specialist Group 2018. *Isurus oxyrinchus*. The IUCN Red List of Threatened Species. Version 2025.

The vertical distribution of this species varies among different studies. Vaudo *et al*. (2016) recorded a maximum depth of 866 m; Santos *et al*. (2021) reported that the depth range extended from the surface down to 979 m; and Abascal *et al*. (2011) documented dives reaching 888 m. However, the species may occur at depths exceeding 1000 m.

Its spatial and vertical distribution is strongly influenced by water temperature, with a clear preference for temperate conditions. In general, these sharks inhabit water masses between 18–22 °C, although they are capable of exploring wider thermal ranges during vertical movements (Vaudo *et al*., 2016; Santos *et al*., 2021). Studies in the Pacific have shown that juvenile makos in the Southern California Bight spend approximately 80% of their time within the upper 12 m of the water column, a zone characterised by higher and more stable temperatures over time and with depth (Sepulveda *et al*., 2004). In the North Atlantic, a similar pattern has been observed, with preferential use of surface layers between 17–22 °C, although occasional dives

into colder waters highlight their ecological flexibility (Vaudo *et al.*, 2016; Santos *et al.*, 2021).

The ability to tolerate substantial thermal variation is supported by a physiological mechanism known as regional endothermy. Unlike most elasmobranchs, mako sharks are able to retain metabolic heat, maintaining specific body regions, namely muscles, viscera, brain, and eyes, between 7–10 °C above ambient water temperature. This is facilitated by complex vascular heat-exchange systems, known as *retia mirabilia*, which reduce heat loss and enable higher activity levels than those observed in strictly ectothermic species. Furthermore, their haemoglobin displays an oxygen affinity less sensitive to temperature changes, ensuring efficient oxygen delivery even when body temperature fluctuates due to vertical movements or sudden environmental changes (Bernal *et al.*, 2001; Bernal *et al.*, 2018; Morrison *et al.*, 2022).

The shortfin mako shark exhibits a generalist and opportunistic feeding strategy, with a clear predominance of bony fishes (teleosts) and cephalopods, which constitute the main component of its diet. A study conducted by Maia *et al*. (2006) on sharks from the north-eastern Atlantic showed that teleosts were present in 87% of the stomachs analysed and accounted for more than 90% of the total prey weight. Crustaceans and cephalopods also contributed to the diet, while other elasmobranchs occurred only in small proportions. No clear selectivity regarding prey size was observed, and seasonal variations in feeding were consistent with the availability of prey in the environment, demonstrating the trophic flexibility of this species.

In contrast, a study by Calle-Morán *et al*. (2023) showed that *I. oxyrinchus* in Ecuadorian waters has a diet dominated by large oceanic squids, mainly *Dosidicus gigas* and *Sthenoteuthis oualaniensis*. This population exhibited a more specialised feeding pattern, with limited variation between sexes and life stages. Furthermore, Preti *et al*. (2012) found that *I. oxyrinchus* displays a more generalist feeding

behaviour compared to other shark species, reinforcing its ecological importance as an apex predator within marine ecosystems.

The shortfin mako is a relatively slow-growing species, a trait which, combined with other life-history characteristics such as low fecundity and late sexual maturity, renders it particularly vulnerable to overfishing. Nevertheless, shortfin makos exhibit rapid early growth, attaining an increase of approximately 39 cm in fork length during the first year of life. Subsequently, males and females display similar but reduced growth rates up to around seven years of age, after which the relative growth of males declines markedly (Liu *et al.*, 2018; Doño *et al.*, 2015; Ribot-Carballal *et al.*, 2005; Bishop *et al.*, 2006; Natanson *et al.*, 2006). In contrast, females reach larger sizes (Vera-Mera *et al.*, 2025). Median age at maturity has been estimated at 7–9 years (180–210 cm) for males, and 19–21 years (260–330 cm) for females (Bishop *et al.*, 2006; Maia *et al.*, 2007; Francis & Duffy, 2005; Cerna & Licandeo, 2009).

This species is aplacental viviparous, with embryos exhibiting oophagy. Litter sizes may range from 4 to 30 pups, depending on the size of the female (Mollet *et al.*, 2002; Costa *et al.*, 2002; Joung & Hsu, 2005; Semba *et al.*, 2011). Gestation periods vary between 15 and 18 months, depending on the region, with parturition typically occurring from late winter through to summer (Joung & Hsu, 2005; Semba *et al.*, 2011; Maia *et al.*, 2007; Costa *et al.*, 2002). Newborns measure between 70 and 80 cm (Joung & Hsu, 2005), and initial growth rates vary considerably between regions, ranging from 16 to 61 cm per year (Bishop *et al.*, 2006; Natanson *et al.*, 2006; Maia *et al.*, 2007; Cerna & Licandeo, 2009).

1.4 Fisheries and conservation status

The shortfin mako shark is one of the most important shark species in pelagic fisheries employing longlines and gillnets, which are primarily targeted at tunas and swordfish in the Atlantic Ocean. In terms of catch volume, only the blue shark (*Prionace glauca*) is more abundant (Campana *et al.*, 2005; Camhi *et al.*, 2008;

Mejuto *et al*., 2009; Coelho *et al*., 2012). Although the capture of makos often occurs as bycatch, shortfin mako specimens are frequently retained due to the high commercial value of their meat and fins (Camhi *et al*., 2008; Dulvy *et al*., 2008b; Stevens, 2008; Rigby *et al*., 2019).

Their aggressive behaviour and remarkable strength have made them one of the most sought-after species in recreational fisheries worldwide (Stevens, 2008). Following their inclusion in Appendix II of CITES in 2019 which stipulates that international trade is permitted only if it can be demonstrated to be legal and sustainable (CITES, 2019), it is likely that the rate of discards has increased. However, like other pelagic sharks, shortfin makos exhibit a low capacity for recovery under intense fishing pressure, due to their biological and life-history traits (Barker & Schluessel, 2005; Dulvy *et al*., 2008b).

This species is regarded as one of the most vulnerable to overfishing in the Atlantic, owing to its low productivity and high susceptibility to capture (Simpfendorfer *et al*., 2008; Cortés *et al*., 2010). Recent studies indicate that the increasing fishing effort over recent decades has had a significant impact on shortfin mako populations in the Atlantic. The recent stock assessment, conducted in 2017 by the International Commission for the Conservation of Atlantic Tunas (ICCAT), concluded that in the South Atlantic there was a 32% probability of overfishing occurring and a 42% probability that the population was already overfished. In the North Atlantic, the combined probability of the stock being both overfished and subject to overfishing reached 90% (de Bruyn, 2017).

In light of these findings, the species has been classified as globally “Endangered” on the IUCN Red List (Rigby *et al*., 2019). Understanding the movements of this species, specifically, how it utilises space and its movement patterns, is essential for interpreting its behaviour and population structure. Furthermore, determining whether individuals move through regions subject to varying types and intensities of fishing activity is critical for predicting the effects of fisheries on populations and on the wider marine food web. Such knowledge also facilitates the identification of

essential habitats and the development of effective management measures (Camhi *et al*., 2008; Rogers *et al*., 2015; Vaudo *et al*., 2016).

1.5 General Objective

The primary aim of the present study is to analyse how different environmental variables influence the vertical behaviour, specifically depth distribution and diel migration movements of the shortfin mako shark (*Isurus oxyrinchus*) in the South Atlantic. Climate change may alter oceanographic conditions that strongly influence the behaviour and ecology of this species. Understanding the behaviour of *I.oxyrinchus* in relation to its environment enables the anticipation of potential shifts in the preferred habitat of the shortfin mako, which could affect its vulnerability to fisheries and the sustainability of its populations.

The aim of this study is, therefore, to provide scientific information that contributes to more effective and adaptive fisheries management, taking into account climate change scenarios and the ecological role of this species within the marine ecosystem.

2. Methods

2.1 Study Area and Species Tagging

A total of twelve shortfin mako sharks (*Isurus oxyrinchus*) were tagged in the South Atlantic Ocean, specifically in offshore waters near Namibia, using pop-off satellite archival tags (PSATs; MiniPAT and Mk-10 models, Wildlife Computers, Redmond, WA, USA), following procedures described in Queiroz *et al*. (2010). Four individuals were tagged between 2021 and 2022 and eight were tagged in 2024. Specimens were captured using commercially baited longlines deployed from industrial fishing vessels.

After capture, sharks were lifted and held in a vertical position perpendicular to the vessel hull while tags were attached. Tags were secured using a monofilament line encased in silicone tubing that was passed through a small hole pierced at the base of the first dorsal fin (Figure 2), providing a secure attachment while minimising impact on the animal's hydrodynamics.

Prior to deployment, PSATs were programmed to record data for either 90, 120 or 180 days depending on the individual, and to release (pop-off) after the programmed interval. Tags were programmed at different times to ensure data collection, but longer durations carried a higher risk of data loss. All tags were bench-tested to confirm positive buoyancy in seawater. During the tagging procedure the following metadata were recorded on-site: date and time (UTC), fork length (FL), GPS position (latitude and longitude), sex, sea surface temperature (SST, °C) and a biological sample.

The PSAT model used in this study was the MiniPAT (Wildlife Computers; Figure 3). MiniPATs archive depth, minimum and maximum temperature, and ambient light level at the deployed sampling frequency; archived data are summarised into 6, 12 or 24-hour bins for satellite transmission depending on the tag configuration. In this study, data from animals tagged in 2021/2022 were summarised at 6-hour intervals, whereas those from 2024 deployments were summarised at 12-hour intervals.

No tags were physically recovered in this study; therefore, only transmitted summary data were available. The MiniPAT records depths between 0–1700 m (resolution 0.5 m; ±1%) and temperatures between −40 °C and +60 °C (resolution 0.05 °C; ±0.1 °C). Tag detachment is achieved by a corrodible pin that dissolves at a pre-programmed date or under conditional-release criteria; once detached, tags float to the surface and begin transmission. After release, archived summaries are transmitted via the Argos satellite system. Summaries included time-at-depth (TAD) and time-at-temperature (TAT) histograms and vertical temperature profiles of the water column.

All tagging procedures were approved by the Animal Welfare and Ethical Review Body (AWERB) of the Marine Biological Association (MBA), UK, and were licensed by

the UK Home Office under Personal and Project Licences in accordance with the Animals (Scientific Procedures) Act 1986. Procedures were conducted by trained personnel and sharks were released within a few minutes with no apparent adverse effects.

Figure 2: Attachment of a pop-off satellite archival tag (PSAT) at the base of the first dorsal fin of a shortfin mako shark (*Isurus oxyrinchus*). The attachment system, consisting of a monofilament tether coated with silicone tubing, can be seen passing through a small hole pierced in the fin (Photograph: Tiago Cidade).

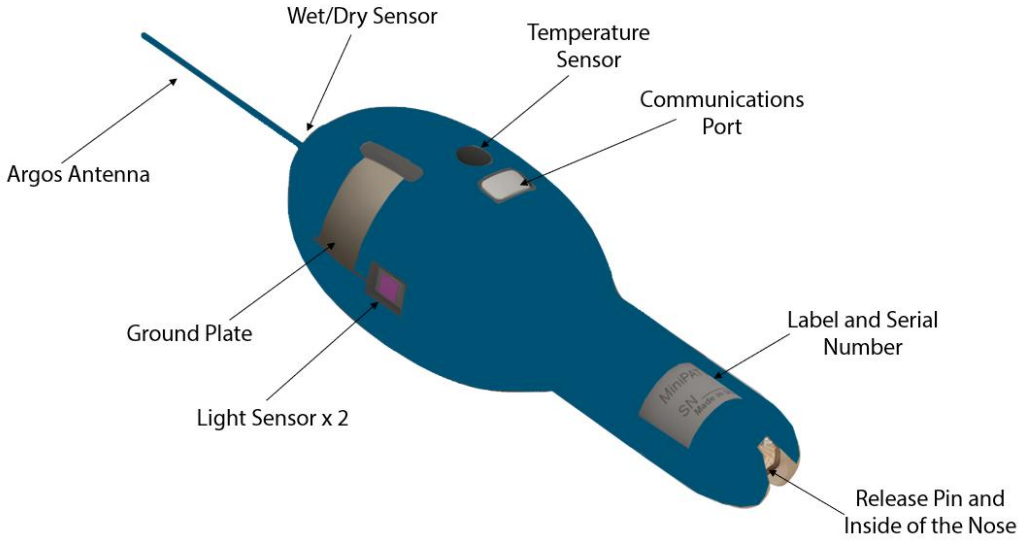

Figure 3: Diagram of a PSAT (pop-off satellite archival tags) with identification of the main components. https://wildlifecomputers.com/our-tags/extras/anti-fouling/.

2.2 Track Processing

The movements of the sharks tagged were estimated based on the satellite-transmitted data from each tag. The locations of each shark, from the moment of tagging until the detachment of the tag (pop-off), were reconstructed using the manufacturer's software (WC-GPE3, Wildlife Computers, USA). This programme uses the maximum daily rate of change in light intensity to estimate local noon or midnight, thereby providing an estimate of longitude. Day length is then used to estimate latitude. Location estimates deemed unreliable, resulting from dive-induced shifts in the estimated sunrise and sunset times derived from light curves, were automatically removed by the software.

Geolocation estimates provided by the system the Wildlife Computer were improved for double-tagged sharks using a Bayesian movement model aniMotum (Jonsen *et al.*,2005) which estimates animal trajectories while accounting for Argos location uncertainty. Argos location class Z (LC Z) fixes, which indicate failed

positioning attempts, were removed. Remaining raw positions (LC 3, 2, 1, 0, A and B) were examined point by point using a 2 m s^{-1} speed filter to exclude outliers. To ensure reliable estimates of space use by the sharks, gaps between consecutive dates in the raw tracking data were interpolated to generate one position per day. However, whenever gaps exceeded 3 days, tracks were not interpolated. This approach avoided the generation of unrealistic locations and ensured more robust results (Queiroz *et al*., 2016; Queiroz *et al*., 2019).

2.3 Data Analyses

The transmitted data were imported into R (version 4.5.1; R Core Team, 2025) and RStudio (Posit team, 2024), where all statistical analyses were conducted., where all statistical analyses were conducted.

For this study, four main file types were considered:

(i) PDT (profiles of depth and temperature), which includes the minimum and maximum depths recorded every 6 or 12 hours depending on the tag configuration, as well as the six intermediate depths with the highest cumulative time-at-depth within the sampling interval, associated with their respective maximum and minimum temperatures;

(ii) Series, containing continuous records of depth and temperature at a resolution of 7 minutes and 30 seconds;

(iii) Histos, which present predefined depth bins (0, 10, 30, 50, 100, 150, 200, 250, 300, 500, 700, 1200 °C) for time-at-depth (TAD) and temperature bins(7, 9, 11, 13, 15, 17, 19, 21, 23, 25, 27, 29 m) for time-at-temperature (TAT), indicating the percentage of time spent within each interval per 6 or 12 hours; and

(iv) MinMaxDepth, derived from the PDT file, which reports the maximum and minimum depths recorded every 6 or 12 hours, depending on the year.

Data processing steps were cross-checked with metadata on transmitter temporal coverage, ensuring that only valid records within the transmission period were

retained. The resulting files were organised to enable the creation of graphs and subsequent statistical analyses.

Bathymetry was obtained from the global GEBCO database (GEBCO Compilation Group, 2025). The bathymetry extraction was carried out using the same method as that employed by Klöcker *et al*. (2025), for each daily position, the value considered corresponded to a weighted mean depth, calculated from the 99% daily utilisation distribution kernel, representing the area in which the study object was located during 99% of the time recorded on that specific day. Weighted Bathymetry data were associated with each daily record. However, on some days, the maximum depth exceeded the local bathymetry assigned. This discrepancy can be explained by the difference in the positional error inherent to daily geolocation estimates, which may lead to mismatches between the actual dive location and the weighted mean bathymetry of the considered cells. Weighted Bathymetry data were used for all daily records, allowing not only the comparison between the maximum recorded depth and the depth of the seafloor, but also the classification of occurrence areas into continental shelf zones (bathymetry < 200 m) and open ocean (bathymetry > 200 m).

Profiles of the environmental variables (chlorophyll, oxygen and temperature) were extracted for each shark location following the same methodology used for bathymetry, using product ID: GLOBAL_MULTIYEAR_BGC_001_029. Temperature profiles were generated at 1-metre depth intervals, from the surface down to 1200 metres, with a 3-day moving window applied to account for temporal variability. Within each window, the geometric mean of temperatures was calculated, producing a final profile representing the shallowest depth observed over the 3-day period. The ELG method was subsequently applied to these daily temperature profiles using MATLAB (MathWorks). This conservative approach was chosen as it provides a more accurate representation of the actual oceanic conditions experienced by the sharks.

The methodology employed to determine the thermocline was based on Klöcker *et al*. (2025), who applied the Exponential Leap Gradient (ELG) method described by Chu and Fan (2017) to identify and characterise both the mixed layer and the

thermocline in temperature profiles. The detection of the thermocline was carried out through the generation of daily temperature profiles derived from the CMEMS (http://marine.copernicus.eu/) Global Ocean Physics Reanalysis model (product ID: GLOBAL_MULTIYEAR_PHY_001_030). Lunar light intensity was calculated in R using the oce package (Kelley & Richards, 2024), estimating the illuminated fraction of the moon for each daily record based on date, longitude, and latitude using the moonAngle function. Daylight duration was determined from nautical sunrise and sunset times for each point.

2.3.1 Analysis of Spatial Representation of Environmental Variables

Different environmental and biological datasets were used to characterise the oceanographic conditions associated with the distribution and behaviour of the analysed sharks. The environmental datasets included chlorophyll concentration, dissolved oxygen, temperature, bathymetry,thermocline position and thermogradient; the biological dataset comprised maximum diving depth. All datasets were harmonised to a common temporal resolution (daily) and time zone (UTC). To determine the daily maximum diving depth, we used the MinMaxDepth file derived from the PDT file.

In addition, daily location data (latitude and longitude) were associated, allowing the combination of maximum diving depth with the geographical position of the individuals. Global maps were generated using the cartographic base from the maps R package (Becker *et al.*, 2024; version 3.4.2.1). Maps display environmental variables at two depths: 0 m depth, representing surface conditions, and 100 m depth, approximating the upper limit of the thermocline, which is particularly relevant to shark diving behaviour and oceanographic gradients.

2.3.2 Analysis Seasonal and Sexual Variation in Depth and Temperature

Minimum and maximum depth data (MinMaxDepth) was used for analysis of seasonal and sexual variation in depth. For each individual, daily mean values of

depth were calculated from all depth samples recorded within the calendar day. Dates were assigned to seasons using the Southern Hemisphere calendar boundaries: Winter (20 June–21 September), Spring (22 September–20 December), Summer (21 December–19 March) and Autumn (20 March–19 June). Individual tag IDs were matched to sex metadata; sex assignment is reported in Table 1 (results).

Descriptive analyses included calculation of measures of central tendency (median) and dispersion (quartiles, interquartile range, minima and maxima) for daily mean depths, stratified by sex and season. Outliers were identified using the 1.5 × IQR rule (Tukey, 1977) unless otherwise stated.

2.3.2 Vertical analysis

Profile of Depth and Temperature (PDT) files from archival tags were processed and analysed in R (R Core Team, 2024). Each PDT contained depth bins and the minimum and maximum temperatures observed within each bin at discrete timestamps. The analysis pipeline was designed to standardise, interpolate and visualise vertical habitat use, with the aim of reconstructing continuous time–depth–temperature profiles for each tagged individual. Relevant columns were selected and the data were reshaped from wide to long format so that each depth–times observation had associated temperature minimum and temperature maximum values. The bin was standardised using lubridate (Spinu *et al.*, 2023), and mean temperature per bin was calculated as the midpoint between minimum and maximum values. Sequential bin identifiers were created to preserve original bin ordering, and the dominant temporal sampling interval was estimated from the time-stamps to guide temporal standardisation.

To address inconsistencies in depth coverage, each PDT profile was interpolated across depth at 1 m resolution using linear interpolation implemented with the zoo package (Zeileis & Grothendieck, 2005). The 1 m resolution was chosen to capture fine vertical structure while remaining coarser than the tags intrinsic resolution. Temporal gaps in the PDT time series were identified by comparing timestamps to a regular datetime sequence at the dominant sampling resolution and, additionally,

by checking for missing values on a 12-hour grid to detect prolonged gaps. Gaps shorter than two sampling intervals (i.e. shorter than twice the dominant sampling interval determined from the data) were filled using neighbouring observations to estimate depth limits and mean temperature profiles; gaps longer than two sampling intervals were flagged and retained as missing to preserve traceability of data quality. The final harmonised dataset therefore integrates original and interpolated PDT values and enables robust analyses of vertical and thermal habitat use.

Histos data were processed and analysed in R. TAD (time-at-depth) and TAT (time-at-temperature) data were imported, and bin headers were harmonised. Specifically, the first row of each file, containing the programmed depth or temperature class labels, was used to rename columns originally labelled Bin1–Bin12; that metadata row was then removed. The bins were pre-programmed in the tags and correspond to fixed depth or temperature ranges, recorded at intervals of either 6 h or 12 h depending on the year of tagging. Data were converted from wide to long format so that each row represented the percentage of time an individual spent in a given depth or temperature bin on a given date. The workflow comprised two sequential steps; the workflow combined procedures for (i) use time-at-depth (TAD) and time-at-temperature (TAT) to make heatmaps and (ii) integrating bathymetric context for each deployment. Bathymetric context was incorporated by merging daily bathymetry estimates with the Histos records using deployment identifier (ID) and date. Values deeper than 2000 m were excluded from plots in order to emphasise time spent in the upper water column, particularly near the thermocline, rather than being visually dominated by occasional very deep dives. For visual comparison of habitat use, a horizontal reference line at 200 m was added to bathymetric plots to distinguish shelf (<200 m) from offshore (>200 m) environments, consistent with the ecological context of the study.

2.3.3 Analysis by Sex

Daily minimum and maximum depth values were extracted from the MinMaxDepth files for each individual. These values were averaged by day and matched with individual ID codes. Individuals were assigned to sex categories based on tag identifiers (Females: S1, S3, S4, S6, S8; Males: all other tags).

To visualise general patterns, data from temperature and depth profiles were used. The columns for depth, minimum temperature, and maximum temperature were transformed from wide to long format, ensuring the correspondence between depth values and their respective minimum and maximum temperatures. Dates were converted to datetime format, and the daily mean temperature for each individual was calculated. Individuals were properly classified by sex (male and female) and by the corresponding year.

2.3.4 Data processing for maximum depth analysis

The PDT data, together with bathymetry, were used to construct scatter plots of the daily maximum depth against date for each individual, as well as the maximum and minimum temperatures recorded for each individual, separated by year, overlaid with a continuous colour scale representing bathymetry, allowing a detailed visualisation of the relationship between the sharks' vertical behaviour and seafloor depth.

For each record, the maximum depth, maximum temperature, and minimum temperature across all bins were extracted. The illuminated fraction of the lunar disc (0–1) was used as a continuous proxy for moonlight intensity, and moon phases were categorised into seven classes (New Moon, Initial Crescent, First Quarter, Waxing Gibbous, Full Moon, Last Quarter, Waning Gibbous). Individuals were grouped into two groups (Year 2021/22 and Year 2024) according to deployment year. Bathymetry was categorised into two zones: Bathymetry <200 m and open ocean (>200 m).

A Generalized Linear Model (GLM) with a Gamma distribution was fitted to evaluate the effect of the thermal gradient on maximum depth and the full open ocean, and in bathymetry less than 200 m. The model predictions were added to the dataset, and the fitted relationship was visualized by overlaying the predicted line on the scatterplots of the observed data. GLM were also constructed to evaluate the relationship between maximum diving depth and different environmental variables. Independent models were fitted considering as predictors: (i) dissolved oxygen concentration, (ii) chlorophyll concentration, (iii) water temperature, (iv) thermocline gradient, (v) thermocline starting depth, and (vi) lunar illuminated fraction. Models were fitted separately for 0 m and 100 m depths, when applicable, and were evaluated based on descriptive statistics and graphical inspection of the model fits. In addition, descriptive statistics (mean, standard deviation, minimum, maximum, and mode) were calculated for each environmental variable, and extreme values (maxima and minima) were identified per individual and per environmental parameter.

2.3.5 Analysis of time spent above the thermocline

Time-series data were also utilised to quantify the proportion of time individuals spent above the thermocline, following the same processing methodology. For each shark and each day, the total number of recordings was calculated (with observations taken at 7.5-minute intervals, yielding approximately 192 expected observations per shark per day). To ensure data quality, only days with at least 60% of the expected recordings were retained. For these days, an additional column was created to classify whether the recorded depth was above or below the onset of the thermocline. For subsequent diel analyses, the days were then aggregated into consecutive blocks.

Filtered datasets were integrated with thermocline characteristics (onset depth, end depth, and thermal gradient) and bathymetry, allowing locations to be classified as either “open ocean” (>200 m) or <200 m depth.

Firstly, GLM were used to evaluate the relationship between the proportion of time spent above the thermocline and selected environmental predictor variables: thermal gradient, surface temperature (0 m at depth), and thermocline onset depth. These predictors were chosen because they had previously shown the strongest influence on maximum depth and were therefore combined to assess their potential role in explaining variation in time spent above the thermocline. Separate models were fitted for open-ocean and shelf regions.

Spatial patterns of thermocline use were mapped by linking daily averages of the percentage of time above the thermocline with georeferenced positions (Longitude and Latitude), providing a geographic overview of horizontal habitat use in relation to vertical oceanographic conditions, using the maps package (Becker & Wilks, 2021; version 3.4.2.1).

To assess how environmental conditions influenced the proportion of time spent above the thermocline, oceanographic variables were extracted at two reference depths: the surface (0 m) and subsurface (100 m). For each tagged individual, daily records of these variables were filtered to include only the high-quality days previously selected (data coverage > 60%) and were subsequently aggregated into the same temporal blocks.

GLMs were applied to test the effects of oxygen, chlorophyll-a, and temperature (with interaction terms for diel phase, i.e. day vs night, used the day-block) on the percentage of time spent above the thermocline. Additionally, the illuminated fraction of the lunar disc (0–1) was used as a continuous proxy for moonlight intensity, and moon phases were categorised into seven classes (New Moon, Initial Crescent, First Quarter, Waxing Gibbous, Full Moon, Last Quarter, Waning Gibbous). The average exposure of the blocks of days moonlight exposure was subsequently incorporated into GLMs to evaluate the influence of lunar cycles, in interaction with diel phase, on time spent above the thermocline.

To investigate which environmental factors best explained the proportion of time spent above the thermocline during day and night, GLMs with binomial distribution and logit link were applied. Prior to modelling, environmental predictors were

standardised by depth. Strongly collinear variables (notably temperature at 0 m and chlorophyll-a at 100 m) were excluded on the basis of pairwise correlation plots and variance homogeneity tests.

The response variable was defined as the proportion of time spent above the thermocline, normalised between 0 and 1. Models were fitted separately for daytime and night-time datasets. Model selection followed a stepwise reduction approach based on Akaike's Information Criterion (AIC). For the night-time subset, the most parsimonious model retained thermocline onset depth, oxygen concentration at 100 m depth, and surface chlorophyll as significant predictors. For the daytime subset, the best-fitting model included thermocline gradient, oxygen concentration at 100 m depth, and surface chlorophyll-a. Predictive effects of the selected variables were visualised using effect plots generated with the allEffects function from the effects package (Fox, 2003; 2019), showing the marginal response of above-thermocline use to environmental gradients while controlling for other predictors.

To account for repeated measures within individuals, generalised linear mixed-effects models (GLMMs) with binomial distribution and logit link were fitted using the lme4 package (Bates *et al.*, 2015). The response variable was again the proportion of time spent above the thermocline, normalised between 0 and 1, with shark identity (ID) included as a random intercept.

Model selection was again conducted using stepwise reduction based on AIC. For the night-time subset, the full model included lunar illuminated fraction, thermocline gradient, thermocline depth, oxygen concentration at 100 m, and surface chlorophyll-a. The most parsimonious model excluded lunar illumination and thermocline gradient, retaining thermocline depth, oxygen concentration at 100 m, and surface chlorophyll-a as significant predictors. Additional sensitivity analyses, restricting thermocline depth to <100 m, produced consistent results.

For the daytime subset, the full model likewise included all five predictors. The best-supported model excluded thermocline depth and thermocline gradient, retaining

lunar illuminated fraction, oxygen concentration at 100 m, and surface chlorophyll-a as significant predictors.

2.3.6 Diel Analysis

The time-series files enabled the assessment of water-column use patterns during both diurnal and nocturnal phases. Each record corresponded to a fixed interval of 7.5 minutes, a resolution determined by the tag programming. This frequency reflects a technical constraint: the tag is unable to transmit all stored data simultaneously, and thus a 7.5-minute interval was adopted as a practical compromise between temporal resolution and transmission capacity. Under ideal conditions, and without transmission failures, 192 records would be obtained per day. However, despite the high temporal resolution, occasional gaps occurred in transmission. These missing values were random, representing moments when the tag failed to transmit, resulting in an absence of data for the corresponding 7.5-minute intervals. Consequently, only the actual number of available records was considered for each period.

The theoretical sampling effort was estimated separately for the diurnal and nocturnal phases, adjusted to the actual duration of each phase according to the times of nautical sunrise and sunset calculated daily for each individual using the suncalc package (Thieurmel & Elmarhraoui, 2022; version 0.5.1). All timestamps were converted into the POSIXct format to ensure temporal consistency and alignment between tag data and solar position files, both confirmed to share the same time zone and geographical coordinates. These files provided the timing of nautical dawn and dusk, allowing each record to be classified as diurnal (between nautical dawn and dusk) or nocturnal (outside this interval).

To facilitate analysis and reduce day-to-day variability, data for each individual were grouped into blocks of five consecutive days, hereafter referred to as day-blocks. This approach allowed clearer identification of behavioural patterns and more robust data management. Only day-blocks in which at least 60% of the actual records were available in both diel phases were retained for analysis. The 60%

threshold was determined empirically: a histogram of data coverage showed that the majority of days retained up to 60% of valid data, which was therefore adopted as the minimum acceptable level of completeness. For each combination of individual, date, and diel phase, the total number of valid records was calculated and used as a reference to compute the percentage of time spent within each depth interval. The procedure was as follows, for each ID, date, and diel phase, the total number of valid records was obtained; each observation was expressed as a percentage of that total; and mean percentages across the days within each day-block were calculated, producing a representative mean value per individual, diel phase, and depth interval. Depth intervals were defined according to the pre-programmed settings of the tag, as represented in the Histos (TAD) files: 0–10 m, 10–30 m, 30–50 m, 50–100 m, 100–150 m, 150–200 m, 200–250 m, 250–300 m, 300–500 m, 500–700 m, 700–800 m, 800–900 m, and 900–1200 m. The proportion of records in each depth range was calculated relative to the total number of records within the same day-block and diel phase.

To incorporate oceanographic structure, the mean thermocline and the mean thermal gradient characteristics were computed for each day-block. These values provided a representative estimate of the vertical temperature structure within each block. In the graphical representations, a horizontal line was added to indicate the average depth of thermocline onset for each block. This line was colour-coded using a continuous viridis scale (Garnier *et al.*, 2024; version 0.6.5) corresponding to the mean thermal gradient, thereby visually linking the strength of the thermocline with the depth-use distribution of each day-block.

The line representing the mean thermocline onset depth was positioned according to the lower boundary of the corresponding depth interval. The same criterion was applied to the daily mean depth estimates to ensure that averaged values were accurately aligned with their respective depth categories.

Mean percentages of use were then computed for each depth interval, diel phase, and day-block, incorporating the associated bathymetric classification and thermocline information. Additionally, the number of records occurring above the

thermocline onset was quantified to enable subsequent comparisons with environmental variables.

3.Results

Of the twelve individuals tagged, it was only possible to obtain data from ten due to failures of unknown origin in the tags. Of these, three were tagged in 2021/22 and seven were tagged in 2024. In total, four males and six females were recorded (Table 1). Most of the tagged individuals are subadults, with the exception of the last individual to be tagged (S10), which is the only adult and also the largest individual. This individual is also the female with the highest number of vertical data records to date.

Table 1: Data for the tagged shortfin mako sharks. For each individual, the identification code (ID), tagging date, pop-off date, number of days at liberty, sex, total length in centimetres (Size (cm)), and life stage.

ID	Tagging date	Pop-off date	Days-atliberty	Sex	Size (cm)	Life stage
S1	26/11/2021	24/02/2022	90 days	female	195	sub-adult
S2	24/11/2021	24/03/2022	120 days	male	195	sub-adult
S3	18/12/2021	17/04/2022	120 days	female	177	sub-adult
S4	23/02/2024	22/06/2024	120 days	female	200	sub-adult
S5	22/02/2024	22/06/2024	121 days	male	220	sub-adult
S6	23/02/2024	23/06/2024	121 days	female	160	sub-adult
S7	13/03/2024	12/07/2024	121 days	male	195	sub-adult
S8	14/03/2024	13/07/2024	121 days	female	210	sub-adult
S9	25/03/2024	21/09/2024	181 days	male	220	sub-adult
S10	17/04/2024	14/10/2024	180 days	female	340	adult

3.1 Horizontal Movements

The tracks of the tagged individuals were recorded in the South Atlantic Ocean, between approximately 40°S and 5°S (Figure 4). The individual tracks revealed diverse movement patterns throughout the tracking period, with a general predominance of movements toward the continental shelf and adjacent waters.

Individuals tagged in 2021/2022 (S1–S3) exhibited trajectories with no differences between sexes. Initially, all individuals tagged during these years showed a tendency to move northwards, later reversing direction towards the south, heading towards the continental shelf. They remained adjacent to it and moved mainly in its proximity until transmission ceased.

Individuals tagged in these years accumulated a total of 10 tracking days in waters shallower than 200 m and 317 tracking days in waters deeper than or equal to 200 m. Although their movements were predominantly oriented towards the continental shelf, the individuals still spent a considerable amount of time in offshore waters while moving towards this region.

In contrast, individuals tagged in 2024 (S4-S10) exhibited more variable and extensive spatial distributions, spanning a wider latitudinal range. Collectively, they accumulated 46 days of tracking in waters <200 m deep and 911 days of tracking in waters ≥200 m deep, indicating a greater use of open ocean areas, similar to that observed in individuals from the previous year. Several individuals followed direct southward trajectories after tagging, often passing near a seamount located within the study area before approaching or entering the continental shelf.

Among the individuals tagged in 2024, some exhibited movement patterns that deviated from the general trends observed. Individuals S4, S7, S8, and S9 crossed a seamount along their trajectories, with S7 and S8 being tagged in its vicinity, while S4 and S9 passed directly over this feature. Individual S6 travelled southwards after approaching the continental shelf, reaching the southernmost coordinates recorded in this study, near Cape Town, South Africa.

Finally, individual S10 displayed the northernmost distribution among all tagged specimens, remaining within a restricted area and reaching the highest latitude recorded, close to the island of Saint Helena. This individual did not approach the continental shelf, nor did it follow the southward movement pattern exhibited by the other individuals.

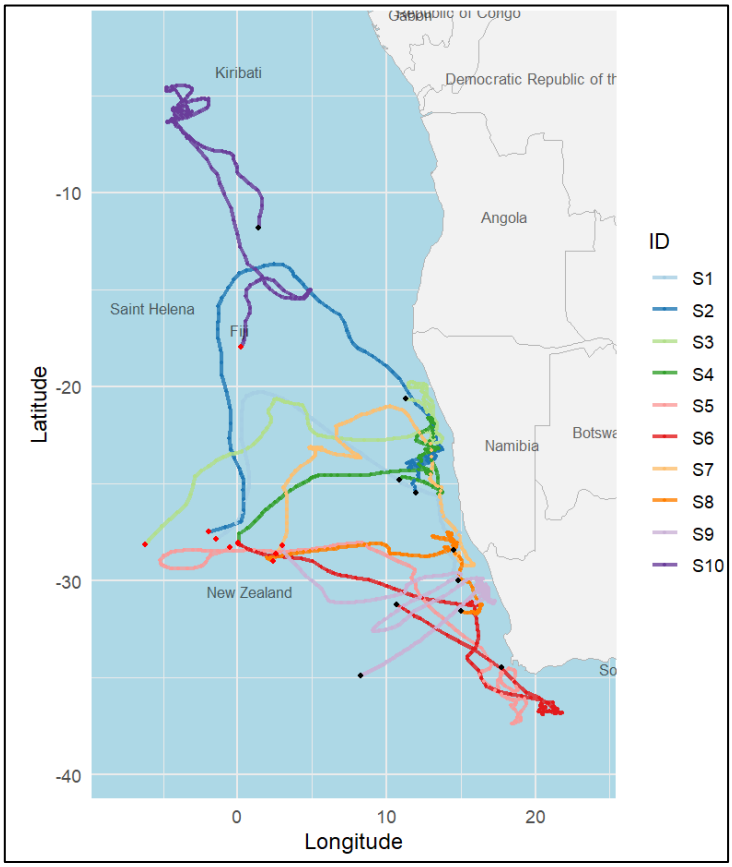

Figure 4: Trajectories of *I. oxyrinchus* individuals tagged with electronic devices in the South Atlantic Ocean. Red circles indicate tagging locations, while black circles represent transmitter pop-off locations.

3.2 Maps of daily environmental variables as a function of individual location

Chlorophyll concentrations exhibited considerable variability. At the surface (0 m), the maximum value of 1.57 µg L^{-1} was recorded on 6 June 2024 by individual S4 at 25.1° S, 13.5° E, whereas the minimum of 0.0463 µg L^{-1} was observed on 28 December 2021 by individual S3 at 24.4° S, 2.41° W. Overall, surface chlorophyll concentrations were higher in coastal regions, particularly between 35° S and 20° S, and decreased towards the open ocean (Figure 5A). At 100 m depth, concentrations were generally lower, with a maximum of 0.448 µg L^{-1} recorded on 28 December 2021 by individual S2 (14.1° S, 3.70° E) and a minimum of 0.0226 µg L^{-1} observed on 13 June 2024 by individual S9 (31.2° S, 17.2° E). These values reflect the vertical stratification of primary productivity (Figure 5B).

Dissolved oxygen concentrations (ml L^{-1}) also displayed pronounced spatial and vertical gradients. At the surface, the maximum of 5.95 ml L^{-1} was recorded on 6 June 2024 by individual S4 (25.1° S, 13.5° E), while the minimum of 4.60 ml L^{-1} was recorded on the same date by individual S10 (10.1° S, 0.869° W). Surface waters were relatively homogeneous in terms of oxygen, maintaining predominantly high concentrations, as expected from gas exchanges between the ocean surface and the atmosphere (Figure 5C). At 100 m, oxygen concentrations were generally lower and more variable, with a maximum of 5.83 ml L^{-1} observed on 20 September 2024 by individual S9 (34.8° S, 8.49° E) and a minimum of 0.199 ml L^{-1} recorded on 16 March 2022 by individual S3 (21.0° S, 13.1° E). The lowest oxygen concentrations were particularly evident along the northern coastal zone, approximately between 5° N and 20° S (Figure 5D).

Temperature (°C) displayed a pronounced latitudinal contrast. At the surface, the maximum of 25.6 °C was recorded on 6 June 2024 by individual S10 (10.1° S, 0.869° W), whereas the minimum of 14.5 °C was observed on 25 June 2024 by individual S7 (29.1° S, 15.9° E). Surface temperatures were highest between 0° and 30° S in oceanic regions and lower near the coast (Figure 5E). At 100 m, temperatures were generally lower, ranging from 11.5 °C (25 June 2024, individual S7; 29.1° S, 15.9° E)

to 19.7 °C (21 December 2021, individual S2; 14.2° S, 0.118° E). This pattern reflects the characteristic vertical cooling of water masses (Figure 5F).

The thermal gradient (ΔT) indicated strong stratification in tropical and northern regions, with a maximum of 0.167 °C recorded on 27 April 2024 by individual S10 (14.6° S, 1.15° E), and weaker stratification in the southern and cooler regions, with a minimum of 0.006 °C observed on 22 April 2024 by individual S9 (30.1° S, 11.6° E) (Figure 5G).

Shark vertical distribution corresponded to these environmental gradients. The maximum depth recorded was 1,168 m, observed on 18 April 2024 by individual S6 (35.2° S, 16.4° E), who also reached the southernmost coordinates of the study area. The minimum depths of 16 m were recorded on 22 May 2024 and 17 September 2024 by individual S10, at 15.4° S, 3.92° E and 7.38° S, 3.15° W, respectively; this individual represented the northernmost location in the study area. In general, sharks in southern regions reached depths exceeding 900 m, whereas those in northern regions typically remained at depths below 500 m, evidencing a clear latitudinal gradient in vertical habitat utilisation (Figure 5H).

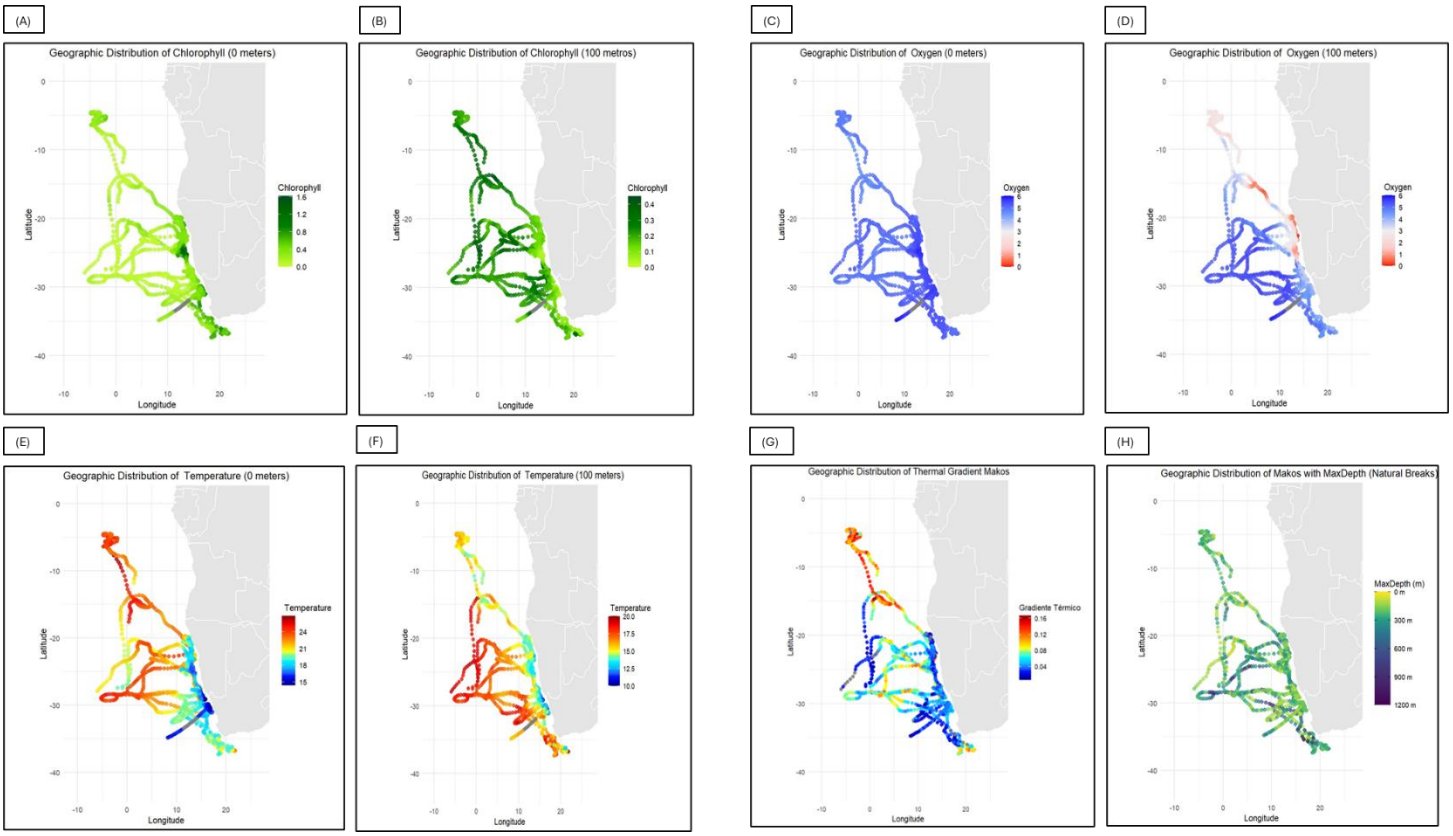

Figure 5: Maps at the surface (0 m) and at 100 m depth showing (A, B) chlorophyll (dark green: high concentration; light green: low), (C, D) dissolved oxygen (blue: high values; red: low), (E, F) temperature (red/orange: warmer waters; green/blue: colder), (G) thermal gradient (warm colours: stronger stratification; cool: weaker), and (H) maximum daily depth (from 600 m onwards, dark tones).

3.3 Seasonal and Sexual Variation in Depth and Temperature Used

Overall, males and females exhibited broadly similar depth-use patterns across seasons, although some sex differences were evident. The most pronounced differences occurred in summer, when females displayed a larger vertical range in dive depths. By contrast, spring and winter showed very similar patterns between sexes. In autumn, females had a slightly higher median depth than males, but this difference was not statistically significant (Figure 6).

During autumn, females (n = 210 dives; median = 206 m, IQR = 180–228 m) and males (n = 239 dives; median = 198 m, IQR = 175–219 m) exhibited very similar depth distributions, with close medians and substantial overlap in the interquartile ranges. Both sexes reached a maximum seasonal depth of 394 m. In spring, both sexes had identical medians (191 m), with females (n = 19 dives; IQR = 145–220 m) and males (n = 20 dives; IQR = 157–213 m) showing comparable depth-use patterns. Most dives in spring occurred between 134 and 245 m, with few outliers outside this interval.

Summer showed the greatest variability in diving depths across the dataset. Females (n = 345 dives; median = 167 m, IQR = 130–268 m) and males (n = 152 dives; median = 191 m, IQR = 138–295 m) reached a maximum observed depth of 486.6 m. During summer, a total of 33 dives exceeding 400 m were recorded for females and 22 for males. Both sexes therefore regularly engaged in deep diving (>400 m), although females displayed a broader interquartile range, indicating greater

variability among individuals. This variability was driven by several females (e.g., IDs S4–S6) whose median and maximum depths exceeded the population range.

In winter, both sexes showed reduced median depths and narrower vertical ranges compared with summer. Females (n = 163 dives; median = 163 m, IQR = 127–192 m) and males (n = 282 dives; median = 161 m, IQR = 128–192 m) reached a maximum observed depth of approximately 281 m.

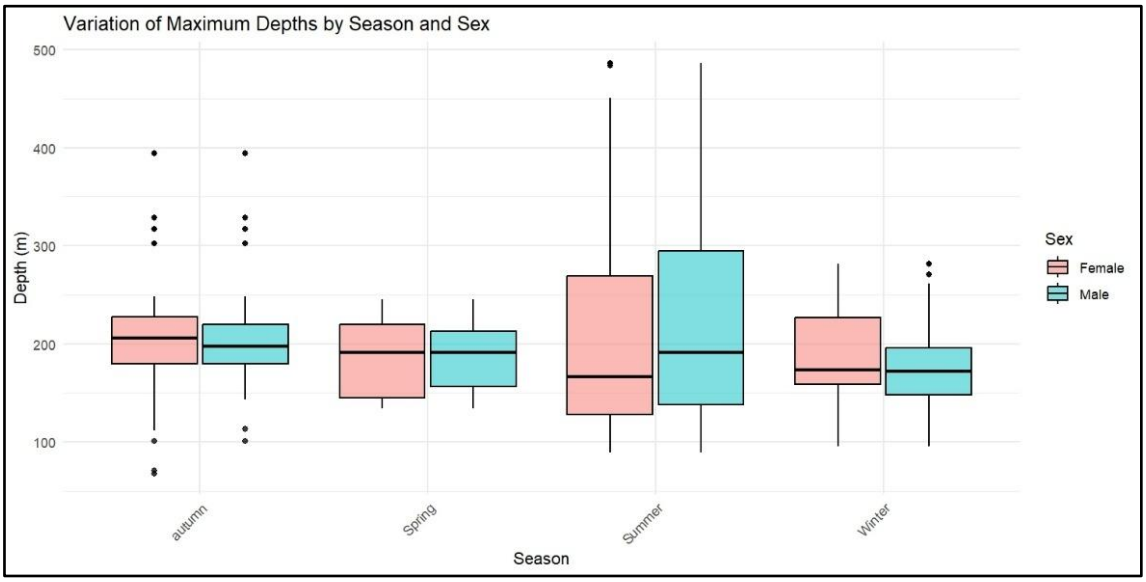

Figure 6: Maximum daily depths recorded for tagged mako sharks *(I.oxyrinchus*) in the South Atlantic, separated by sex (females in pink and males in blue) and season. Boxes represent the interquartile range (IQR), the centre line indicates the median, and dots represent outliers.

3.4 Depth and Temperature Profile Analysis

The overall analysis of vertical profiles revealed a predominant occupation of depths between 10 and 500 m, with marked inter-individual variability in both depth utilisation and temperature exposure. Among all tagged individuals (n = 10), median depths ranged from 40 to 112 m (mean depths: 69–166 m), while maximum recorded depths varied between 456 and 1168 m. The proportion of time spent in the surface layer (0–10 m) ranged from 17% to 26%. Minimum recorded temperatures were

between 3.4 and 8 °C, and maximum temperatures ranged from 22.2 to 26.9 °C, resulting in thermal ranges of approximately 14.6–23.2 °C.

A general trend was observed towards longer residence times in warmer mid-depth waters (200–350 m), interspersed with occasional deep dives, particularly during the warmer months. These temporal variations often coincided with changes in thermal stratification, suggesting a potential relationship between the vertical thermal structure and the vertical behaviour of individuals.

However, it was also observed that when temperatures in the 0–10 m layer were elevated, individuals tended to perform deeper dives. For example, individual S4 initially encountered relatively warm waters (0–150 m; up to 21 °C) in March, during which it conducted deep dives reaching 900 m. From April onwards, as the water cooled (15–20 °C), the individual increasingly occupied shallower layers (0–150 m) (Figure A1D). Similarly, individual S5 (Figure A1E) was associated with higher temperatures (21–27 °C) between March and April, a period characterised by several deep dives beyond 1000 m. From May onwards, temperatures decreased markedly (9–15 °C), and a pronounced thermal gradient developed by June, when the individual remained within 0–300 m.

Among the monitored individuals, distinct depth–temperature patterns were identified. Individuals S5 (Figure A1E) and S6 (Figure A1F) stood out for exhibiting the greatest median and maximum dive depths, reaching 1056 m and 1168 m, respectively. Both experienced the lowest minimum temperatures (3.6 °C and 3.4 °C) and spent little time in surface waters (0–10 m; 18.1% and 17.4% of the total time). These individuals also displayed the widest thermal ranges (23.2 °C and 20.7 °C).

Individual S9 initially experienced homogeneous and warm thermal conditions (21–27 °C; 0–500 m), but from June onwards there was a sharp drop in temperature (9–15 °C), particularly within the 0–250 m range (Figure 7A). Individual S10 (Figure 7B) experienced the highest maximum temperatures (up to 25 °C) and showed the lowest proportion of time spent in the surface layer (17%), remaining mostly

between 0 and 600 m. Despite the elevated surface temperatures, this individual did not perform dives deeper than 600 m.

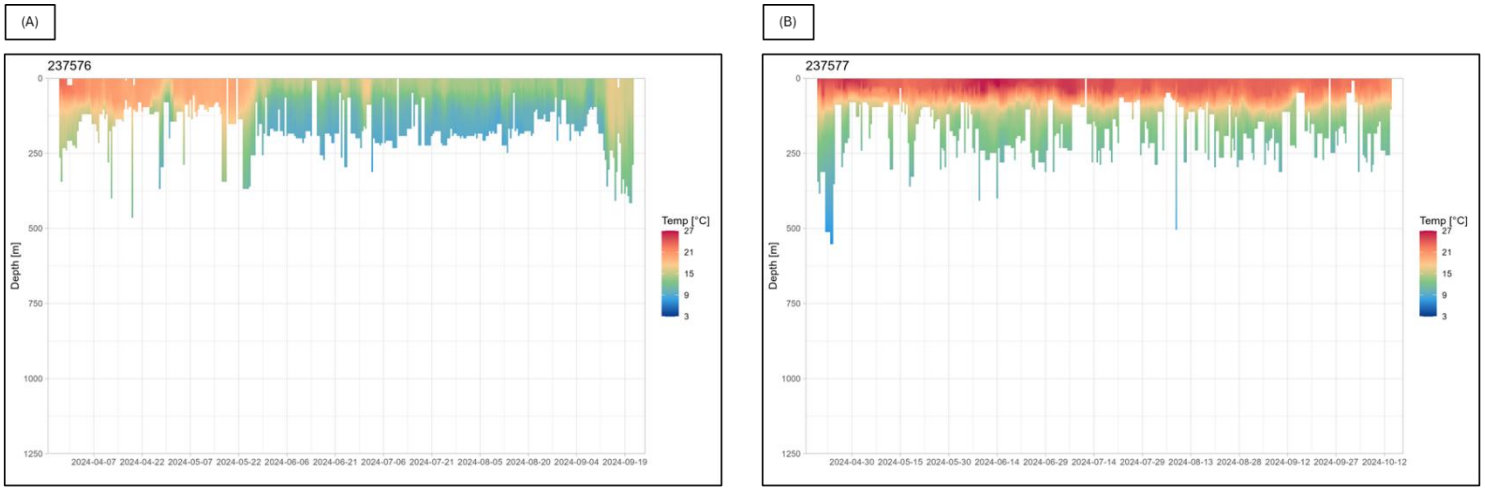

Figure 7: Depth and temperature profiles recorded by *I. oxyrinchus* individuals during the tagging period. (A) S9; (B) S10. Lines represent depth over time, while colour shading indicates water temperature.

3.5 Variation in the Percentage of Time Spent by Sharks at Different Depths and Temperatures

In general, individuals moved between coastal and oceanic zones, spanning depths of approximately 200 m to over 2,000 m. In most cases, the greatest depths were recorded at the onset of movements, immediately following offshore tagging. Although there was a general tendency to approach the continental shelf, several individuals never entered areas shallower than 200 m during the monitoring period.

S1 remained exclusively in waters >200 m for 92 days. Similar patterns were observed for S4, S5, S8 (121 days) and S10, none of which were recorded at depths <200 m (Figure A2A; 2D; 2E; 2H and 2J). In contrast, S2, S3, S6, S7 and S9 occasionally moved onto the continental shelf, albeit infrequently. S2 spent 119 days >200 m and 2 days <200 m; S3 120 days >200 m and 8 days <200 m; S6 115 days >200 m and 6 days <200 m; S7 113 days >200 m and 8 days <200 m; S9 149

days >200 m and 32 days <200 m. These results indicate a clear preference for deeper habitats, even among individuals that sporadically approached shallower shelf areas (Figure A2B; 2C; 2F; 2G and 2I).

TAD results show that the monitored individuals demonstrated a clear preference for the upper layers of the water column, irrespective of the available depth. Most of the tracked time was spent in shallow waters (<50 m), ranging from 53.4% to 77.5%, followed by the mid-depth range of 50–200 m (25.4–44.6%). Occupancy of deeper waters (>200 m) was minimal, representing between 1.59% and 23.2% of the total tracking time. These results confirm that sharks predominantly remain in surface layers, even when local bathymetry allows access to much deeper habitats. Dives exceeding 200 m were rare and isolated, even in individuals tracked over areas with pronounced bathymetry, such as S1, S4, S5, S8 and S10 (Figure A2A; 2D; 2E; 2H and 2J). Individuals such as S2, S3, S6, S7 and S9 occasionally approached depths <200 m, but these incursions were infrequent (Figure A2B; 2C; 2F; 2G and 2I).

TAT results further indicate that sharks preferred temperate waters, with the highest frequency recorded between 19 °C and 25 °C. During the early months of the year (January–March), occupation of warmer waters (23–25 °C) predominated, whereas from April to July there was a greater occurrence of lower temperatures (17–19 °C), reflecting migration to shallower waters with greater thermal variability. Occasional deep dives exposed some individuals to extreme temperatures, reaching 7 °C in isolated cases (e.g., S6, S9 and S10). Overall, 87.1–99.2% of the recorded time was spent in waters between 15 and 25 °C. Temperatures below 15 °C were observed only sporadically (0.797–12.9%), and temperatures above 25 °C were virtually absent (<1%). These results indicate a strong preference for moderate thermal conditions, with only occasional exposure to colder waters during deep dives.

3.6 Distribution of Average Maximum and Minimum Depths and Temperature by Sex and years

The analysis of the mean maximum diving depth of shortfin mako sharks by sex (Figure 8B) did not reveal substantial differences between females and males. Both groups exhibited identical medians of 188 m. The first and third quartiles ranged from 146–237 m in females and 159–223 m in males, indicating slightly greater variability among females, which may reflect individual differences in vertical habitat utilisation. The whiskers extended from 68 to 355 m in females and from 89.7 to 318 m in males. A total of 38 outliers were identified in females and 42 in males, with values exceeding 355 m (up to approximately 400 m). These data confirm that some individuals undertook markedly deep dives, although such occurrences were infrequent.

Regarding the mean minimum diving depth (Figure 8A), a strong similarity between sexes was again observed. Females exhibited a median of 2 m, whereas males showed a median of 1.82 m. The whiskers ranged from 0 to 8.22 m in females and from 0 to 9.21 m in males. Outliers were also recorded, with 21 in females and 12 in males, reaching maximum depths of approximately 20–30 m. These results suggest that both sexes frequently utilise the upper layers of the water column, with no marked differences in near-surface behaviour.

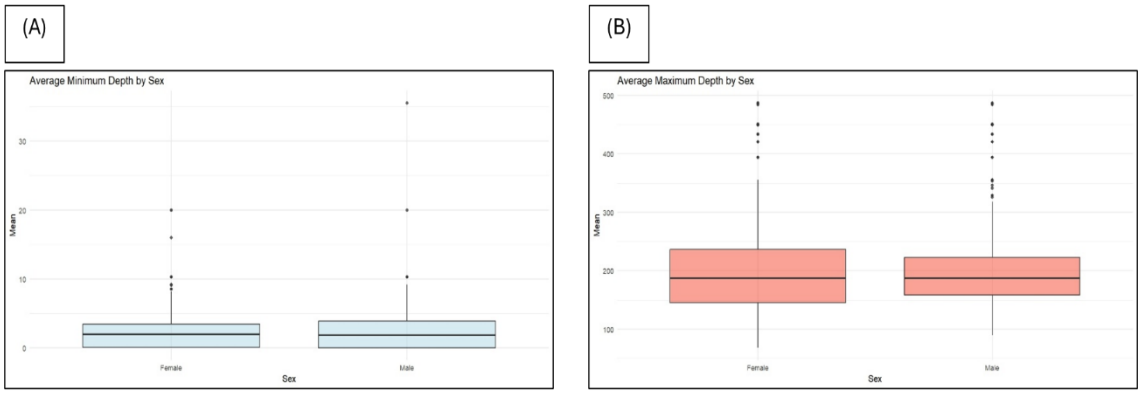

Figure 8: Boxplots of the daily average of maximum (A) and minimum (B) depths recorded by individuals of *I. oxyrinchus*, broken down by sex.

Potential differences in habitat utilisation between males and females were examined by analysing the distributions of mean daily depth and mean daily temperature associated with each individual throughout the monitoring period.

In the distribution of mean daily depth utilised by individuals according to sex. Both sexes display similar patterns, with peak densities concentrated between 90 and 100 metres. This overlap suggests that both sexes exhibit a broadly similar pattern of habitat use in terms of depth. Nevertheless, subtle differences are apparent. Females tend to show slightly higher densities at shallower depths (<80 m), whereas males exhibit a more pronounced tail at depths exceeding 120 m, indicating that some males more frequently explore deeper environments Figure 9C and Figure 9D.

Descriptive statistics reinforce this difference: the mean depth was 97.8 m for females (median = 91.1 m) and 100.0 m for males (median = 92.9 m). The Wilcoxon test indicated that this difference was statistically significant ($p < 0.001$), demonstrating that males generally occupied slightly greater depths than females over the sampling period.

The mean daily temperature recorded for each sex is presented in Figure 9D. In both sex, there was a higher frequency of use at temperatures between 16°C and 18°C, suggesting a shared thermal preference. However, females exhibited a broader distribution, with a notable proportion occurring at temperatures above 19°C. In contrast, males displayed a narrower distribution, with activity more concentrated within intermediate thermal ranges. Descriptive statistics indicate that the mean daily temperature was essentially identical between sexes: 16.6°C for females (median = 16.6°C) and 16.6°C for males (median = 16.5°C). The Wilcoxon test revealed no statistically significant difference between the groups ($p = 0.0545$), indicating that, at the 5% significance level, thermal variation was insufficient to infer a differentiated pattern between sexes.

The distributions of mean daily temperature and depth of tagged sharks revealed significant interannual differences, indicating that sharks occupied shallower and warmer waters in 2021/22, whereas in 2024 they explored deeper and cooler

environments, suggesting potential environmental or behavioural shifts between years. Individuals from 2024 reaching depths beyond 200 m represent an exceptional pattern, likely reflecting adaptive or exploratory behaviour.

In Figure 9A, the pink curve (2021/22) indicates a concentration of higher temperatures, predominantly between 18°C and 20°C. Conversely, the blue curve (2024) reveals a shift towards lower temperatures, concentrated between 14°C and 17°C. Descriptive statistics corroborate this trend: in 2021/22, the mean temperature was 17.7°C (median = 17.6°C), whereas in 2024 it was 16.1°C (median = 16.3°C). The Wilcoxon test confirms that this difference is statistically significant ($p < 0.001$).

Figure 9B illustrates the distribution of mean daily depth between years. In 2021/22 depths were more concentrated between 50 and 100 metres, with a mean of 78.2 m and a median of 77.7 m. In 2024, the distribution shifted towards greater depths, peaking around 100 metres and extending beyond 200 metres, indicating increased variability. The mean was 107 m and the median 95.3 m. The Wilcoxon test reinforced this difference ($p < 0.001$), confirming a significant increase in depth utilisation between years.

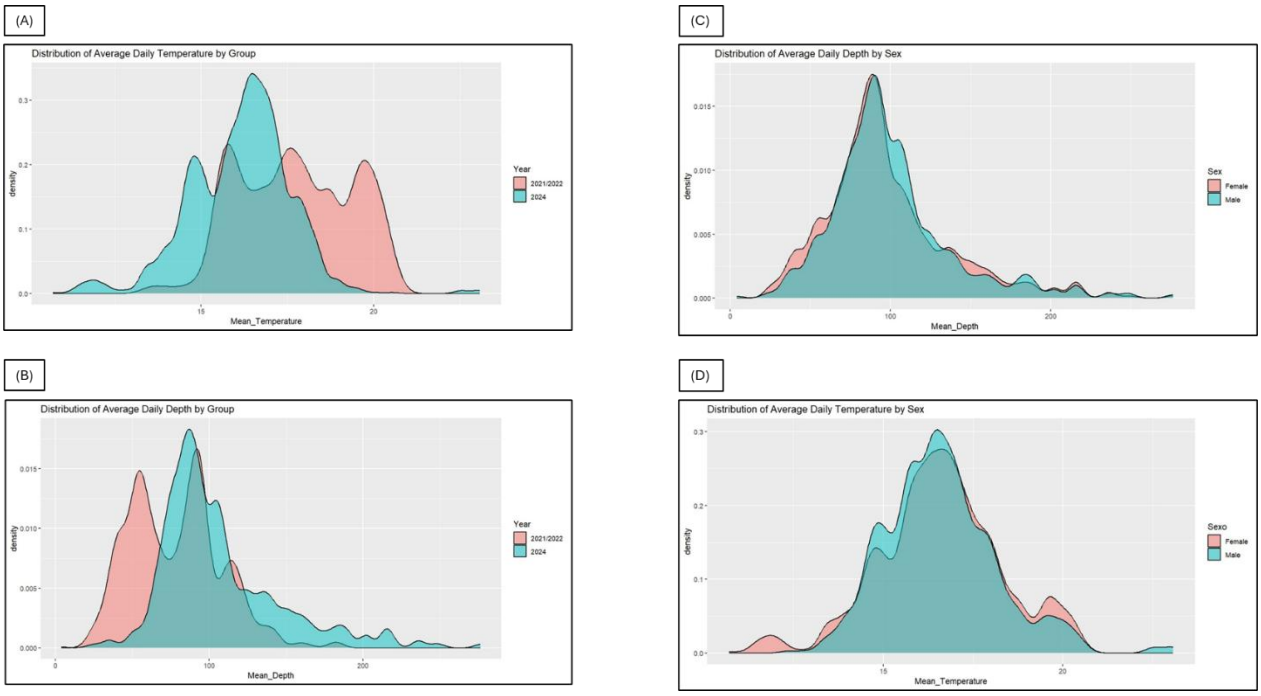

Figure 9: Distribution of mean depth (m) and temperature (°C) used by individuals throughout the monitoring period, stratified by year (A–B) and sex (C–D).

3.7 Analysis of Maximum Depth and Bathymetry

Integration of bathymetric data indicated that individuals in 2021/22 were predominantly located in areas deeper than 200 m (491 records; mean depth = 153 m, maximum = 712 m), with only 13 records in shallower regions (mean depth = 139 m). In 2024, sharks continued to conduct the majority of dives in open-ocean habitats (1,198 records; mean depth = 219 m, maximum = 1,168 m), with a smaller number of records in shallower areas (54 records; mean depth = 173 m), indicating a slightly broader habitat use compared to 2021/22 (Figure 10).

In 2021/22, individuals generally exhibited relatively shallow dives. By contrast, in 2024, dives were considerably deeper and associated with greater thermal variability. Figure 10 illustrates the daily variation in maximum recorded depth (MaxDepth) for individuals tagged in 2024 (Figure 10 C and D) and in 2021/22 (Figure 10 A and B). Points are coloured according to bathymetry levels (m), highlighting the

relationship between the maximum depth reached and the depth available at the respective sites.

Individual S6 (Figure 11A) was the most distinct. This shark exhibited both the greatest maximum depth (1,168 m) and the highest mean depth (338 m), as well as recording the lowest mean minimum temperature (10.3 °C). These values indicate that this individual dives deeper and accesses colder waters, suggesting a more oceanic and exploratory behaviour. Individual S5 (Figure A3 E), also stood out for its considerable depths, reaching maximum values of up to 1,056 m, closely following S6. Individual S4 (Figure A3 D), exhibited a similar pattern, attaining nearly 1,000 m in maximum depth, albeit at slightly higher temperatures.

By contrast, individual S10 (Figure 11B) was remarkable for a different reason, displaying an extremely high bathymetry (4,366 m), reflecting its presence over a very deep oceanic region. Moreover, it recorded the highest mean maximum temperature (24.4 °C), suggesting that it spends more time in shallower, warmer waters, despite having access to deeper zones.

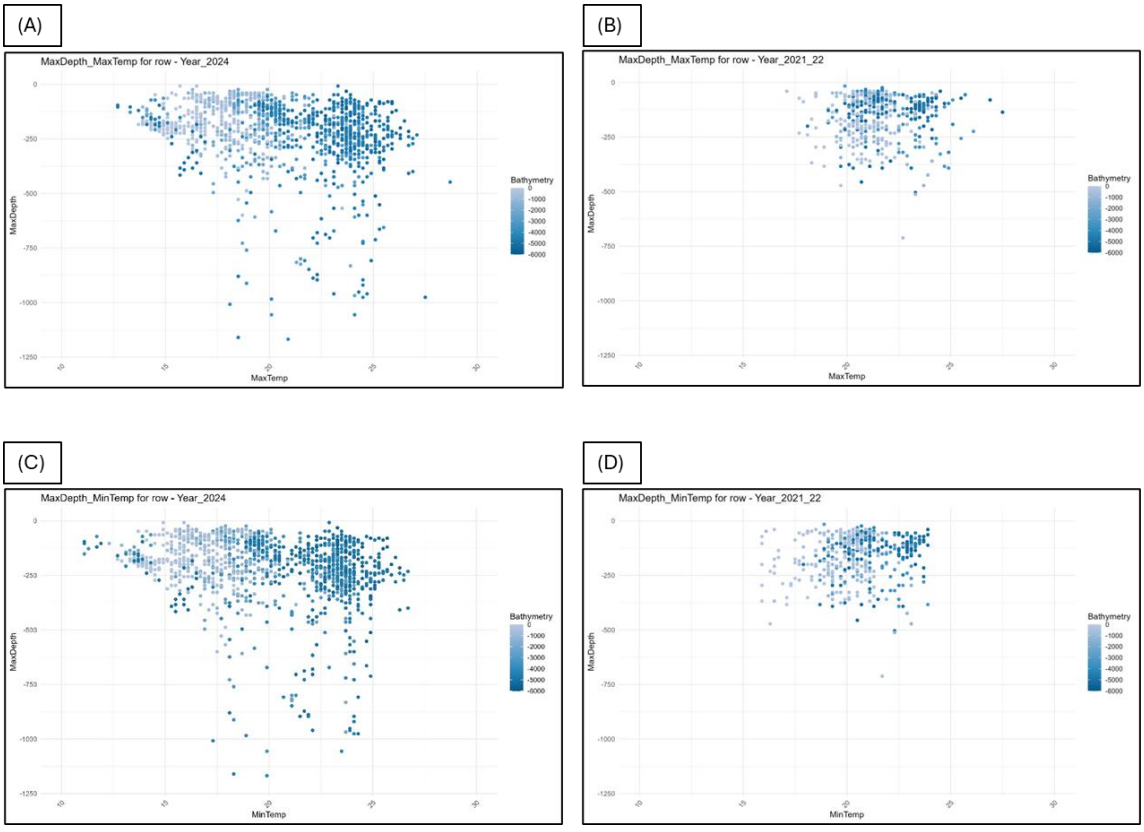

Figure 10: Daily variation in maximum recorded depth (MaxDepth) for individuals tagged in 2024 (C and D) and individuals tagged in 2021/22 (A and B). The points are coloured according to the bathymetry levels (m), illustrating the relationship between the maximum depth reached and the depth available at the site.

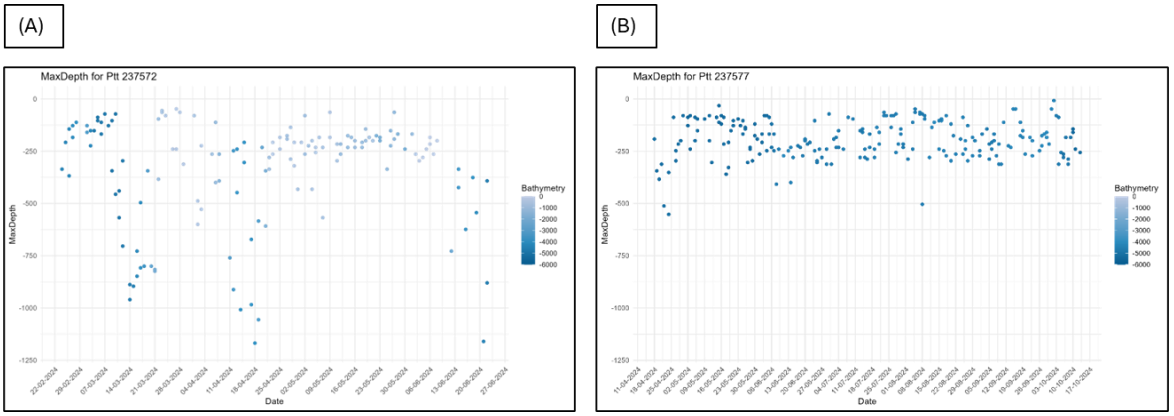

Figure 11: Relationship between maximum depth and maximum (MaxTemp) and minimum (MinTemp) temperature for ID S6 (A) and S10 (B). Points are coloured according to local bathymetry at the time of recording.

3.8 Relationship between Thermal Gradient and Maximum Diving Depth

The analysis of maximum dive depths of shortfin mako sharks revealed that most dives occurred in relatively shallow waters, with the highest concentration within the 200–400 m range (46.3%), followed by the 0–200 m range (43.8%). Together, these two depth intervals accounted for approximately 90% of all recorded dives, highlighting the predominant use of the upper layers of the water column by this species.

Deep dives were comparatively rare. Approximately 5.4% occurred between 400 and 600 m, 2.2% between 800 and 1000 m, and only 0.5% exceeded 1000 m (six cases in total). All these deeper dives occurred under conditions of reduced thermal

gradient (<0.1). The frequency of dives deeper than 600 m decreased markedly with increasing thermal gradient, representing only 0.47% of dives in gradients ≥0.1 compared with 5.1% in gradients <0.1 (Figure 12A). These results reinforce the predominance of shallow-water activity and suggest that steep thermal gradients may constrain dive depth, possibly due to physiological limitations or reduced prey availability in colder waters. This trend of decreasing maximum dive depth with increasing thermal gradient was confirmed by the Gamma regression model (log-link), which yielded a coefficient of –1.55 ($p < 0.01$). The result indicates a significant negative relationship between the two variables, albeit with a moderate effect size.

Analysis of the thermal gradient values associated with the deepest dives revealed similar mean conditions between the two sampling years. In 2021/2022, the mean gradient was 0.0649 (range: 0.011–0.151), with individual values ranging from S3 (0.0457) to S2 (0.0789). In 2024, the mean value was 0.0656 (range: 0.006–0.167), with the highest gradient recorded for S10 (0.115) and the lowest for S9 (0.0429). These findings suggest a stable vertical thermal structure between years, with no substantial interannual differences in the intensity of the thermocline experienced by the sharks.

Given this overall pattern, an additional analysis was conducted to assess whether bathymetry influenced the relationship between thermal gradient and maximum dive depth. The relationship was examined under two distinct contexts: oceanic environments (depths >200 m) and coastal regions with bathymetry <200 m.

In oceanic waters (Figure 12B), thermal gradients ranged from 0.006 to 0.167, while maximum dive depths varied between 5 and 1168 m (mean = 191 m; median = 160 m). Dive distribution indicated a clear predominance of shallow and mid-depth ranges, with 529 dives between 0–200 m and 574 between 200–400 m. Deep dives were infrequent, with 68 recorded between 400–600 m, 23 between 600–800 m, 28 between 800–1000 m, and only 6 exceeding 1000 m. These very deep dives occurred under reduced thermal gradients (0.018–0.048; mean = 0.032). Spearman's rank correlation analysis indicated a positive but weak association between thermal gradient and maximum depth ($p < 0.001$). These results suggest that, despite wide

variation in thermal gradients, dive depth is primarily determined by other environmental or biological factors rather than by thermal stratification alone.

In coastal regions (<200 m bathymetry) (Figure 12C), thermal gradients ranged from 0.018 to 0.123, while maximum dive depths varied between 8 and 476 m (mean = 173 m; median = 176 m). Dives were strongly concentrated in shallower depth classes, with 34 dives recorded between 0–200 m and 21 between 200–400 m. In this context, the correlation between thermal gradient and maximum dive depth was not statistically significant ($p > 0.01$).

A direct comparison between the two bathymetric contexts revealed significant differences in thermal gradients (Wilcoxon test, $p < 0.001$), whereas maximum dive depths did not differ significantly ($p > 0.1$). These results indicate that, although thermal gradients vary between oceanic and coastal zones, this variability is not consistently reflected in the maximum dive depths reached by individual sharks.

Linear models fitted separately for each context revealed distinct temporal patterns. In oceanic waters (>200 m), a significant annual effect was observed ($\beta = 82.55$; $p = 0.001$), whereas the thermal gradient and its interaction with year showed no significant influence ($p > 0.1$), explaining only ~2% of the variance ($R^2 = 0.022$). In contrast, in coastal regions (<200 m), year had a significant negative effect on maximum dive depth ($\beta = –151.89$; $p = 0.01$), while both the thermal gradient and the year × gradient interaction remained non-significant. The explanatory power was higher in this context ($R^2 = 0.366$).

To assess whether the overall relationship observed under oceanic conditions might have been disproportionately influenced by a single individual, an additional analysis was conducted. When all individuals were included, the linear model revealed a significant negative relationship between thermal gradient and maximum dive depth ($\beta = –389.8$; $p > 0.001$). However, after excluding individual S10, this relationship was no longer statistically significant ($\beta = –245.2$; $p > 0.1$). This result indicates that the significance of the thermal gradient effect was largely driven by that individual, highlighting its distinctive behavioural contribution within the dataset.

Overall, the behavioural pattern of shortfin mako sharks was consistent across years and bathymetric contexts, characterised by a predominance of shallow dives (0–400 m) and a limitation of deep dives under conditions of pronounced thermal stratification. Individual S10 displayed atypical behaviour, accounting for much of the detected statistical effect, whereas S3 and S2 showed lower thermal gradients and more stable diving patterns.

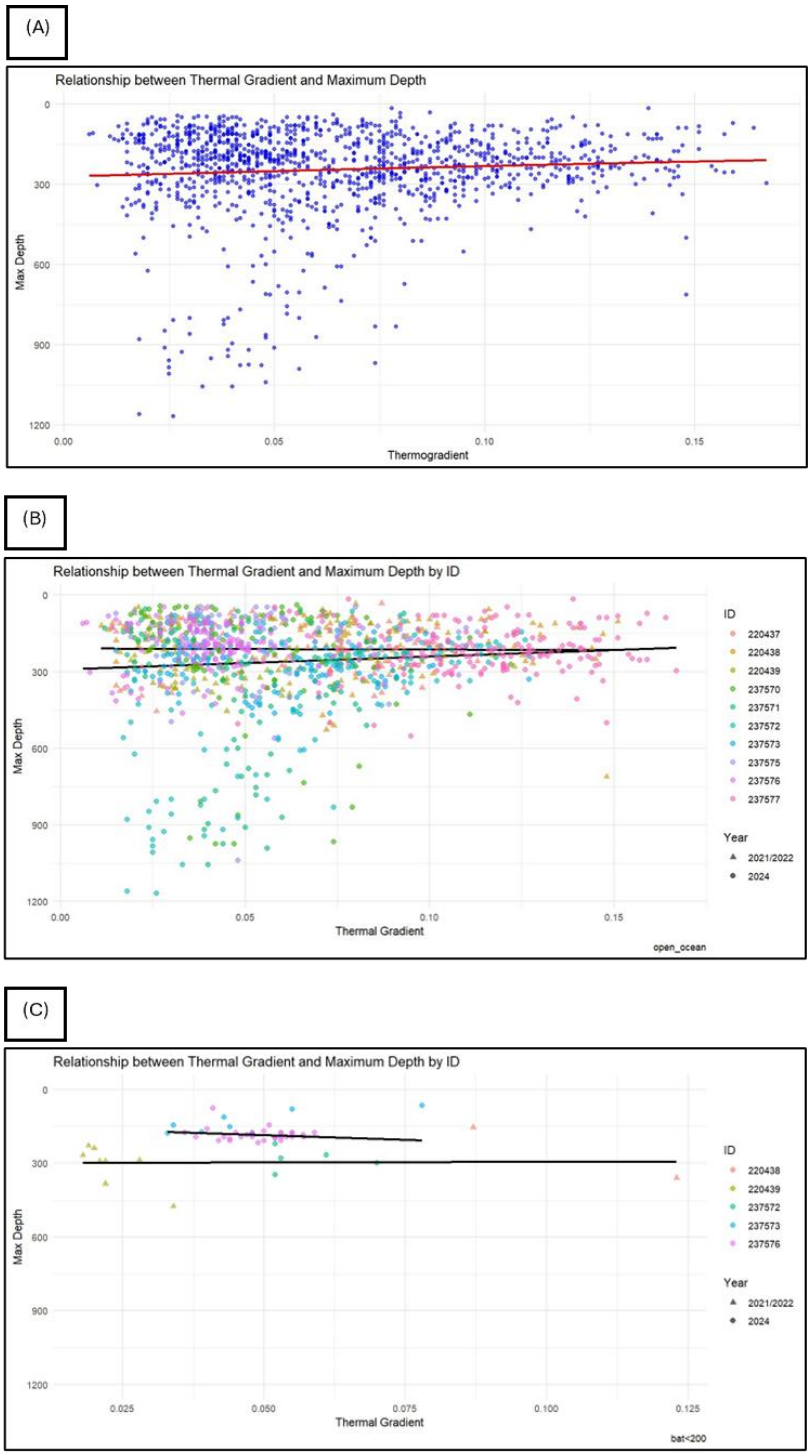

Figure 12: Relationship between thermal gradient and maximum diving depth of tagged mako sharks: (A) all dives combined (open-ocean and <200 m bathymetry), (B) dives in open-ocean environments, and (C) dives in regions with bathymetry <200 m. Each point represents an individual dive (triangles: 2021/22; circles: 2024).

3.9 Influence of Environmental Variables on Maximum Daily Depth

The analysis of environmental factors revealed distinct patterns in how they influence the maximum diving depth of sharks. Overall, the mean maximum depth recorded remained at 258.5 ± 180.5 m, with values ranging between 32 m and 1168 m, regardless of the environmental parameter considered. For each variable (chlorophyll concentration, dissolved oxygen, temperature, thermocline gradient and onset depth, and lunar illumination), generalised linear models (GLMs) were fitted and complemented with descriptive statistics to characterise the observed variation.

For chlorophyll, surface concentrations (0 m) averaged 0.30 ± 0.25 $\mu g \cdot L^{-1}$ (min = 0.05; max = 1.57), with the highest concentration recorded in individual S4 (1.57 $\mu g \cdot L^{-1}$, maximum depth 43 m) and the lowest in S3 (0.046 $\mu g \cdot L^{-1}$, maximum depth 120 m). The model revealed a significant negative relationship between chlorophyll and maximum depth (coefficient = –119.84; $p < 0.001$), suggesting that increases in chlorophyll are associated with shallower dives (Figure 13A). At 100 m, the mean concentration was lower (0.20 ± 0.09 $\mu g \cdot L^{-1}$, range 0.02–0.45), varying from 0.448 $\mu g \cdot L^{-1}$ (individual S2, maximum depth 104 m) to 0.023 $\mu g \cdot L^{-1}$ (individual S9, maximum depth 208 m). The model showed a significant positive relationship (coefficient = 359.09; $p < 0.001$), indicating that higher chlorophyll concentrations at this depth are linked to deeper dives (Figure 13B).

Regarding dissolved oxygen, surface concentrations (Figure 13C) averaged 5.16 ± 0.24 $mg \cdot L^{-1}$ (range 4.60–5.95), with the maximum recorded in individual S4 (5.95 $mg \cdot L^{-1}$, maximum depth 43 m) and the minimum in S10 (4.60 $mg \cdot L^{-1}$, maximum depth 232 m). The model revealed a significant negative relationship (coefficient = –141.88; $p < 0.001$), indicating that higher oxygen values are associated with shallower dives. At 100 m (Figure 13D), the mean concentration was 4.12 ± 1.28 $mg \cdot L^{-1}$ (range 0.20–5.83), with the maximum observed in S9 (5.83 $mg \cdot L^{-1}$, maximum depth 416 m) and the minimum in S3 (0.20 $mg \cdot L^{-1}$, maximum depth 239.5 m). A

significant positive relationship was observed between oxygen and maximum depth (coefficient = 36.95; $p < 0.001$).

For temperature, the mean at the surface was 20.6 ± 2.5 °C (range 14.5–25.6), ranging from 25.6 °C (individual S10, maximum depth 232 m) to 14.5 °C (S8, maximum depth 79.75 m). The model indicated a significant positive relationship (coefficient = 12.85; $p < 0.001$) (Figure 13E). At 100 m (Figure 13F), the mean temperature was lower (15.7 ± 1.7 °C, range 11.5–19.7), with extremes recorded in S3 (19.7 °C, maximum depth 112 m) and S7 (11.5 °C, maximum depth 79.75 m). A significant positive association with maximum depth was also observed (coefficient = 23.77; $p < 0.001$).

With respect to the thermal gradient (Figure 13G), a mean of 0.063 ± 0.030 °C·m^{-1} (range 0.01–0.16) was recorded, with extremes of 0.159 °C·m^{-1} (S10, maximum depth 71.75 m) and 0.011 °C·m^{-1} (S3, maximum depth 120 m). The model revealed a significant negative relationship between thermal gradient and maximum depth (coefficient = –693.75; $p = 0.004$). Dives deeper than 700 m were not observed when the gradient exceeded 0.08 °C·m^{-1}, highlighting the importance of thermal stability in the water column for deep-diving behaviour.

For the depth of thermocline onset (Figure 13 H), mean values were 35.5 ± 18.8 m (range 5–149), with maximum thermocline depths of 149 m recorded in individuals S6 (maximum dive depth 376 m) and S9 (384 m), and a minimum of 5 m in S4 (maximum depth 66.5 m). A significant positive relationship was found with maximum dive depth (coefficient = 2.75; $p < 0.001$), indicating that deeper thermoclines are associated with correspondingly deeper dives.

Finally, in the case of lunar illumination (Figure 13I), the mean illuminated fraction was 0.53 ± 0.35 (range 0.00–1.00), with the maximum close to full moon (0.999, individual S5, maximum depth 104 m) and minima of 0.00022 recorded in the same individual (maximum depth 233.5 m) and in S8 (maximum depth 48 m). The model did not reveal a statistically significant relationship (coefficient = –14.10; $p = 0.51$). The observed trend remained virtually stable, suggesting that moon phase does not exert a relevant influence on daily vertical behaviour.

(A)

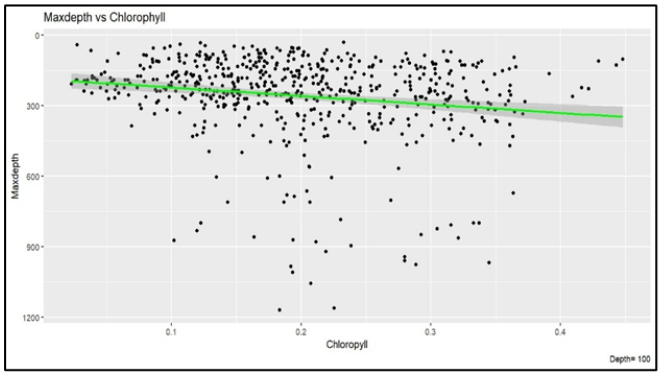
Maxdepth vs Chlorophyll
Maxdepth
Chloropyll
Depth= 100

(B)

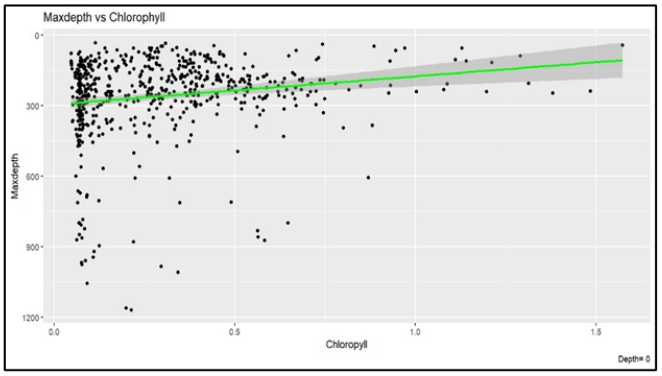
Maxdepth vs Chlorophyll
Maxdepth
Chloropyll
Depth= 0

(C)

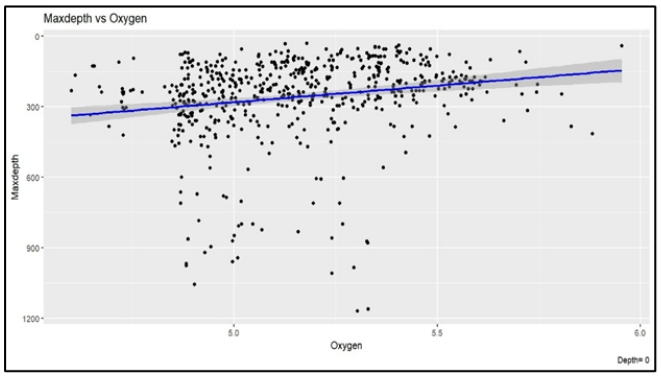
Maxdepth vs Oxygen
Maxdepth
Oxygen
Depth= 0

(D)

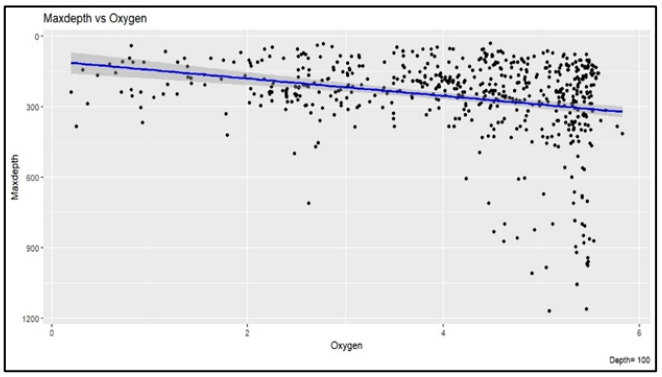
Maxdepth vs Oxygen
Maxdepth
Oxygen
Depth= 100

(E)

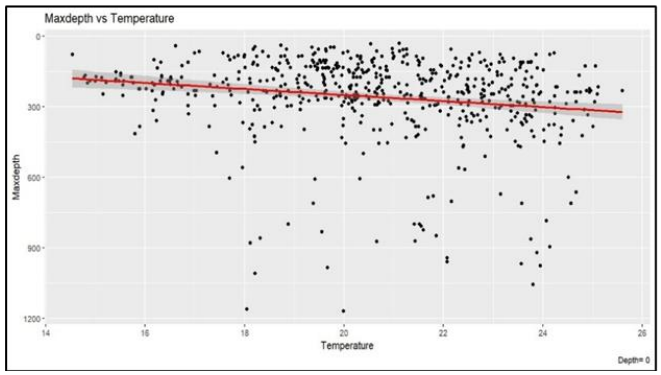
Maxdepth vs Temperature
Maxdepth
Temperature
Depth= 0

(F)

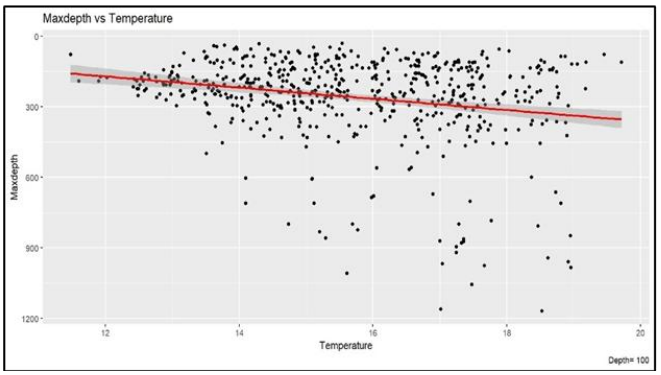
Maxdepth vs Temperature
Maxdepth
Temperature
Depth= 100

(G)

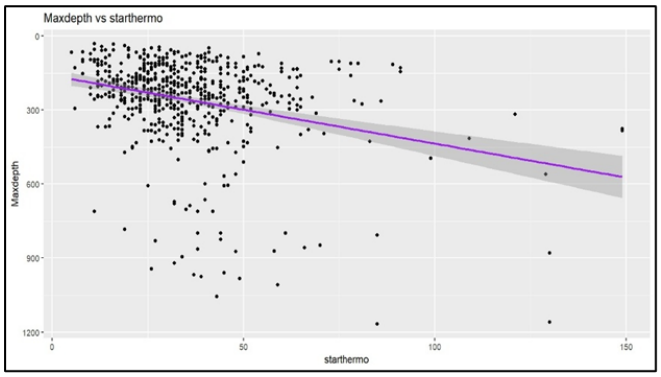
Maxdepth vs starthermo
Maxdepth
starthermo

(H)

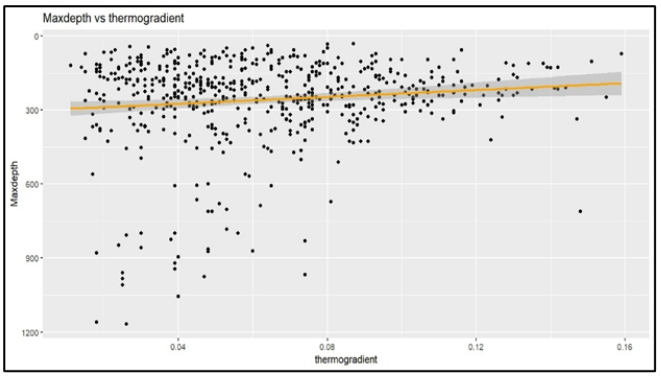
Maxdepth vs thermogradient
Maxdepth
thermogradient

(I)

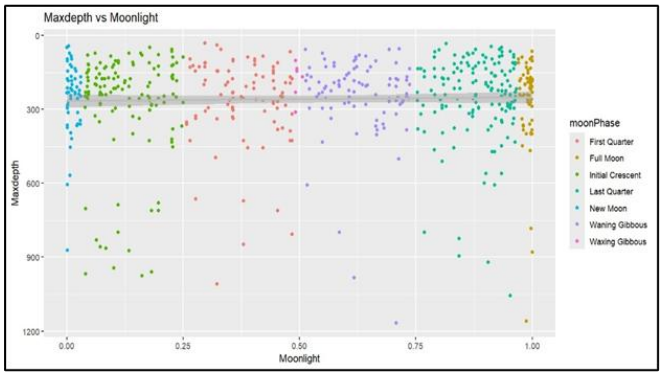

Figure 13: Relationships between maximum diving depth and environmental variables: (A, B) chlorophyll concentration at the surface and at 100 m depth; (C, D) dissolved oxygen at the surface and at 100 m depth; (E, F) temperature at the surface and at 100 m depth; (G) thermal gradient; (H) depth of the thermocline onset; (I) lunar phase (percentage of illumination).

3.10 Time Distribution by Depth Interval during Day and Night

The records of ten individuals were analysed over 154 distinct weeks, considering only those with more than 60% data availability per individual, resulting in a total of 78 valid weeks. Overall, occupancy was concentrated between 0 and 100 m depth, with a predominant use of the surface layer (0–10 m) both during the day (33.1%) and at night (31.7%). Collectively, individuals exhibited a consistent pattern, characterized by a higher frequency of deeper occupancy during daytime periods (Figure 14).

However, six individuals displayed atypical behaviours, expressed as occasional nocturnal displacements to depths exceeding 200–250 m, in some cases reaching 700–800 m. Although infrequent and representing a low percentage of overall activity, these episodes constitute notable deviations from the predominant pattern observed across most individuals.

None of the individuals exhibited nocturnal predominance at depths greater than 150–200 m. However, detailed analysis revealed that several individuals reached depths exceeding 200 m during the night, which is not typical behaviour, namely Individual S4 (Figure A7), S5 (Figure 15A and 15B; Figure A8) and S6 (Figure 16A, 16B and 16C; Figure A9). Less frequent occurrences at depth were observed in individuals S7 (Figure A10), S8 (Figure A11) and S10 (Figure A13).

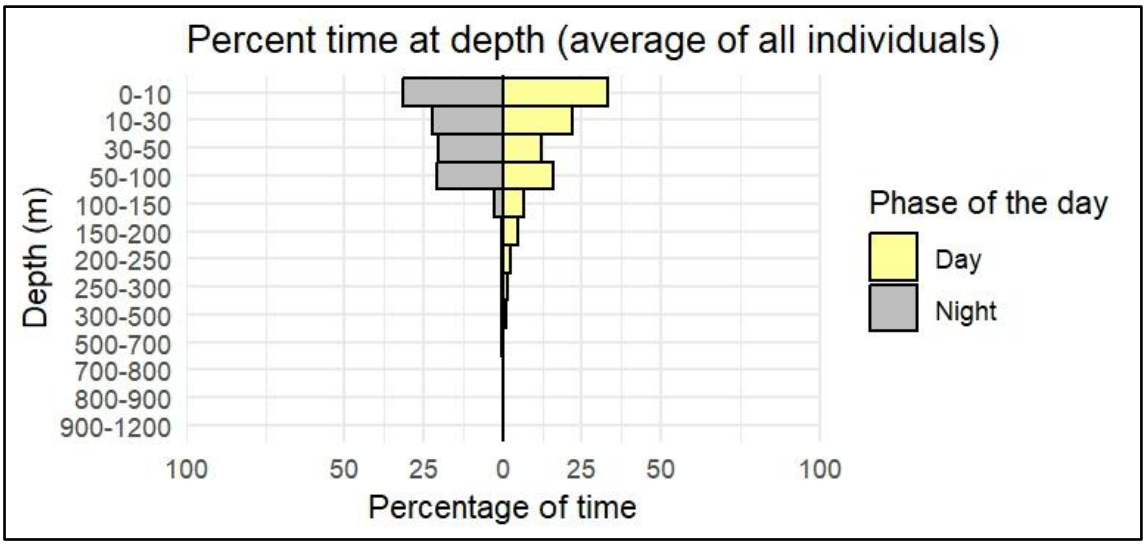

Figure 14: Distribution of the percentage of time spent by individuals across different depth intervals.

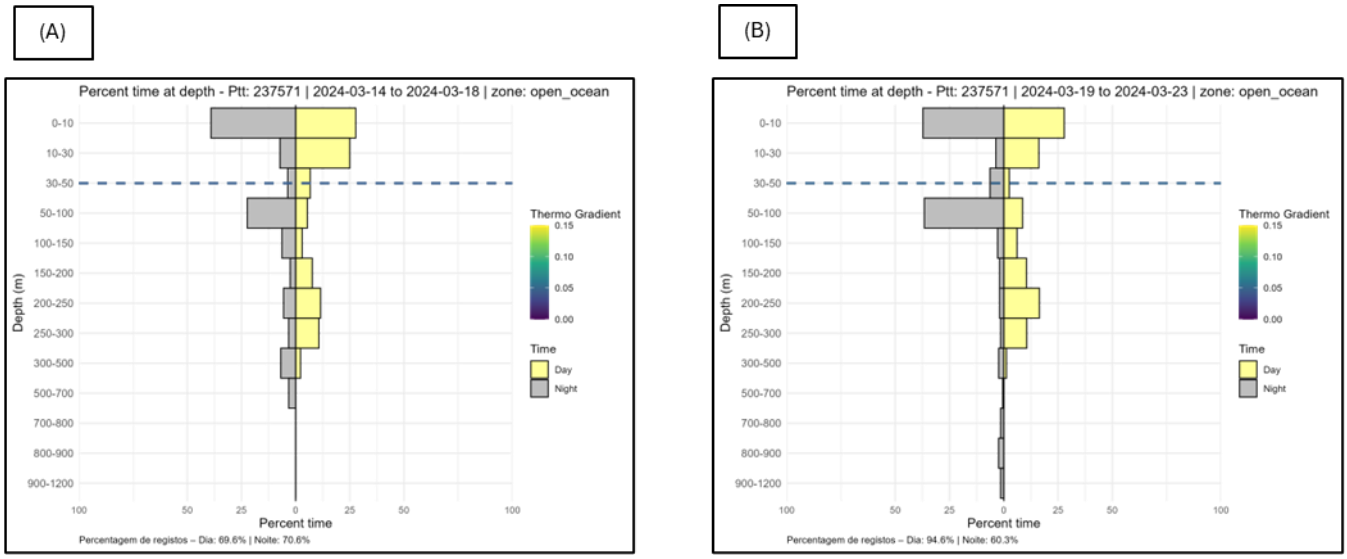

Figure 15: Distribution of daytime and nighttime occurrence percentages by depth stratum for individual S5 during weeks 5 (A) and 6 (B).

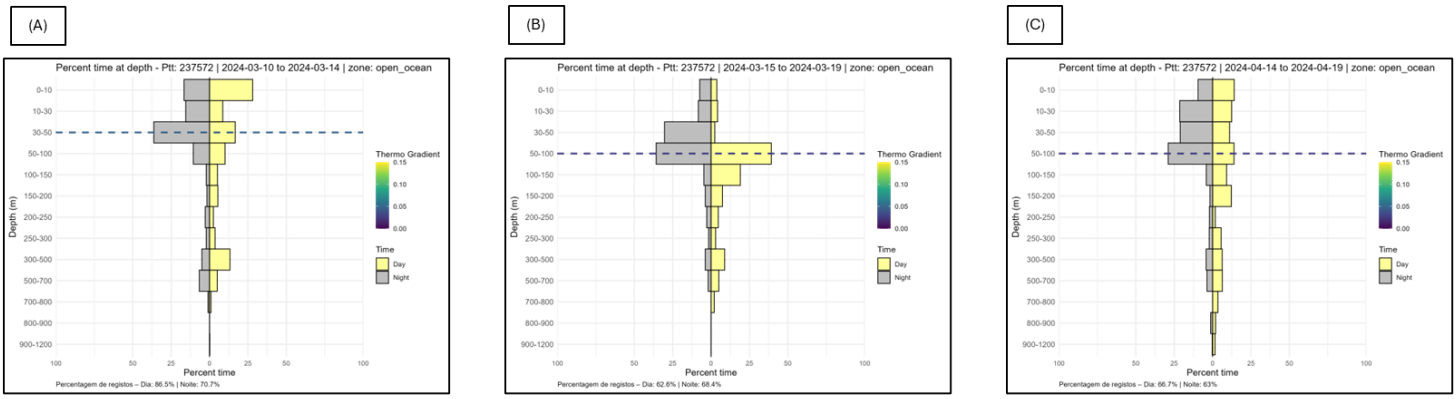

Figure 16: Distribution of daytime and nighttime occurrence percentages by depth stratum for individual S6 during weeks 4 (A) 5 (B) and 9 (C).

3.11 Analyses of Time Above the Thermocline

Observation of the trajectories of the IDs (Figure 17), coloured according to the time spent above the thermocline, shows that individuals spent more time above the thermocline between latitudes –20° and –30°, particularly in coastal areas. Extended periods above the thermocline were also observed in areas farther north.

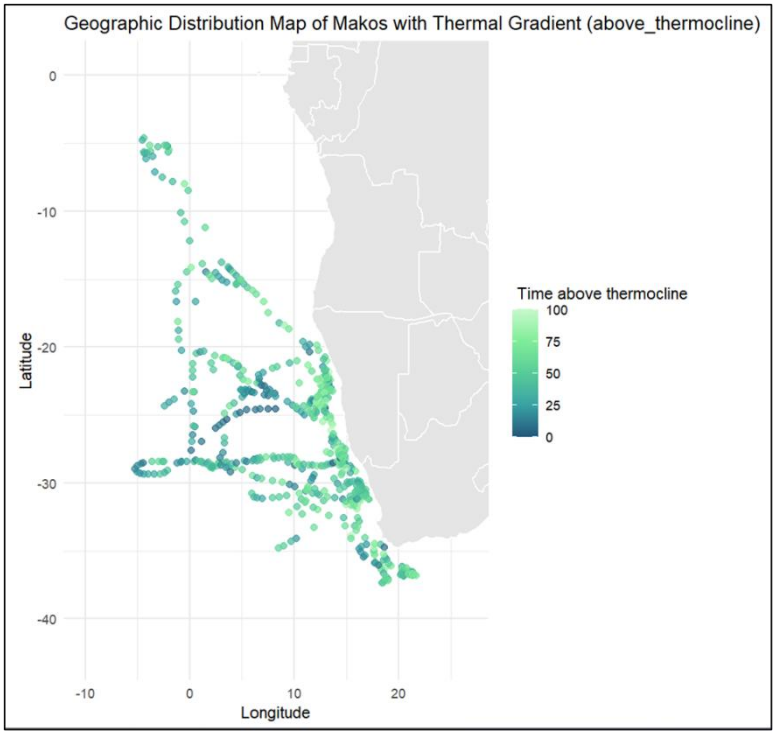

Figure 17: Spatial distribution of time spent above the thermocline, based on the trajectories of tagged individuals. The colour scale represents the percentage of time spent above the thermocline along individual trajectories.

The relationship between the thermal gradient and the time spent above the thermocline showed no significant association in either open-ocean environments or coastal areas with bathymetry shallower than 200 m, In the open ocean (Figure 18A), a total of 212 valid observations were obtained, with thermal gradient values ranging from 0.01 to 0.15 °C m^{-1} (mean = 0.06 ± 0.03 °C m^{-1}, SD). The simple linear model did not identify a statistically significant relationship between the thermal gradient and the time spent above the thermocline ($\beta = 16.2 \pm 53.5$; $p > 0.1$), and the

explained variance was negligible (adjusted R^2 = −0.004). The data exhibited high dispersion, with substantial inter-individual variability in vertical distribution regardless of gradient intensity.

In areas with bathymetry <200 m (Figure 18 B), only three valid observations were available. Thermal gradient values ranged from 0.02 to 0.12 °C m^{-1} (mean = 0.04 ± 0.04 °C m^{-1}). The corresponding linear model also revealed no significant association between thermal gradient and time above the thermocline (β = 3044.9 ± 3330.9; p > 0.1), and the adjusted R^2 value was negative (−0.090), reflecting both the extremely limited sample size and the lack of explanatory power of the model.

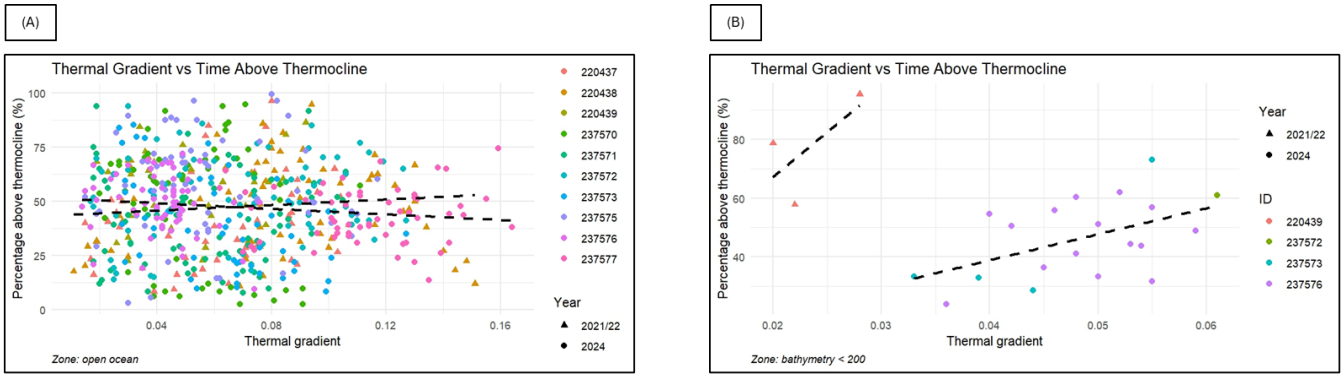

Figure 18: Relationship between the percentage of time spent above the thermocline and the thermal gradient. (A) Data from the open ocean. (B) Data from coastal areas with bathymetry <200 m. Linear regressions with confidence intervals are shown.

The relationship between the depth of thermocline onset and the time spent above it showed more consistent trends. In the open ocean (Figure 19A), the depth of thermocline onset varied between 5 and 81 m (mean = 26.1 ± 10.5 m). The univariate model identified a significant positive association (β = 0.39 ± 0.15; p < 0.01), indicating that a deeper thermocline onset was generally linked to a longer time spent above it. However, the explained variance remained low (adjusted R^2 = 0.028). A dense cluster of points was observed for thermocline depths between 0 and 40 m, reflecting substantial variability under these conditions.

In the bathymetry <200 m dataset (Figure 19B), comprising only three valid observations, the onset depth ranged from 24 to 42 m (mean = 35 ± 9.6 m). The model suggested a positive slope (β = 1.86 ± 0.58), but the effect was not statistically significant ($p > 0.1$), likely due to the small sample size. These results indicate that, while a positive relationship may exist, it cannot be robustly confirmed in the limited coastal dataset.

When both predictors, the depth of thermocline onset and the thermal gradient, were included in a multiple regression model for the open ocean (Figure 19C), the thermal gradient did not show a significant effect (β = 43.25 ± 53.57; $p > 0.1$), whereas the depth of thermocline onset remained positively associated with time spent above the thermocline (β = 0.42 ± 0.15; $p < 0.01$). The explanatory power of the model remained low (adjusted $R^2 = 0.027$), indicating that these environmental variables together explained only a small fraction of the observed variability. In the coastal dataset (Figure 19D), the regression including both predictors could not be reliably evaluated due to the very small sample size (n = 3). The model output indicated a perfect fit ($R^2 = 1$), but the parameter estimates were statistically unreliable, with undefined p-values.

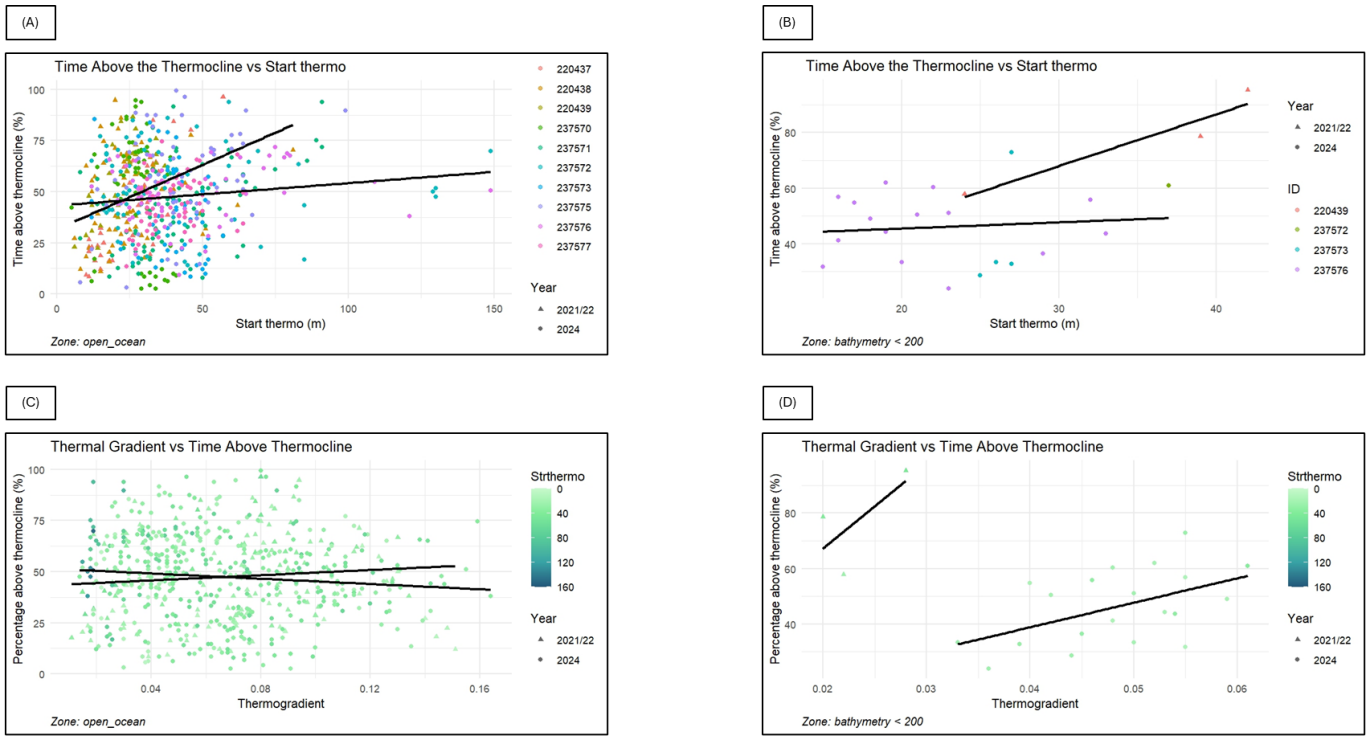

Figure 19: Scatterplots of time above the thermocline versus initial thermocline depth and thermal gradient. (A) Open ocean. (B) Coastal areas <200 m; (C) Thermal gradient, points colour-coded by thermocline onset depth in the open ocean; (D) Thermal gradient, points colour-coded by thermocline onset depth in areas <200 m.

Surface temperature also showed a clear influence on the time spent above the thermocline. In the open ocean (Figure 20A), surface temperature ranged from 16.4 °C to 24.5 °C (mean = 21.1 ± 1.92 °C, SD). The simple linear model revealed a significant negative association (β = −3.85 ± 0.81; t = −4.76; p < 0.001), indicating that higher surface temperatures were linked to reduced time spent above the thermocline. When the thermal gradient was added to the model (Figures 20C), both predictors remained significant. Surface temperature retained a strong negative effect (β = −4.91 ± 0.89; t = −5.54; p < 0.001), while the thermal gradient exhibited a significant positive effect (β = 151.7 ± 55.7; p <0.01). The combined model explained slightly more variance (adjusted R^2 = 0.120), although the coexistence of opposite effects suggests possible collinearity or suppression between predictors.

In the coastal dataset (bathymetry <200 m), the relationship between surface temperature and time above the thermocline was not statistically significant (β = 19.8 ± 13.4; p >0.1), despite a relatively high R^2 (0.685) (Figure 20D). The recorded temperatures ranged from 18.7 °C to 21.4 °C (mean = 19.9 ± 0.95 °C, SD). However, given the extremely limited sample size these results should be interpreted with caution.

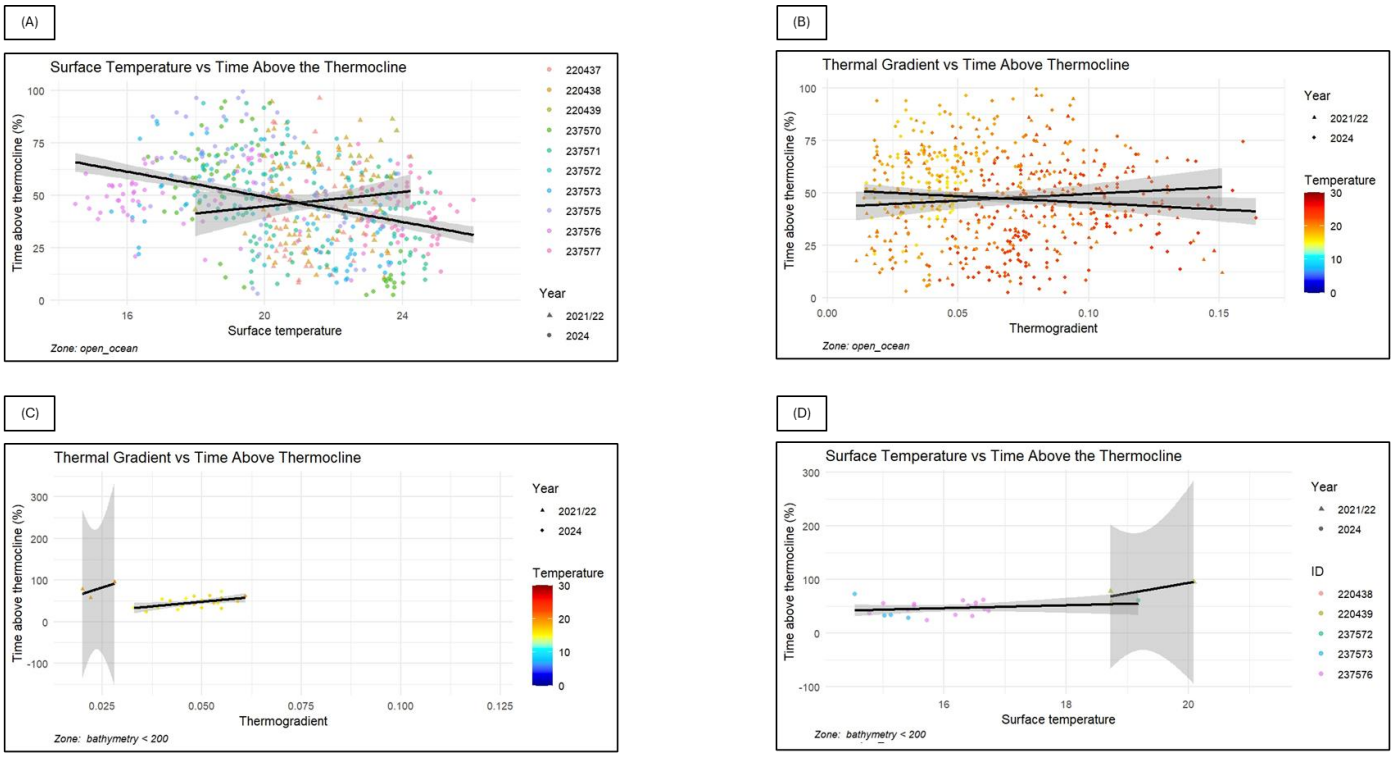

Figure 20: (A) Percentage of time spent above the thermocline in relation to surface water temperature, with fitted regression line; (B) bathymetry <200 m; (C) Open-ocean data showing the relationship between time above the thermocline, surface temperature (colour scale), and thermal gradient. (D) bathymetry <200 m data showing the relationship between time above the thermocline and surface temperature and thermal gradient.

3.11.1 Influence of environmental variables on time spent above the thermocline on daytime and nighttime vertical distribution

The physico-chemical characterisation of the water column provided a description of the predominant environmental patterns at the surface (0 m) and at depth (100 m), as well as the intensity of thermal stratification and the influence of external factors such as moonlight. For each variable analysed (dissolved oxygen, chlorophyll, temperature, thermal gradient, and lunar illumination), minimum, maximum, and mean values were calculated, together with the most frequent intervals (modes) and the mean percentage of time spent above the thermocline associated with each interval. This approach enabled the vertical distribution to be related to the most representative environmental conditions, both during daytime and night-time periods.

3.11.1.1 Oxygen

At the surface (Figure 21A), dissolved oxygen values ranged from 4.63 to 5.76 mg L^{-1} (mean = 5.18 mg L^{-1}), with low variability indicating relatively stable conditions. The most frequent interval was 5–5.2 mg L^{-1}, associated with a mean percentage of time above the thermocline of 71.4% during the day and 79.3% at night. At 100 m depth, oxygen concentrations were lower and more heterogeneous (0.66–5.61 mg L^{-1}; mean = 4.07 mg L^{-1}). The modal interval was 5–5.5 mg L^{-1}, with mean percentages of time above the thermocline of 53.1% during the day and 58.1% at night (Figure 21B).

Behavioural analysis revealed a negative relationship between oxygen and time spent above the thermocline at 100 m, particularly during the day. In contrast, at the surface, the trend was positive, with higher oxygen concentrations associated with greater presence above the thermocline, especially at night.

3.11.1.2 Chlorophyll

At the surface, chlorophyll values ranged from 0.046 to 1.17 µg L^{-1} (mean = µg L^{-1}), with the most frequent interval being 0–0.2 µg L^{-1}, associated with mean percentages of 53.8% during the day and 60.4% at night (Figure 21C). At 100 m (Figure 21D), values were lower and more stable (0.032–0.42 µg L^{-1}, mean = 0.19 µg

L^{-1}). The modal interval was 0.15–0.2 µg L^{-1}, associated with higher mean percentages of time above the thermocline (77.9% during the day and 82% at night).

At 100 m, higher chlorophyll concentrations were negatively related to time above the thermocline, with this trend being more pronounced during the day. At the surface, however, the trend was positive: higher chlorophyll concentrations were associated with longer periods above the thermocline. Nevertheless, a wide scatter of points was observed at concentrations between 0.0 and 0.5 µg L^{-1} both day and night.

3.11.1.3 Temperature

At the surface (Figure 21E), temperature ranged from 14.7 to 25.1 ºC (mean = 20.5 ºC), with the most frequent interval of 20–21 ºC, associated with 71.9% above the thermocline during the day and 79.6% at night. At 100 m, values ranged from 11.8 to 18.9 ºC (mean = 15.5 ºC), with the modal interval of 14–15 ºC, associated with 71.6% of time above the thermocline during the day and 78.4% at night (Figure 21F).

Behavioural analysis indicated a predominantly negative trend between temperature and time above the thermocline at both depths. At the surface the individuals tended to remain above the thermocline at lower surface temperatures. At 100 m, higher temperatures were also linked to shorter time above the thermocline, with the trend being somewhat stronger during the day. In both cases, substantial scatter in the data suggests a variable response of individuals to thermal conditions.

3.11.1.4 Thermal Gradient

The mean gradient ranged (Figure 21G) from 0.016 to 0.14 ºC m^{-1} (median = 0.056 ºC m^{-1}), with the modal interval of 0.04–0.06 ºC m^{-1} associated with mean percentages of 65.2% during the day and 76.1% at night. When examined in relation to vertical behaviour, the gradient showed a negative relationship with time spent above the thermocline during both day and night. As stratification intensity increased, individuals tended to remain below the thermocline, with this trend slightly more pronounced at night.

3.11.1.5 Lunar illumination

The illuminated fraction of the moon (Figure 21H) ranged from 0.03 to 0.98 (mean = 0.50), with the most frequent interval being 0.9–1 (full or nearly full moon). This range was associated with 64.9% of time above the thermocline during the day and 72.7% at night. Behavioural analysis confirmed that lunar illumination influenced only the nocturnal phase, showing a subtle negative trend: higher moonlight intensity coincided with shorter time above the thermocline. As expected, no direct relationship was observed during the day.

(A)

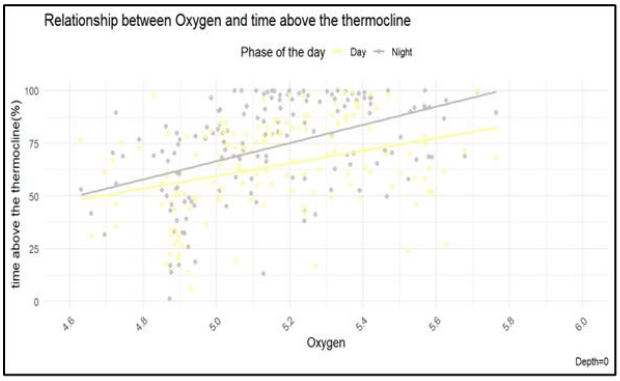
Relationship between Oxygen and time above the thermocline
Phase of the day Day Night
time above the thermocline(%)
Oxygen
Depth=0

(B)

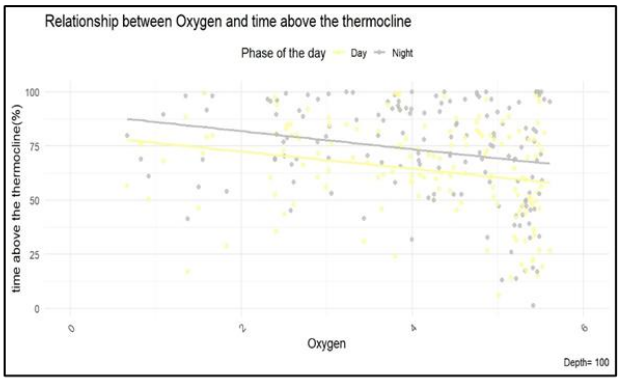
Relationship between Oxygen and time above the thermocline
Phase of the day Day Night
time above the thermocline(%)
Oxygen
Depth= 100

(C)

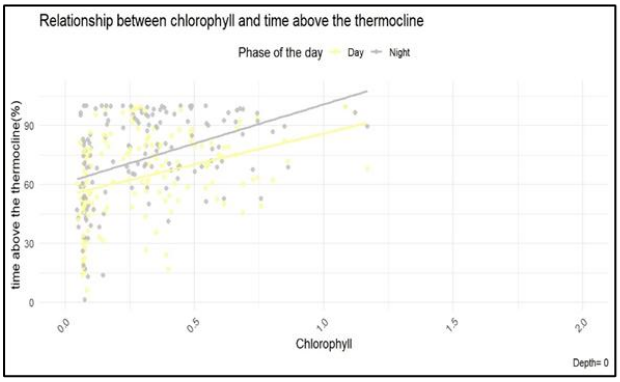
Relationship between chlorophyll and time above the thermocline
Phase of the day Day Night
time above the thermocline(%)
Chlorophyll
Depth= 0

(D)

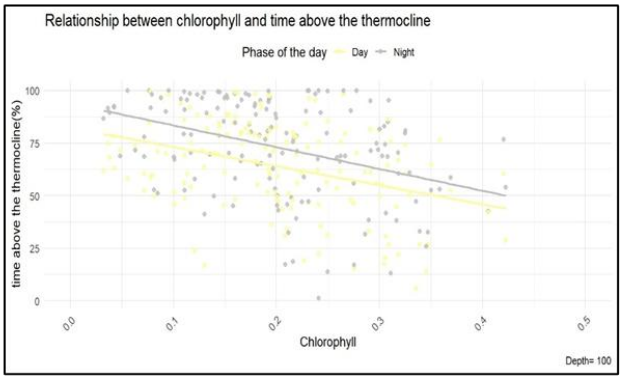
Relationship between chlorophyll and time above the thermocline
Phase of the day Day Night
time above the thermocline(%)
Chlorophyll
Depth= 100

(E)

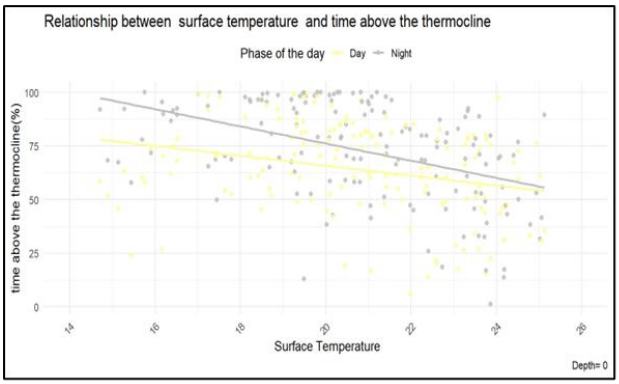
Relationship between surface temperature and time above the thermocline
Phase of the day Day Night
time above the thermocline(%)
Surface Temperature
Depth= 0

(F)

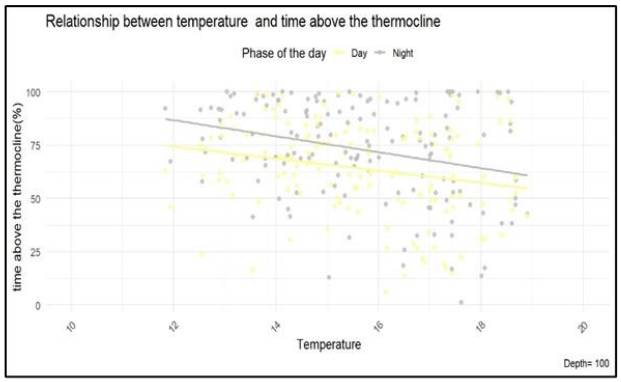
Relationship between temperature and time above the thermocline
Phase of the day Day Night
time above the thermocline(%)
Temperature
Depth= 100

(G)

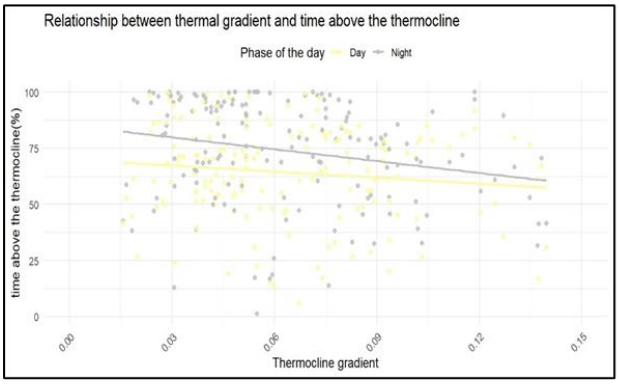
Relationship between thermal gradient and time above the thermocline
Phase of the day Day Night
time above the thermocline(%)
Thermocline gradient

(H)

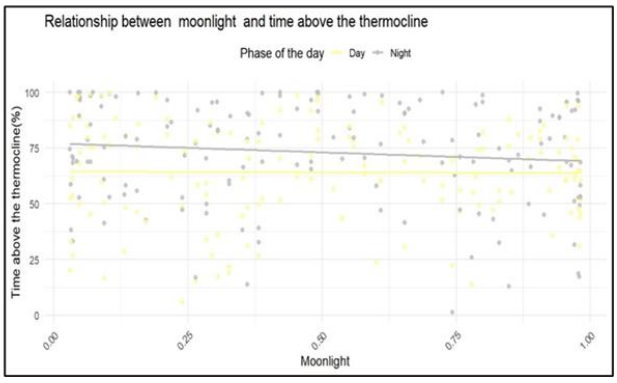
Relationship between moonlight and time above the thermocline
Phase of the day Day Night
Time above the thermocline(%)
Moonlight

Figure 21: Time spent above the thermocline in relation to environmental variables and the day/night period: (A, B) dissolved oxygen at the surface and at 100 m depth; (C, D) chlorophyll at 100 m depth and at the surface; (E, F) temperature at the surface and at 100 m depth; (G) thermal gradient of the thermocline; (H) lunar illumination.

3.11.2 Model Analyses

Generalized linear (GLM) and mixed (GLMM) models were adjusted to investigate the effects of environmental variables on the dependent variable (time spent above the thermocline). Effect plots present the relationship between each predictor and the response variable, based on the best models selected for the day and night periods.

A total of N = 296 observations from 10 individuals were analysed, with a mean of 29.6 ± 7.11 observations per individual (range 16–38). Observations were evenly distributed between day and night periods (148 each). During the daytime, individuals spent a mean proportion of 0.639 of their time above the thermocline (SD = 0.223; median = 0.656). At night, the mean proportion increased to 0.727 (SD = 0.231; median = 0.768).

For the nocturnal GLM, surface chlorophyll concentration had a significant positive effect on time spent above the thermocline (β = 2.528, p > 0.1), while thermocline onset depth exhibited a marginal positive effect (β = 0.031, p > 0.01). Oxygen concentration at 100 m showed a negative but non-significant effect (β = −0.170, p > 0.1). Model fit improved relative to the null model, with deviance decreasing from 43.641 to 31.542. Coefficients are reported in Table 2, and effect patterns are illustrated in Figure A 14C.

Table 2: Coefficients of the GLM for the nighttime period, relating time above thermocline to environmental variables (start thermocline, oxygen at 100 m depth, and chlorophyll at 0 m depth).

RESPONSE VARIABLE	PREDICTOR	ESTIMATE	STD. ERROR	Z VALUE	P-VALUE
TIME ABOVE THERMOCLINE	(Intercept)	-0.03478	0.96534	-0.036	0.9713
	Start thermocline	0.03078	0.01593	1.933	0.0532
	Oxygen at 100 m	-0.16985	0.18476	-0.919	0.3579
	chlorophyll at 0 m	2.52766	1.11259	2.272	0.0231

During daylight, the GLM incorporated mean thermal gradient, oxygen at 100 m, and surface chlorophyll. The mean thermal gradient had a negative but non-significant coefficient ($\beta = -3.886$, $p > 0.1$), oxygen at 100 m showed a non-significant negative effect ($\beta = -0.112$, $p > 0.1$), and surface chlorophyll retained a positive but non-significant association ($\beta = 1.112$, $p > 0.1$). The model produced a modest improvement over the null model (null deviance 34.858 → residual deviance 30.550). Model selection indicated that the best daytime GLM excluded thermocline onset depth and illuminated fraction, suggesting that thermal stratification and moonlight did not substantially improve explanatory power (Table 3).

Table 3: Coefficients of the GLM for the daytime period, relating time above thermocline to environmental variables (thermogradient, oxygen at 100 m depth, and chlorophyll at 0 m depth).

RESPONSE VARIABLE	PREDICTOR	ESTIMATE	STD. ERROR	Z VALUE	P-VALUE
TIME ABOVE THERMOCLINE	(Intercept)	0.9672	1.1431	0.846	0.397
	Thermogradient	-3.8864	6.4630	-0.601	0.548
	Oxygen at 100 m	-0.1118	0.1706	-0.655	0.512
	Chlorophyll at 0 m	1.1115	0.9233	1.204	0.229

Incorporating a random intercept for individual ID, the nocturnal GLMM (Laplace approximation) substantially improved model fit compared with the GLM, although a singular fit was observed, indicating near-zero variance for the random effect. Among fixed effects in nighttime, mean thermal stratification had a significant positive effect ($\beta = 0.0793$, $p < 0.01$), and surface chlorophyll showed a strong positive association ($\beta = 13.6009$, $p < 0.001$). Oxygen at 100 m remained non-significant ($p > 0.1$). Graphical inspection (Figure A14 B) revealed saturation patterns for thermal stratification (~40 units) and surface chlorophyll (~0.4 units), indicating thresholds beyond which further increases had diminishing effects. Oxygen at depth retained a negative relationship, with smoother and more stable predicted effects compared to the GLM. Coefficients are summarised in Table 4.

Table 4: Coefficients of the GLMM for the nighttime period, including random effect of ID and fixed effects (start thermocline, oxygen at 100 m depth, and chlorophyll at 0 m depth).

RESPONSE VARIABLE	PREDICTOR	ESTIMATE	STD. ERROR	Z VALUE	P-VALUE
TIME ABOVE THERMOCLINE	(Intercept)	-1.54587	1.75670	-0.880	0.3789
	Start thermocline	0.07930	0.02786	2.847	0.0044
	Oxygen at 100 m	-0.45204	0.29086	-1.554	0.1202
	Chlorophyll at 0 m	13.60088	3.84528	3.537	0.0004

The best daytime GLMM included illuminated fraction, oxygen at 100 m, and surface chlorophyll as fixed effects. Surface chlorophyll was significant (β = 2.736, $p > 0.01$), while illuminated fraction showed a marginal positive trend (β = 1.0499, $p > 0.05$), and oxygen at 100 m remained non-significant ($p > 0.1$). Effect plots (Figure A14 A) support these associations, with surface chlorophyll showing saturation at higher values and illuminated fraction indicating a potential positive influence on time spent near the surface. Coefficients are reported in Table 5.

Table 5: Coefficients of the GLMM for the daytime period, including random effect of ID and fixed effects (illuminatedFraction, at oxygen 100 m depth, and chlorophyll 0 m depth).

RESPONSE VARIABLE	PREDICTOR	ESTIMATE	STD. ERROR	Z VALUE	P-VALUE
TIME ABOVE THERMOCLINE	(Intercept)	0.8428	1.0753	0.784	0.4331
	IlluminatedFraction	1.0499	0.6324	1.660	0.0969
	Oxygen at 100 m	-0.2368	0.1978	-1.197	0.2313
	Chlorophyll at 0 m	2.7363	1.1969	2.286	0.0222

The analysis and visualization of the graphs of each model confirmed the analysed results. The results of the best GLM model fitted for the daytime period (Figure A 14D) indicate distinct patterns in the influence of environmental variables on the response variable. The analysis of partial effects revealed that the thermal gradient shows a slightly negative relationship with the time spent above the thermocline, suggesting that higher values of thermal stratification may be associated with a slight reduction in the response variable. Similarly, a negative effect of oxygen concentration at 100 metres depth was observed, indicating that higher oxygen levels in this layer are associated with lower values of time spent above the thermocline.

In contrast, mean surface chlorophyll exhibited a clearly positive effect, showing that higher levels of phytoplankton biomass are associated with an increase in the time spent above the thermocline. This pattern suggests that surface primary productivity may play an important role in explaining the variability of the response variable.

The results of the best-fitting GLM for the nocturnal period (A 14C) reveal clear patterns in the influence of environmental variables on the time spent above the thermocline.

The start thermocline variable exhibited a strongly positive and non-linear relationship, indicating that, as thermal stratification intensifies, the time spent above the thermocline increases markedly. The effect is more pronounced at low values of start thermocline, stabilising near the maximum as the thermocline becomes stronger. This pattern suggests that the thermal structure of the water column plays a key role in nocturnal vertical behaviour, with individuals preferentially remaining in the upper layers when stratification is pronounced.

In contrast, the oxygen concentration at 100 metres depth displayed a gently negative relationship, with higher oxygen levels associated with a slight reduction in time spent above the thermocline. This gradual decline indicates that, even at night, more oxygenated conditions in deeper layers may be linked to reduced utilisation of the surface zones.

Finally, the surface chlorophyll concentration showed a well-defined positive relationship, with a consistent increase in time spent above the thermocline as chlorophyll concentrations rise. The pattern suggests a slight saturation effect at higher values, indicating that beyond a certain level of surface productivity, the additional gain in time above the thermocline tends to stabilise.
The results of the best GLMM model fitted for the periods of the day revealed clear and consistent patterns in the influence of environmental variables on the time spent above the thermocline (Figure A14 A and B).

The analysis of the moon light effect showed a positive relationship, indicating that as the illuminated fraction of the moon increases, sharks tend to spend more time above the thermocline. This suggests that lunar illumination may influence vertical activity patterns, possibly by enhancing visibility or altering prey behaviour near the surface.

The oxygen concentration at 100 metres depth exhibited a slightly negative relationship. Although the overall time spent above the thermocline remained relatively high, a gradual decline was observed as oxygen levels increased. This pattern is like that recorded during the night, though slightly more pronounced during daylight hours.

The mean surface chlorophyll concentration demonstrated a positive relationship with a saturation pattern, comparable to that observed in the nocturnal model. Increases in chlorophyll near the surface were associated with longer periods above the thermocline, although this effect tended to stabilise at higher chlorophyll concentrations. This consistency across diel periods reinforces the role of surface productivity as a key structuring factor influencing vertical behaviour.

Finally, the start thermocline showed a strong, non-linear positive relationship. When the average thermocline strength was low (indicating a shallower thermocline), the proportion of time spent above it increased sharply. Beyond a threshold (around "start thermocline ≈ 20), the relationship plateaued and remained consistently high. This pattern suggests that the position and intensity of the thermocline exert a major influence on vertical distribution, with sharks spending substantially more time in upper layers when stratification is weaker or shallower.

4.Discussion

4.1 Vertical movements

Although information on the habitat preferences of mako sharks in the South Atlantic Ocean is limited when compared to that available for the North Atlantic, the combined analysis of vertical water column use, considering time spent at different depths and temperatures, reveals patterns consistent with other studies. The thermal preferences observed here agree with those previously reported for this species. Loefer et al. (2005) showed that tagging data from a specimen captured in the southeastern United States indicated movements between the surface and 556 m depth, within a temperature range of 10.4 °C to 28.6 °C. Similarly, Vaudo et al. (2016) reported that mako sharks tagged in the northeastern United States and the Gulf of Mexico experienced temperatures between 5.2 °C and 31.1 °C, while occupying depths from the surface to 866 m. Gibson et al. (2021) further demonstrated that this species frequents areas encompassing a broad range of sea

surface temperatures, between 10.0 °C and 31.0 °C. In the present study, sharks showed a preference for occupying layers between 0 and 150 m, despite the availability of greater depths across all study areas. A tendency for prolonged residence between 10 and 50 m was observed in several individuals (particularly S1, S2, S3, S7, S8, and S9), which is consistent with the vertical profile analyses indicating increased time spent in warmer waters (19–25 °C), with a predominance between 21 and 23 °C.

This occupation of relatively shallow and warmer waters is consistent with the thermal and ecological behaviour described for the species, which, although highly migratory and capable of extensive vertical movements, tends to prefer environments with higher temperatures close to its optimal thermal range. In a study conducted by Santos *et al*. (2021), individuals of the same species spent most of their time in temperate waters (18–22 °C) above 90 m, while this preference for warmer surface waters is also consistent with observations in other pelagic shark species, such as the blue shark (*Prionace glauca*), which preferentially occupies surface waters even in deep ocean regions (Queiroz *et al*., 2012; Vandeperre *et al*., 2014), and the tiger shark (*Galeocerdo cuvier*), was spent most of its time in the first 50 m of the water column, at temperatures between 22 and 25 °C (Lipscombe *et al*., 2020). The occasional presence of temperatures below 10 °C, associated with deeper dives, suggests that these movements are specific and not dominant behaviours in the ecological strategy of the monitored individuals.

However, despite their frequent presence in areas with bathymetries exceeding 2,000 meters, deep dives (>500 m) were occasional, which may be related to prey availability and the optimization of body temperature. The deep-diving pattern is presumed to be linked to the foraging behaviour in pelagic shark species such as the blue shark (*Prionace glauca*), tiger shark (*Galeocerdo cuvier)*, Scalloped hammerhead (*Sphyrna lewini*), big-eyed thresher shark (*Alopias superciliosus*), and oceanic whitetip shark (*Carcharhinus longimanus*) (Stevens *et al*., 2010; Nakamura *et al*., 2011; Hoffmayer *et al*., 2013; Howey-Jordan *et al*., 2013). Another widely accepted explanation for this type of behaviour points to the need to re-establish

body temperature following thermal losses resulting from incursions into cold waters (Peter Klimley *et al*., 2002).

The analysis of time spent at different depth intervals during the day and night reveals a typical pattern of diel vertical migration (DVM). Most individuals remained predominantly within the upper 150 m of the water column, with greater use of the 0–10 m and 10–30 m strata within the mixed layer depth (MLD) both day and night. A higher occupation of deeper layers was observed during the day and a preference for shallower layers at night, consistent with a diel vertical migration strategy previously described for the species. Nasby-Lucas *et al*. (2019) also reported that, although some individuals remained within the MLD both during the day and at night, the general trend was towards deeper distributions during daylight hours. Santos *et al*. (2021) showed that sharks tagged in the open waters of the Central and Northwestern regions tended to exhibit daily vertical movements characterised by shallower mean depths at night and greater mean depths during the day. Similarly, Vaudo *et al*. (2016); Loefer *et al*. (2005) and Abascal *et al*. (2011) observed the same pattern.

Epipelagic fishes adjust their vertical movements to exploit diel vertical migration (DVM), either directly or indirectly, by following the movements of their prey such as squids or smaller fishes which themselves feed on nektonic and planktonic organisms (Hays, 2003). Thus, this behaviour of spending more time in shallower layers at night has been associated with foraging activity. This behaviour is common among other large pelagic predators and teleosts (Dewar *et al*., 2011; Weng & Block, 2004; Coffey *et al*., 2017). However, exceptions to the classical DVM pattern were recorded, particularly among individuals S4, S5, and S6, which exhibited deep dives to depths ≥500–700 m during the night. This behaviour indicates a degree of behavioural plasticity that may be associated with the opportunistic exploitation of deep-water resources or with specific oceanographic conditions. Movement patterns of the porbeagle (*Lamna nasus*) have shown that some individuals exhibited reverse diel vertical migration (ascending at dawn and descending at dusk) in well-mixed coastal waters, while others displayed normal diel vertical migration in deeper, thermally stratified waters (Pade *et al*., 2009). Such patterns have been

documented in blue sharks (*Prionace glauca*) (Queiroz *et al*., 2012; Nosal *et al*., 2019) and in more recent studies (Mas *et al*., 2024).

In this study, the role of the thermal gradient was particularly evident in diel behaviour. Low gradients (0.02–0.05 °C/m) frequently coincided with deeper dives (>200 m), especially in individuals such as S4, S5, and S6 during days of weak stratification, whereas intermediate gradients (0.06–0.09 °C/m) promoted longer residence times within the 10–30 m or 30–50 m intervals, corresponding to the thermocline, and steeper gradients (≥0.1 °C/m) restricted individuals to the upper layers (0–10 m). During the day, sharks tended to occupy the thermocline (10–50 m), moving to deeper layers (50–100 m or more) when gradients were weak, whereas at night the predominant behaviour was a return to surface waters (0–10 m), particularly under strong gradients.

The results of the analyses regarding the time spent above the thermocline, during both day and night, support this hypothesis. In open waters, the thermal gradient exhibited a negative relationship with the time spent above the thermocline, during both day and night. In water columns characterised by strong stratification (steeper gradients), individuals reduced their epipelagic occupation (65.2% during the day; 76.1% at night). The thermal stratification model indicated a positive and significant effect only at night. During the day, stratification had limited explanatory power, suggesting that other environmental factors, such as surface temperature and solar radiation, may play a more dominant role in determining vertical distribution. When the thermal gradient was analysed together with temperature, a positive effect was observed, steeper gradients appeared to promote persistence in the upper layers of the thermocline. This findings suggests that the thermal gradient may exert a more significant influence than temperature alone on vertical behaviour.

The relationship between the thermal gradient and maximum diving depth further explains observed differences in diving behaviour. The deepest dives occurred in areas of weak stratification (<0.1 °C/m), suggesting that more homogeneous water columns facilitate wider vertical movements, possibly due to lower energetic costs. Previous studies corroborate this pattern: in the North Atlantic, Brill *et al*. (2002)

reported that bluefin tuna remained closer to the surface under marked thermoclines, while performing deeper dives under weak stratification. In the Mediterranean, Bauer *et al*. (2017) associated alternation between surface and depth with the thermal structure of the water column. These findings support the notion that strong stratification can act as a physiological or ecological barrier, limiting vertical exploration.

The initial depth of the thermocline showed a significant positive association with the time spent above this layer in open waters, although the explained variance was low. This result indicates that deeper thermoclines may allow individuals to remain longer in surface waters, possibly avoiding colder or less productive layers consistent with patterns observed in maximum diving depth. Abascal *et al*. (2011) similarly demonstrated that thermoclines between 100 and 150 m influence vertical activity, with individuals concentrating in the mixed layer (<150 m) after thermal homogenisation.

In areas shallower than 200 m, despite the observed positive trend, statistical significance was not achieved due to the limited number of observations. When the initial depth of the thermocline and the thermal gradient were considered together, the effect of the gradient remained non-significant, whereas thermocline depth showed a consistent positive association. This pattern suggests that the relative depth of the thermocline may be a more influential factor than gradient intensity in determining vertical behaviour. The deepest dives occurred when the thermocline was below 75 m, indicating that a thicker mixed layer facilitates deeper incursions by reducing the energetic cost of traversing steep thermal transitions. The positive relationship between initial thermocline depth and maximum diving depth suggests that, in environments with reduced upper-layer stratification, sharks can more efficiently exploit deeper zones. Electronic tagging data have shown that various aspects of the thermal structure generally constrain the vertical distributions of pelagic fish. Some species primarily utilise the surface mixed layer. Madigan *et al*. (2021) analysed the vertical habitat use of 12 species in the tropical South Atlantic and found that seven of these species preferred to spend time above the

thermocline. Similar patterns have been reported in other studies (Musyl *et al*., 2011; Howey-Jordan *et al*., 2013; Andrzejaczek *et al*., 2018)

Nevertheless, the majority of dives were concentrated between 200 and 400 m, regardless of thermal gradient. Dives exceeding 600 m occurred mainly in environments with reduced gradients. The statistical model revealed a significant association between thermal gradient and depth but explained only a small portion of the variability and was heavily influenced by a single individual (S10). Excluding this individual, the relationship was no longer significant, suggesting that the thermal gradient has a limited and non-generalizable effect. Other factors, such as prey availability, oxygen profiles, or individual characteristics, may play a more decisive role in dive depth (Andrzejaczek *et al*., 2019).

Simultaneously, the effect of surface temperature revealed a negative impact on the time spent above the thermocline, particularly in areas with depths less than 200 m. Individuals tend to remain above the thermocline both during the day and at night when surface temperatures are lower. A similar pattern is observed at 100 m, higher temperatures were associated with reduced time above the thermocline, with the trend being slightly stronger during the day, indicating that at higher temperatures individuals spend less time at depths shallower than 100 m. Other studies report comparable findings. Vaudo *et al*. (2016) showed that in warmer waters, sharks spent 36% of the daytime below 150 m, whereas in colder waters only 1% of the time was spent at these depths. These patterns suggest that organisms adjust their behaviour in response to thermal conditions, likely to remain within an optimal temperature range, as observed by Loefer *et al*. (2005), who noted that with increasing surface temperatures, nocturnal excursions into very shallow waters became less frequent; studies in the Atlantic have reported broader and deeper daytime depth ranges under warmer conditions (Santos *et al*., 2021), and in the Southeast Pacific, water temperature was identified as a key factor in determining vertical range, with deeper average daytime distributions and prolonged surface residence under colder conditions (Abascal *et al*., 2011).

The association between maximum depth and recorded temperature (both maximum and minimum) reinforces these patterns, showing that deeper dives

occurred preferentially under higher temperature conditions, particularly above 15 °C, despite cooler surface layers in 2024. Other studies indicate that as sea surface temperatures increased, mako sharks spent less time in the upper 50 m of the water column, likely seeking thermal refuges in deeper waters (Vaudo *et al*., 2016; Byrne *et al*., 2024). This behaviour has also been observed in other species with regional endothermy, namely the salmon shark *Lamna ditropis* (Weng *et al*., 2005) and the porbeagle *L. nasus* (Campana *et al*., 2010), but also in the ectothermic blue shark *Prionace glauca* (Campana *et al*., 2011).

Nevertheless, clear differences between individuals were evident. For example, S10 was associated with comparatively higher average temperatures (~24 °C), whereas S6 exhibited substantially lower values (16–17 °C), corresponding to movements towards more northern and southern latitudes, respectively. Interestingly, while high surface temperatures are generally associated with deeper dives, S10 predominantly remained in the surface layers throughout its trajectory, even in areas of considerable bathymetric depth. However, this individual experienced a high thermal gradient along its trajectory, whereas S6 exhibited low gradients on multiple occasions, enabling it to perform deeper dives in response to elevated temperatures. This suggests that factors beyond temperature, such as local thermal gradients or stratification, may limit deep-diving behaviour in certain individuals, highlighting the complex interaction between environmental variation and individual behavioural strategies.

Regarding chlorophyll-a concentration at 100 m, a negative relationship was observed with the time spent above the thermocline, both during the day and at night, particularly during the day. The same pattern was observed in the maximum depth results, with higher chlorophyll values associated with deeper dives. This suggests that elevated primary productivity at 100 m drives individuals to explore deeper layers, as observed by Vedor *et al*. (2021a), in which blue sharks adopt a depth-oriented diel vertical migration (DVM), following prey aggregations in deeper zones, such as cephalopods or mesopelagic fish. Similar behaviour has been reported in blue sharks in the North Atlantic (Campana *et al*., 2011; Queiroz *et al*., 2012). Other top predators feeding on similarly vertically migrating prey, such as

tuna and swordfish, also exhibit dives to the deep scattering layer (DSL), likely to maximise foraging success (Schaefer *et al*., 2009; Dewar *et al*., 2011; Sepulveda *et al*., 2018).At the surface, the relationship was inverse, particularly at night; higher chlorophyll levels were also associated with shallower dives, consistent with the classic DVM of species migrating to the surface at night, reinforcing the idea that more productive areas promote residence in this layers.

Environmental variable modelling analyses revealed that surface productivity, measured via chlorophyll concentration, consistently emerged as the most robust predictor in both periods, supporting the notion that the availability of trophic resources guides water column utilisation. Interestingly, a saturation pattern was observed, beyond a certain chlorophyll threshold (~0.4 μg L^{-1}), further increases in productivity did not correspond to proportional gains in time spent above the thermocline, suggesting that other factors modulate vertical behaviour once resource availability reaches sufficient levels.

Gibson Banks *et al*. (2025) noted in their study a reduction in movement persistence in regions with elevated chlorophyll-a concentrations; this persistence serves as an indicator of marine productivity (Benoit-Bird & Au, 2003). Although interpreting foraging behaviour from movement persistence is challenging without prior knowledge of prey availability (Florko *et al*., 2023) or foraging success (Bestley *et al*., 2008), areas where mako sharks remain longer continue to be essential for habitat conservation and protection (Hays *et al*., 2019). Similar patterns were observed in salmon sharks (*Lamna ditropis*), close relatives of mako sharks, which displayed slower and more tortuous swimming patterns in regions with high chlorophyll concentrations in the eastern North Pacific Ocean (Weng *et al*., 2008). Likewise, seasonal patterns of mako sharks in the eastern North Pacific Ocean tracked variations in temperature and elevated chlorophyll-a concentrations (Block *et al*., 2011; Nasby-Lucas *et al*., 2019).

Surface oxygen reinforced the chlorophyll results, as dissolved oxygen at the surface exhibited a positive relationship with the time spent above the thermocline, most evident at night, and again associated with diel vertical migration (DVM). This suggests that well-oxygenated waters promote epipelagic residence, leading

individuals to remain preferentially in shallower waters rather than performing deep dives.

In contrast, oxygen concentration at 100 m showed a negative association with the time spent above the thermocline in both periods, a result consistent with maximum dive depth data, indicating that when oxygen concentrations at 100 m are elevated, individuals tend to reach greater depths. This suggests that mako sharks exploit deeper zones when oxygen conditions allow. In a study in the southeast Pacific Ocean, mako shark dives frequently terminated at depths corresponding to an oxygen concentration of 3 ml L^{-1} (Abascal *et al.*, 2011), while off the coast of California, mako sharks rarely descended to depths with oxygen concentrations below 2 ml L^{-1} (Vetter *et al.*, 2008). In the Gulf of Mexico, sharks frequently reached depths with oxygen concentrations between 2.5 and 3 ml L^{-1} (Garcia *et al.*, 2014), demonstrating that oxygen influences the vertical behaviour of this species.

In the present study, oxygen concentration at 100 m consistently showed a negative, though non-significant, effect in both periods. This suggests that physiological limitations associated with low oxygen levels in deeper waters are not the primary determinants of vertical distribution, although they may exert a secondary or indirect influence, potentially related to metabolism or prey availability.

Finally, the influence of lunar illumination on the studied organisms was weak and restricted to the nocturnal period, exhibiting negative relationship brighter nights were associated with reduced time spent above the thermocline (epipelagic occupation of 72.7%). Andrzejaczek *et al*. (2024) reported consistent patterns across multiple taxa, observing deeper vertical movements with increasing lunar illumination. This pattern likely reflects prey responses, as both plankton and mesopelagic fish tend to remain at greater depths during the full moon as a predator avoidance strategy (Hays, 2003; Last *et al.*, 2016). In top predators, such as tuna and swordfish (*Xiphias gladius*), deeper distributions during full moon nights were associated with greater foraging success on prey aggregated at shallower depths (Musyl *et al.*, 2003; Dewar *et al.*, 2011; Abascal *et al.*, 2015).

In contrast, the mixed model for the daytime period revealed an almost significant positive effect of lunar illumination ($\beta = 1.05$; $p = 0.097$). This suggests an indirect effect of moonlight, possibly modulating nocturnal behaviour in a way that manifests during the following day. At maximum depth, lunar illumination had a negligible effect, remaining largely stable throughout the lunar cycle, although a slight reduction in depth was observed during the new moon.

The analysis of seasonal and sexual differences in the vertical behaviour of mako sharks reveals a general trend towards similar depth patterns between males and females, although with occasional variations, more evident during summer. In autumn and spring, the overlap of interquartile depth ranges between sexes and the low dispersion of values suggests behavioural homogeneity, possibly associated with thermal stability of the water column during these seasons. However, the greater dispersion in depths used by females in autumn, as well as the occurrence of extreme deeper values, may indicate the existence of differentiated individual habitat exploration strategies.

During summer, more pronounced differences were observed, with females exhibiting a wider vertical range of water column utilisation. This greater variability may be related to distinct physiological requirements, particularly those associated with reproductive strategies, thermoregulation, or prey search. The higher behavioural heterogeneity in summer may also reflect an adaptive response to warmer surface waters, compelling individuals to seek deeper and thermally more stable layers, as previously documented in Atlantic mako shark studies. This behavioural pattern finds parallels in earlier research on the vertical ecology of large elasmobranchs. Andrzejaczek *et al*. (2018) observed that *Carcharhinus longimanus* increases the amplitude and duration of vertical oscillations during summer, tending to avoid surface waters when temperatures exceed 28 °C, and highlighted sexual differences in vertical behaviour. Complementarily, Doherty *et al*. (2019) demonstrated that basking sharks (*Cetorhinus maximus*) in the Northeast Atlantic exhibit vertical water column utilisation influenced by seasonality, remaining in shallower waters during summer and autumn, and moving to greater depths as winter approaches. These patterns are explained by prey distribution and the

presence of physical barriers, such as the thermocline, factors that may also influence the patterns observed in the present study.

Regarding maximum depth reached, despite these seasonal variations, analysis of mean maximum and minimum depths reveals remarkable similarity between sexes. Both groups demonstrated a strong association with surface layers, with very low medians for mean minimum depth and mean maximum depths concentrated below 200 metres. These results reinforce the notion that habitat use near the surface is a common characteristic of the species vertical ecology, irrespective of sex. The occasional occurrence of deep dives, with maximum values exceeding 400 metres, indicates that both sexes are capable of large-amplitude vertical movements, although such behaviour is sporadic.

Analysis of daily mean depth and temperature revealed relatively similar habitat occupation patterns between males and females, with some subtle but statistically significant differences. Both sexes exhibited a peak in depth utilisation between 90 and 100 metres, indicating a shared general vertical utilisation pattern. Despite overlapping distributions, males tended to utilise depths greater than 120 metres more frequently, whereas females exhibited higher densities in shallower waters (<80 metres). Although small in absolute terms, this difference was statistically significant ($p < 0.001$), suggesting possible behavioural variations associated with sex-specific factors, such as physiological demands or differentiated foraging strategies.

In terms of temperature, both males and females displayed a clear preference for temperatures between 16 °C and 18 °C, indicating a common thermal activity range. However, females showed greater dispersion, with significant occurrences in warmer waters (>19 °C). Nevertheless, statistical testing did not reveal significant differences between sexes ($p > 0.01$), suggesting that these thermal discrepancies do not robustly translate into sex-specific patterns.

Overall, the observed seasonal variation with a tendency for greater permanence in shallower waters, especially in autumn/winter, may be related to changes in the thermal structure of the water column. This dynamic was especially evident in

individuals as IDs S4, S5, and S8, which appeared to adjust their preferred depth depending on water temperature. The association between depth and temperature, especially in individuals that frequented areas of high bathymetry at the beginning of their journey and migrated to shallower areas as winter approached, suggests a behavioural response to environmental conditions. This pattern is consistent with that described by Block *et al*., 2011, who identified a clear seasonality in the behaviour of resident populations in the Open Western Atlantic, associated with shelf and slope waters.

Notable interannual variations were also observed. During 2021/2022, individuals remained predominantly in the upper layers of the water column (mean depth 155 m, maximum 712 m), even in areas of steep bathymetry. This pattern suggests reduced vertical exploration, possibly associated with more homogeneous and favourable thermal conditions in the upper layers, as described by Block *et al*. (2011). In contrast, in 2024, individuals exhibited greater vertical range, with regular dives to 500 m and occasional excursions beyond 1000 m whenever bathymetry permitted. This pattern reflects more intensive water column exploration, likely as an adaptive response to environmental or trophic changes occurring that year. Behavioural responses of this type have been documented by several authors. Andrzejaczek *et al*. (2019) reinforced this notion, describing how changes in the physical structure of the water column may lead epipelagic sharks to spend more time at depth as a strategy to maintain stable body temperature and access diversified food resources.

These differences in depth may be associated with temperatures experienced in the different years, as sharks frequented warmer waters in 2021/2022 (mean 17.7 °C), whereas 2024 exhibited cooling, with mean temperatures of 16.1 °C, showing a significant difference between years ($p < 0.001$). These interannual variations likely reflect changes in water masses associated with regional climatic phenomena or variations in thermocline depth, including influences from marginal currents, meso-scale oceanic gyres, and regional upwelling systems (Liu *et al*., 2022; Zhai *et al*., 2025; Sayol *et al*., 2023). The lower mean temperatures recorded in 2024 may be linked to a higher frequency of deep dives that year or reflect seasonal variations,

given that most individuals tagged in 2021/2022 were recorded during warmer months, while a large portion of 2024 individuals traversed periods characterised by cooler thermal conditions along their respective tracks.

Bathymetry did not appear to be a limiting factor in any of the analysed years. When the thermal gradient was examined in different bathymetric contexts, distinct patterns were evident. In the open ocean, characterised by greater depths, more pronounced variability in dives was observed, including descents exceeding 800 m, as well as a slight tendency to avoid deeper layers under intense thermal gradients. In contrast, in shallow coastal regions (<200 m), no correlation was detected between thermal gradient and maximum depth, suggesting that in these shallow environments, physical limitations imposed by bathymetry override the influence of thermal variables in determining vertical behaviour. It is also noteworthy that thermal gradients differed significantly between open ocean and coastal zones, reflecting the distinct thermal conditions provided by each environment. However, in both cases, neither the thermal gradient nor its interaction with year had statistically significant effects.

4.2 Horizontal movements

The horizontal movements of the tagged mako sharks indicate a clear preference for areas adjacent to the southeastern continental shelf, although individuals also utilised nearby oceanic waters. Similar spatial patterns have been reported in other studies, Santos *et al*. (2021) found that satellite-tracked shortfin makos exhibited variable horizontal movements but tended to concentrate in shelf waters and along the slopes of the Southwest Atlantic Subtropical Convergence Zone. Coelho *et al*. (2020) reported comparable findings, with the majority of makos tagged off Cape Verde moving towards the African shelf. Overall, our results are consistent with previous research.

The tendency of most individuals to move towards the continental shelf is likely influenced, at least in part, by prey availability. Vaudo *et al*. (2024) demonstrated that mako foraging in pelagic environments results from interactions between

horizontal and vertical movements and is strongly influenced by water temperature and seasonal productivity; individual variability and regional differences also modulate these patterns.

These areas are attractive because they support higher primary productivity as well as greater prey diversity and abundance compared with the open ocean (Gattuso *et al.*, 2006; Chen *et al.*, 2000; Francis *et al.*, 2019). Several studies indicate that residency is more common on or near continental shelves and other productive areas, with limited residency in offshore waters (Block *et al.*, 2011; Kai *et al.*, 2015; Rogers *et al.*, 2015; Adams *et al.*, 2016; Vaudo *et al.*, 2017; Byrne *et al.*, 2019). In our study, surface chlorophyll-a concentrations were higher over the shelf, whereas chlorophyll at 100 m depth was relatively higher in offshore waters; this vertical separation of productivity may partly explain movements between shelf and oceanic habitats.

Notably, the horizontal movements of two individuals (S6 and S10) reached the most extreme latitudes within the study area: S6 moved southwards to latitudes near Cape Town, South Africa, while S10 moved northwards towards Saint Helena. Both individuals were female; S6 was the smallest and S10 the largest tagged specimen. This behavioural diversity may reflect different ecological strategies associated with size, age, sex, physiological condition, or dynamic environmental contexts. Nasby-Lucas *et al*. (2019) suggested that body size often has a stronger influence on large-scale mako movements than sex, which could explain some of the differences observed. Alternatively, these long-distance movements may reflect directed migrations along environmental gradients (e.g., temperature, oxygen, bathymetry) or journeys to known feeding or reproductive areas.

The overlay of environmental variables onto individual trajectories further supports the previously described horizontal behaviour, providing an integrated perspective on how physical and biogeochemical factors shape the spatial behaviour of the mako shark.

The analysis of time spent above the thermocline revealed clear patterns of spatial variability and responses to oceanographic factors. It was observed that individuals

remained longer above the thermocline between latitudes –20° and –30°, particularly in coastal areas. This trend suggests that proximity to the coast at shallower depths may create favourable conditions for prolonged presence in the surface layer. Sea surface temperature exhibited a distinct north–south gradient. Warmer waters dominated equatorial and oceanic regions (as experienced by S10), whereas cooler waters occurred closer to the coast, reflecting coastal upwelling that enhances nutrient supply and primary productivity (Bakun *et al*., 2015). This upwelling is consistent with higher surface chlorophyll-a concentrations along the coast, notably between approximately 35°S and 20°S. Elevated chlorophyll levels indicate greater phytoplankton biomass, which can aggregate epipelagic prey and, indirectly, attract top predators.

Multiple studies report increased residency of mako sharks in productive areas of the continental slope and frontal zones (Block *et al*., 2011; Kai *et al*., 2015; Rogers *et al*., 2015; Adams *et al*., 2016; Vaudo *et al*., 2017). Our results, showing a tendency of sharks to move towards areas with high surface chlorophyll, are consistent with an indirect trophic association driven by prey aggregation. Similarly, Coelho *et al*. (2020) observed movements towards the African slope in individuals tagged off Cape Verde. In southwestern Uruguay, sharks demonstrated fidelity to the Subtropical Convergence Zone, where convergent currents create a rich ecosystem capable of supporting high trophic levels (Acha *et al*., 2004; Jiménez *et al*., 2011; Gaube *et al*., 2017).

Dissolved oxygen maps revealed strong vertical stratification: surface waters were generally well-oxygenated and homogeneous, consistent with continuous gas exchange between air and sea, whereas oxygen concentrations declined at 100 m, particularly along the northwest coast between approximately 5°S and 20°S. Regions of low oxygen are located near oxygen minimum zones (OMZs) and may influence vertical distribution (Stramma *et al*., 2010; Helly & Levin, 2004; Vedor *et al*., 202b), as exemplified by individual S10, which experienced the lowest oxygen concentrations, approached the OMZ more closely than other individuals, and did not undertake dives exceeding 500 m. Studies show that blue sharks and salmon sharks reduce their maximum diving depth when encountering low oxygen levels at

depth, remaining in shallower, better-oxygenated layers (Coffey *et al*., 2017; Vedor *et al*., 2021b).

Consistently, sharks tended to restrict their dives to shallower depths (<500 m), whereas in less stratified southern regions they penetrated more deeply (>900 m), likely taking advantage of deeper, better-oxygenated waters.

4.3 Vertical Habitat Use of Mako Sharks and Its Conservation Significance under Climate and Fishery Pressures

There remain relatively few studies that comprehensively address the interactions between sharks and their environment, alongside the spatial overlap with fishing vessels. A study conducted by Queiroz *et al*. (2016) was the first to quantify, at the scale of the North Atlantic basin, the interactions between oceanic sharks and the environment, together with the spatial overlap with pelagic fishing fleets, mainly Spanish and Portuguese longliners.

In that study, 99 sharks from several species were tracked, including the species examined in the present work. The results showed that sharks spent more time in habitats characterised by strong temperature gradients and high local productivity areas typically associated with elevated concentrations of nutrients and prey.

Regarding overlap with fisheries, it was found that pelagic longliners also tend to concentrate in these frontal zones, leading to a considerable spatial coincidence between sharks and fishing operations. Among the species analysed, the shortfin mako shark exhibited a higher risk of capture than the blue shark, as it showed a stronger preference for frontal habitats the same areas most frequently targeted by longliners.

Although the present study did not directly assess overlap with fisheries, the findings of Queiroz *et al*. (2016) emphasise the importance of understanding how environmental factors shape species' behaviour and distribution. Several individuals tracked in this study moved towards areas of high primary productivity and elevated oxygen concentrations, regions that also attract other pelagic species

and, consequently, fishing activity. Furthermore, the study area spans two Exclusive Economic Zones (EEZs), Namibian territorial waters (564,700 km^2) and South African waters (1,535,538 km^2). These extensive maritime zones encompass productive coastal and oceanic habitats, which are important both for pelagic shark populations and for commercial fisheries, highlighting the need to assess spatial overlap and potential conflicts between conservation and exploitation.

Given that the distribution and movement patterns of pelagic sharks are strongly influenced by environmental factors, and that there is a high degree of spatial and temporal overlap between sharks and fishing vessels, it is essential to implement international management measures and catch limitations to ensure the protection and conservation of these pelagic shark species. Consequently, any climate-driven changes in oceanographic conditions are likely to modify shark behaviour and habitat use, which in turn may alter the degree of spatial and temporal overlap between sharks and fisheries.

Several studies have already documented shifts in the behaviour of the shortfin mako shark (*Isurus oxyrinchus*) in response to environmental variability. Vaudo *et al*. (2016) suggested that the strong association between mako shark habitat use and temperature may be affected by increasing ocean temperatures. Specifically, ocean warming could lead to an expansion of the depths utilised by this species as its lower thermal limit deepens, while simultaneously reducing the amount of time individuals spend near the surface. Similarly, Hazen *et al*. (2013) projected that suitable habitat for mako sharks in the Northeast Pacific could decrease by more than 25% by the year 2100, based on predicted changes in sea surface temperature (SST) and chlorophyll concentrations. However, since their model did not account for oxygen levels or the expansion of oxygen minimum zones (OMZs), the actual habitat loss could be even greater.

Data from the present study also indicated that individuals tended to move towards cooler and deeper waters when temperatures were elevated. Although oxygen appeared to influence the sharks' vertical behaviour, it did not emerge as a limiting environmental variable for vertical movement within the study area. Nevertheless, other studies have demonstrated that deoxygenation and OMZ expansion can

significantly affect the behaviour and distribution of this species. Byrne *et al*. (2024), for instance, reported that the ongoing expansion of OMZs, driven by climate change-induced deoxygenation, poses a major threat to mako sharks and other large pelagic fishes.

Despite these challenges, mako sharks may be capable of tolerating moderate hypoxia, at least for short periods. Individuals tracked within the Eastern Tropical Pacific (ETP) typically remained in waters with oxygen concentrations above 3.0 mL $O_2 \cdot L^{-1}$and rarely encountered levels below 2.0 mL $O_2 \cdot L^{-1}$. However, during deep dives exceeding 300 m, they were estimated to experience oxygen concentrations as low as 1.3 mL $O_2 \cdot L^{-1}$ (Abascal *et al*., 2011; Vetter *et al*., 2008).

These findings collectively suggest that climate-driven alterations in ocean temperature and oxygen availability have the potential to reshape the spatial ecology of the shortfin mako, with cascading implications for its vulnerability to fisheries and the effectiveness of conservation measures.

The vertical behaviour of mako sharks reflects a multifactorial balance between the physical and biological characteristics of the water column. Surface productivity, expressed by chlorophyll concentration, emerges as the primary determinant of their vertical distribution, indicating that the availability of food resources strongly guides habitat use. Temperature and thermal stratification constitute secondary structural factors, yet they exert relevant influence in limiting or facilitating vertical movements, strong stratification translates into physiological constraints, whereas weak stratification allows greater diving amplitude.

Oxygen acts as a complementary modulator, adjusting behaviour according to prevailing environmental conditions. Observed inter-individual and interannual differences demonstrate marked behavioural plasticity, highlighting the species' capacity to adapt vertical exploration strategies to local and seasonal variations.

Overall, it can be concluded that mako sharks dynamically adjust their vertical behaviour to maximise energetic efficiency and foraging success, simultaneously responding to thermal constraints, trophic availability, and the structural characteristics of their environment.

The present study aims to contribute to the understanding of how environmental variables shape the behaviour of the *I.oxyrinchus* in the South Atlantic, a region where information on this species remains scarce. These findings enhance our understanding of how multiple environmental factors interact in shaping vertical behavioural patterns within aquatic ecosystems, highlighting the dynamic and multifactorial nature of water column utilisation.

However, the conservation of oceanic sharks remains hindered by fundamental gaps in knowledge regarding where these species aggregate across different oceanic zones. *I.oxyrinchus* is of particular conservation concern, being listed on the IUCN Red List. Despite these concerns, the availability of both fishery and biological data continues to be limited, especially within the study area, thus constraining the development and implementation of effective conservation measures.

Future research should assess the effects of climatic variability and long-term oceanographic changes on the distribution and migratory phenology of shortfin mako sharks. It is particularly important to determine whether their movements are beginning to shift beyond current spatial management zones that have offered protection from commercial fishing and bycatch. Understanding how climate-driven habitat changes may affect exposure risk is essential to ensure that conservation measures remain effective under continuously changing oceanic conditions.

6.References

Abascal, F. J., Mejuto, J., Quintans, M., García-Cortés, B., & Ramos-Cartelle, A. (2015). Tracking of the broadbill swordfish, Xiphias gladius, in the central and eastern North Atlantic. Fisheries Research, 162, 20-28. https://doi.org/10.1016/j.fishres.2014.09.011.

Abascal, F. J., Quintans, M., Ramos-Cartelle, A., & Mejuto, J. (2011). Movements and environmental preferences of the shortfin mako, *Isurus oxyrinchus*, in the southeastern Pacific Ocean. Marine Biology, 158(5), 1175-1184. https://doi.org/10.1007/s00227-011-1639-1.

Acha, E. M., Mianzan, H. W., Guerrero, R. A., Favero, M., & Bava, J. (2004). Marine fronts at the continental shelves of austral South America: physical and ecological processes. Journal of Marine systems, 44(1-2), 83-105. https://doi.org/10.1016/j.jmarsys.2003.09.005.

Adams, G. D., Flores, D., Flores, O. G., Aarestrup, K., & Svendsen, J. C. (2016). Spatial ecology of blue shark and shortfin mako in southern Peru: local abundance, habitat preferences and implications for conservation. *Endangered Species Research*, *31*, 19-32. https://doi.org/10.3354/esr00744.

Afonso, A. S., & Hazin, F. H. (2015). Vertical movement patterns and ontogenetic niche expansion in the tiger shark, Galeocerdo cuvier. PloS one, 10(1), e0116720. https://doi.org/10.1371/journal.pone.0116720.

Andrzejaczek, S., Gleiss, A. C., Jordan, L. K., Pattiaratchi, C. B., Howey, L. A., Brooks, E. J., & Meekan, M. G. (2018). Temperature and the vertical movements of oceanic whitetip sharks, Carcharhinus longimanus. Scientific reports, 8(1), 8351. https://doi.org/10.1038/s41598-018-26485-3.

Andrzejaczek, S., Gleiss, A., Pattiaratchi, C., & Meekan, M. (2019). Patterns and drivers of vertical movements of the large fishes of the epipelagic. Reviews in Fish Biology and Fisheries, 29, 335–354. https://doi.org/10.1007/s11160-019-09555-1.

Andrzejaczek, S., DiGiacomo, A. E., Mikles, C. S., Pagniello, C. M., Reimer, T. E., & Block, B. A. (2024). Lunar cycle effects on pelagic predators and fisheries: insights into tuna, billfish, sharks, and rays. Reviews in Fish Biology and Fisheries, 1-18. https://doi.org/10.1007/s11160-024-09914-7.

Arnold, G., & Dewar, H. (2001). Electronic tags in marine fisheries research: a 30-year perspective. In Electronic Tagging and Tracking in Marine Fisheries: Proceedings of the Symposium on Tagging and Tracking Marine Fish with Electronic Devices, February 7–11, 2000, East-West Center, University of Hawaii (pp. 7-64). Dordrecht: Springer Netherlands. https://doi.org/10.1007/978-94-017-1402-0_2.

Bakun, A., Black, B. A., Bograd, S. J., Garcia-Reyes, M., Miller, A. J., Rykaczewski, R. R., & Sydeman, W. J. (2015). Anticipated effects of climate change on coastal upwelling ecosystems. Current Climate Change Reports, 1(2), 85-93. https://doi.org/10.1007/s40641-015-0008-4.

Bandara, K., Varpe, Ø., Wijewardene, L., Tverberg, V., & Eiane, K. (2021). Two hundred years of zooplankton vertical migration research. Biological Reviews, 96(4), 1547-1589. https://doi.org/10.1111/brv.12715.

Barker, M. J., & Schluessel, V. (2005). Managing global shark fisheries: suggestions for prioritizing management strategies. *Aquatic Conservation: Marine and Freshwater Ecosystems*, *15*(4), 325-347. https://doi.org/10.1002/aqc.660.

Bates, D., Maechler, M., Bolker, B., & Walker, S. (2015). Fitting linear mixed-effects models using *lme4*. *Journal of Statistical Software,* *67*(1), 1–48. https://doi.org/10.18637/jss.v067.i01.

Bauer, R. K., Fromentin, J. M., Demarcq, H., & Bonhommeau, S. (2017). Habitat use, vertical and horizontal behaviour of Atlantic bluefin tuna (Thunnus thynnus) in the Northwestern Mediterranean Sea in relation to oceanographic conditions. Deep Sea Research Part II: Topical Studies in Oceanography, 141, 248-261. https://doi.org/10.1016/j.dsr2.2017.04.006.

Becker, O., Minka, A., & Deckmyn, A. (2024). *maps: Draw geographical maps* (R package versão 3.4.2.1) . CRAN. https://CRAN.R-project.org/package=maps.

Benoit-Bird, K. J., & Au, W. W. (2003). Prey dynamics affect foraging by a pelagic predator (Stenella longirostris) over a range of spatial and temporal scales. *Behavioral Ecology and Sociobiology*, *53*(6), 364-373. https://doi.org/10.1007/s00265-003-0585-4.

Bernal, D., Sepulveda, C., & Graham, J. B. (2001). Water-tunnel studies of heat balance in swimming mako sharks. Journal of Experimental Biology, 204(23), 4043-4054. https://doi.org/10.1242/jeb.204.23.4043.

Bernal, D., Reid, J. P., Roessig, J. M., Matsumoto, S., Sepulveda, C. A., Cech Jr, J. J., & Graham, J. B. (2018). Temperature effects on the blood oxygen affinity in sharks. Fish Physiology and Biochemistry, 44(3), 949-967. https://doi.org/10.1007/s10695-018-0484-2.

Bestley, S., Patterson, T. A., Hindell, M. A., & Gunn, J. S. (2008). Feeding ecology of wild migratory tunas revealed by archival tag records of visceral warming. *Journal of Animal Ecology*, *77*(6), 1223-1233. https://doi.org/10.1111/j.1365-2656.2008.01437.x.

Bishop, S. D. H., Francis, M. P., Duffy, C., & Montgomery, J. C. (2006). Age, growth, maturity, longevity and natural mortality of the shortfin mako shark (*Isurus oxyrinchus*) in New Zealand waters. Marine and Freshwater Research, 57(2), 143-154. https://doi.org/10.1071/MF05077.

Block, B. A., Dewar, H., Farwell, C., & Prince, E. D. (1998). A new satellite technology for tracking the movements of Atlantic bluefin tuna. Proceedings of the National Academy of Sciences, 95(16), 9384-9389. https://doi.org/10.1073/pnas.95.16.9384.

Block, B. A., Jonsen, I. D., Jorgensen, S. J., Winship, A. J., Shaffer, S. A., Bograd, S. J., ... & Costa, D. P. (2011). Tracking apex marine predator movements in a dynamic ocean. Nature, 475(7354), 86-90. https://doi.org/10.1038/nature10082.

Brill, R., Lutcavage, M., Metzger, G., Bushnell, P., Arendt, M. D., Lucy, J., ... & Foley, D. (2002). Horizontal and vertical movements of juvenile bluefin tuna (Thunnus thynnus), in relation to oceanographic conditions of the western North Atlantic, determined with

ultrasonic telemetry. Fishery Bulletin, 100(2), 155. https://scholarworks.wm.edu/handle/internal/18700.

Bruno, J. F., Bates, A. E., Cacciapaglia, C., Pike, E. P., Amstrup, S. C., Van Hooidonk, R., ... & Aronson, R. B. (2018). Climate change threatens the world's marine protected areas. Nature Climate Change, 8(6), 499-503. https://doi.org/10.1038/s41558-018-0149-2.

Byrne, M. E., Vaudo, J. J., Harvey, G. C. M., Johnston, M. W., Wetherbee, B. M., & Shivji, M. (2019). Behavioural response of a mobile marine predator to environmental variables differs across ecoregions. Ecography, 42(9), 1569-1578. https://doi.org/10.1111/ecog.04463.

Byrne, M., Dewar, H., Vaudo, J., Wetherbee, B., & Shivji, M. (2024). You Shall Not Pass: The Pacific Oxygen Minimum Zone Creates a Boundary to Shortfin Mako Shark Distribution in the Eastern North Pacific Ocean. Diversity and Distributions, 30. https://doi.org/10.1111/ddi.13924.

Calle-Morán, M. D., Erazo-Garcés, H. M., Hernández-Téllez, A. R., Galván-Magaña, F., & Estupiñán-Montaño, C. (2023). Feeding ecology of the shortfin mako shark, *Isurus oxyrinchus*, in the Ecuadorian Pacific Ocean. *Journal of the Marine Biological Association of the United Kingdom*, *103*, e96. DOI:10.1017/S0025315423000863.

Camhi, M. D., Lauck, E., Pikitch, E. K., & Babcock, E. A. (2008). A global overview of commercial fisheries for open ocean sharks. Sharks of the open ocean: Biology, fisheries and conservation, 166-192.

Campana, S. E., Marks, L., & Joyce, W. (2005). The biology and fishery of shortfin mako sharks (*Isurus oxyrinchus*) in Atlantic Canadian waters. *Fisheries Research*, *73*(3), 341-352. https://doi.org/10.1016/j.fishres.2005.01.009.

Campana, S. E., Joyce, W., & Fowler, M. (2010). Subtropical pupping ground for a cold-water shark. Canadian Journal of Fisheries and Aquatic Sciences, 67(5), 769-773. https://doi.org/10.1139/F10-020.

Campana, S. E., Dorey, A., Fowler, M., Joyce, W., Wang, Z., Wright, D., & Yashayaev, I. (2011). Migration pathways, behavioural thermoregulation and overwintering grounds of

blue sharks in the Northwest Atlantic. PloS one, 6(2), e16854. https://doi.org/10.1371/journal.pone.0016854.

Campana, S. E., Joyce, W., Fowler, M., & Showell, M. (2016). Discards, hooking, and post-release mortality of porbeagle (Lamna nasus), shortfin mako (*Isurus oxyrinchus*), and blue shark (Prionace glauca) in the Canadian pelagic longline fishery. ICES Journal of Marine Science, 73(2), 520-528. https://doi.org/10.1093/icesjms/fsv234.

Cantin, N. E., Cohen, A. L., Karnauskas, K. B., Tarrant, A. M., & McCorkle, D. C. (2010). Ocean warming slows coral growth in the central Red Sea. *Science*, *329*(5989), 322-325. DOI: 10.1126/ciência.1190182.

Cao, L., Wang, S., Zheng, M., & Zhang, H. (2014). Sensitivity of ocean acidification and oxygen to the uncertainty in climate change. Environmental Research Letters, 9(6), 064005. https://doi.org/10.1088/1748-9326/9/6/064005.

Carilli, J., Donner, S. D., & Hartmann, A. C. (2012). Historical temperature variability affects coral response to heat stress. *PloS one*, *7*(3), e34418. https://doi.org/10.1371/journal.pone.0034418.

Cerna, F., & Licandeo, R. (2009). Age and growth of the shortfin mako (*Isurus oxyrinchus*) in the south-eastern Pacific off Chile. Marine and Freshwater Research, 60(5), 394-403. https://doi.org/10.1071/MF08125.

Chen, X., Lohrenz, S. E., & Wiesenburg, D. A. (2000). Distribution and controlling mechanisms of primary production on the Louisiana–Texas continental shelf. Journal of Marine Systems, 25(2), 179-207. https://doi.org/10.1016/S0924-7963(00)00014-2.

CITES (2019). Summary of the Twelfth Session of Committee I. Available online at: https://cites.org/sites/default/files/eng/cop/18/Com_I/SR/E-CoP18-Com-I-Rec-12-R1.pdf .

Coelho, R., Fernandez-Carvalho, J., Lino, P. G., & Santos, M. N. (2012). An overview of the hooking mortality of elasmobranchs caught ina swordfish pelagic longline fishery in the Atlantic Ocean. *Aquatic Living Resources*, *25*(4), 311-319.doi:10.1051/alr/2012030.

Coelho, R., Macías, D., de Urbina, J. O., Martins, A., Monteiro, C., Lino, P. G., ... & Santos, M. N. (2020). Local indicators for global species: pelagic sharks in the tropical northeast Atlantic, Cabo Verde islands region. Ecological Indicators, 110, 105942. https://doi.org/10.1016/j.ecolind.2019.105942.

Coffey, D. M., Carlisle, A. B., Hazen, E. L., & Block, B. A. (2017). Oceanographic drivers of the vertical distribution of a highly migratory, endothermic shark. Scientific reports, 7(1), 10434. https://doi.org/10.1038/s41598-017-11059-6.

Compagno, L. J. (2001). Sharks of the world: an annotated and illustrated catalogue of shark species known to date (Vol. 1). Food & Agriculture Org.

Cortés, E., Arocha, F., Beerkircher, L., Carvalho, F., Domingo, A., Heupel, M., ... & Simpfendorfer, C. (2010). Ecological risk assessment of pelagic sharks caught in Atlantic pelagic longline fisheries. *Aquatic Living Resources*, *23*(1), 25-34. Doi:10.1051/alr/2009044.

Costa, F. E. S., Braga, F. M. D. S., Arfelli, C. A., & Amorim, A. F. (2002). Aspects of the reproductive biology of the shortfin mako, *Isurus oxyrinchus* (Elasmobranchii Lamnidae), in the southeastern region of Brazil. Brazilian Journal of Biology, 62, 239-248. https://doi.org/10.1590/S1519-69842002000200007.

de Bruyn, P. (2017). Report of the 2017 ICCAT Shortfin mako assessment meeting. *International Commission for the Conservation of Atlantic Tunas, Madrid*.

de Perera, T. B., Holbrook, R., Davis, V., Kacelnik, A., & Guilford, T. (2013). Navigating in a volumetric world: metric encoding in the vertical axis of space. Behavioural & Brain Sciences, 36(5). DOI:10.1017/S0140525X13000344.

Dedman, S., Moxley, J. H., Papastamatiou, Y. P., Braccini, M., Caselle, J. E., Chapman, D. D., ... & Heithaus, M. R. (2024). Ecological roles and importance of sharks in the Anthropocene Ocean. Science, 385(6708), adl2362. DOI: 10.1126/science.adl2362.

Delong, R. L., Stewart, B. S., & Hill, R. D. (1992). Documenting migrations of northern elephant seals using day length. Marine Mammal Science, 8(2), 155-159. https://doi.org/10.1111/j.1748-7692.1992.tb00375.x.

Dewar, H., Prince, E. D., Musyl, M. K., Brill, R. W., Sepulveda, C., Luo, J., ... & McNaughton, L. M. (2011). Movements and behaviours of swordfish in the Atlantic and Pacific Oceans examined using pop-up satellite archival tags. Fisheries Oceanography, 20(3), 219-241. https://doi.org/10.1111/j.1365-2419.2011.00581.x.

Doherty, P. D., Baxter, J. M., Godley, B. J., Graham, R. T., Hall, G., Hall, J., ... & Witt, M. J. (2019). Seasonal changes in basking shark vertical space use in the north-east Atlantic. *Marine Biology*, *166*(10), 129. https://doi.org/10.1007/s00227-019-3565-6.

Doney, S. C., Ruckelshaus, M., Duffy, J. E., Barry, J. P., Chan, F., English, C. A., ... & Talley, L. D. (2012). Climate change impacts on marine ecosystems. Annual review of marine science, 4(2012), 11-37. https://doi.org/10.1146/annurev-marine-041911-111611.

Doño, F., Montealegre-Quijano, S., Domingo, A., & Kinas, P. G. (2015). Bayesian age and growth analysis of the shortfin mako shark *Isurus oxyrinchus* in the Western South Atlantic Ocean using a flexible model. Environmental Biology of Fishes, 98(2), 517-533. https://doi.org/10.1007/s10641-014-0284-1.

Dulvy, N. K., Rogers, S. I., Jennings, S., Stelzenmüller, V., Dye, S. R., & Skjoldal, H. R. (2008a). Climate change and deepening of the North Sea fish assemblage: a biotic indicator of warming seas. *Journal of Applied Ecology*, *45*(4), 1029-1039. https://doi.org/10.1111/j.1365-2664.2008.01488.x.

Dulvy, N. K., Baum, J. K., Clarke, S., Compagno, L. J., Cortés, E., Domingo, A., ... & Valenti, S. (2008b). You can swim but you can't hide: the global status and conservation of oceanic pelagic sharks and rays. *Aquatic conservation: marine and freshwater ecosystems*, *18*(5), 459-482. https://doi.org/10.1002/aqc.975.

Duncanson, L., Liang, M., Leitold, V., Armston, J., Krishna Moorthy, S. M., Dubayah, R., ... & Zvoleff, A. (2023). The effectiveness of global protected areas for climate change mitigation. Nature Communications, 14(1), 2908. https://doi.org/10.1038/s41467-023-38073-9.

Ekau, W., Auel, H., Pörtner, H. O., & Gilbert, D. (2010). Impacts of hypoxia on the structure and processes in pelagic communities (zooplankton, macro-invertebrates and fish). *Biogeosciences*, *7*(5), 1669-1699. https://doi.org/10.5194/bg-7-1669-2010.

Ferretti, F., Worm, B., Britten, G. L., Heithaus, M. R., & Lotze, H. K. (2010). Patterns and ecosystem consequences of shark declines in the ocean. Ecology letters, 13(8), 1055-1071. https://doi.org/10.1111/j.1461-0248.2010.01489.x.

Florko, K. R., Shuert, C. R., Cheung, W. W., Ferguson, S. H., Jonsen, I. D., Rosen, D. A., ... & Auger-Méthé, M. (2023). Linking movement and dive data to prey distribution models: new insights in foraging behaviour and potential pitfalls of movement analyses. *Movement Ecology*, *11*(1), 17. https://doi.org/10.1186/s40462-023-00377-2.

Fox, J. (2003). Effect displays in R for generalised linear models. *Journal of Statistical Software, 8*(15), 1–27. https://doi.org/10.18637/jss.v008.i15.

Fox, J., & Weisberg, S. (2019). *An R companion to applied regression* (3.ª ed.). Thousand Oaks, CA: Sage. https://socialsciences.mcmaster.ca/jfox/Books/Companion/index.html.

Francis, M. P., & Duffy, C. (2005). Length at maturity in three pelagic sharks (Lamna nasus, *Isurus oxyrinchus*, and Prionace glauca) from New Zealand. Fishery Bulletin-National Oceanic and Atmospheric Administration, 103(3), 489.

Francis, M. P., Shivji, M. S., Duffy, C. A., Rogers, P. J., Byrne, M. E., Wetherbee, B. M., ... & Meyers, M. M. (2019). Oceanic nomad or coastal resident? Behavioural switching in the shortfin mako shark (*Isurus oxyrinchus*). Marine Biology, 166(1), 5. https://doi.org/10.1007/s00227-018-3453-5.

Garcia, H. E., Locarnini, R. A., Boyer, T. P., Antonov, J. I., Baranova, O. K., Zweng, M. M., Reagan, J. R., & Johnson, D. R. (2014). *World Ocean Atlas 2013, Volume 3: Dissolved Oxygen, Apparent Oxygen Utilization, and Oxygen Saturation* (S. Levitus, Ed., A. Mishonov, Technical Ed.). NOAA Atlas NESDIS 75. U.S. Department of Commerce, Silver Spring, MD.

Garnier, S., Ross, N., Rudis, R., Camargo, A. P., Sciaini, M., & Scherer, C. (2024). viridis(Lite) – Colorblind-friendly color maps for R (R package version 0.6.5).

Gattuso, J. P., Gentili, B., Duarte, C. M., Kleypas, J. A., Middelburg, J. J., & Antoine, D. (2006). Light availability in the coastal ocean: impact on the distribution of benthic photosynthetic organisms and their contribution to primary production. Biogeosciences, 3(4), 489-513. https://doi.org/10.5194/bg-3-489-2006.

Gaube, P., & McGillicuddy Jr, D. J. (2017). The influence of Gulf Stream eddies and meanders on near-surface chlorophyll. *Deep Sea Research Part I: Oceanographic Research Papers*, *122*, 1-16. https://doi.org/10.1016/j.dsr.2017.02.006

GEBCO Compilation Group. (2025). *GEBCO 2025 Grid*. DOI:10.5285/37c52e96-24ea-67ce-e063-7086abc05f29.

Gibson, K. J., Streich, M. K., Topping, T. S., & Stunz, G. W. (2021). New insights into the seasonal movement patterns of shortfin mako sharks in the Gulf of Mexico. Frontiers in Marine Science, 8, 623104. https://doi.org/10.3389/fmars.2021.623104.

Gibson Banks, K., Coffey, D. M., Fisher, M. R., & Stunz, G. W. (2025). To stay or go: movement, behavior, and habitat use of shortfin mako sharks (*Isurus oxyrinchus*) in the Gulf of Mexico. *Frontiers in Marine Science*, *12*, 1562581. https://doi.org/10.3389/fmars.2025.1562581.

Gilly, W. F., Beman, J. M., Litvin, S. Y., & Robison, B. H. (2013). Oceanographic and biological effects of shoaling of the oxygen minimum zone. Annual review of marine science, 5(1), 393-420. https://doi.org/10.1146/annurev-marine-120710-100849.

Hammerschlag, N., Gallagher, A. J., & Lazarre, D. M. (2011). A review of shark satellite tagging studies. Journal of Experimental Marine Biology and Ecology, 398(1-2), 1-8. https://doi.org/10.1016/j.jembe.2010.12.012.

Hays, G. C. (2003). A review of the adaptive significance and ecosystem consequences of zooplankton diel vertical migrations. Hydrobiologia, 503(1), 163-170. https://doi.org/10.1023/B:HYDR.0000008476.23617.b0.

Hays, G. C., Bradshaw, C. J. A., James, M. C., Lovell, P., & Sims, D. W. (2007). Why do Argos satellite tags deployed on marine animals stop transmitting? Journal of Experimental Marine Biology and Ecology, 349(1), 52-60. https://doi.org/10.1016/j.jembe.2007.04.016.

Hays, G. C., Bailey, H., Bograd, S. J., Bowen, W. D., Campagna, C., Carmichael, R. H., ... & Sequeira, A. M. (2019). Translating marine animal tracking data into conservation policy and management. Trends in ecology & evolution, 34(5), 459-473. DOI: 10.1016/j.tree.2019.01.009.

Hazen, E. L., Jorgensen, S., Rykaczewski, R. R., Bograd, S. J., Foley, D. G., Jonsen, I. D., ... & Block, B. A. (2013). Predicted habitat shifts of Pacific top predators in a changing climate. Nature Climate Change, 3(3), 234-238. https://doi.org/10.1038/nclimate1686.

Helly, J. J., & Levin, L. A. (2004). Global distribution of naturally occurring marine hypoxia on continental margins. Deep Sea research part I: Oceanographic research papers, 51(9), 1159-1168. https://doi.org/10.1016/j.dsr.2004.03.009.

Henderson, C. J., Gilby, B. L., Turschwell, M. P., Goodridge Gaines, L. A., Mosman, J. D., Schlacher, T. A., ... & Olds, A. D. (2024). Long term declines in the functional diversity of sharks in the coastal oceans of eastern Australia. Communications Biology, 7(1), 611. https://doi.org/10.1038/s42003-024-06308-0.

Hoffmayer, E. R., Franks, J. S., Driggers, W. B., & Howey, P. W. (2013). Diel vertical movements of a scalloped hammerhead, Sphyrna lewini, in the northern Gulf of Mexico. *Bulletin of Marine Science*, *89*(2), 551-557. https://doi.org/10.5343/bms.2012.1048.

Horton, T. W., Birch, S., Block, B. A., Hawkes, L. A., van der Kooij, J., Witt, M. J., & Righton, D. (2024). Maximising the value of transmitted data from PSATs tracking marine fish: a case study on Atlantic bluefin tuna. *Animal Biotelemetry*, *12*(1), 2. https://doi.org/10.1186/s40317-023-00356-9.

Howey-Jordan, L. A., Brooks, E. J., Abercrombie, D. L., Jordan, L. K., Brooks, A., Williams, S., ... & Chapman, D. D. (2013). Complex movements, philopatry and expanded depth

range of a severely threatened pelagic shark, the oceanic whitetip (Carcharhinus longimanus) in the western North Atlantic. *PloS one*, *8*(2), e56588. https://doi.org/10.1371/journal.pone.0056588.

Hussey, N. E., Kessel, S. T., Aarestrup, K., Cooke, S. J., Cowley, P. D., Fisk, A. T., ... & Whoriskey, F. G. (2015). Aquatic animal telemetry: a panoramic window into the underwater world. Science, 348(6240), 1255642. DOI: 10.1126/ciência.1255642.

Jewett, L. & A. Romanou. (2017). Ocean acidification and other ocean changes. In: Climate Science Special Report: Fourth National Climate Assessment, Volume I [Wuebbles, D.J., D.W. Fahey, K.A. Hibbard, D.J.Dokken, B.C. Stewart, and T.K. Maycock (eds.)]. U.S. Global Change Research Program, Washington, DC, USA, pp. 364-392, doi: 10.7930/J0QV3JQB.

Jiménez, S., Domingo, A., Abreu, M., & Brazeiro, A. (2011). Structure of the seabird assemblage associated with pelagic longline vessels in the southwestern Atlantic: implications for bycatch. Endangered Species Research, 15(3), 241-254. https://doi.org/10.3354/esr00378.

Jonsen, I. D., Flemming, J. M., & Myers, R. A. (2005). Robust state–space modeling of animal movement data. *Ecology*, *86*(11), 2874-2880. https://doi.org/10.1890/04-1852.

Jorda, G., Marbà, N., Bennett, S., Santana-Garcon, J., Agusti, S., & Duarte, C. M. (2020). Ocean warming compresses the three-dimensional habitat of marine life. Nature Ecology & Evolution, 4(1),109-114. https://doi.org/10.1038/s41559-019-1058-0.

Joung, S. J., & Hsu, H. H. (2005). Reproduction and embryonic development of the shortfin mako, *Isurus oxyrinchus* Rafinesque, 1810, in the northwestern Pacific. ZOOLOGICAL STUDIES-TAIPEI-, 44(4), 487. https://www.researchgate.net/publication/288802127.

Kai, M., Shiozaki, K., Ohshimo, S., & Yokawa, K. (2015). Growth and spatiotemporal distribution of juvenile shortfin mako (*Isurus oxyrinchus*) in the western and central North Pacific. Marine and Freshwater Research, 66(12), 1176-1190. https://doi.org/10.1071/MF14316.

Keeling, R. F., Körtzinger, A., & Gruber, N. (2010). Ocean deoxygenation in a warming world. *Annual review of marine science*, *2*(1), 199-229. https://doi.org/10.1146/annurev.marine.010908.163855.

Kelley, D., & Richards, C. (2024). *oce: Analysis of oceanographic data* (versão 1.8-3) [R package]. CRAN. https://CRAN.R-project.org/package=oce.

Klöcker, C. A., Bjelland, O., Ferter, K., Arostegui, M. C., Braun, C. D., da Costa, I., ... & Junge, C. (2025). Basking sharks of the Arctic Circle: year-long, high-resolution tracking data reveal wide thermal range and prey-driven vertical movements across habitats. *Animal Biotelemetry*, *13*(1), 15. https://doi.org/10.1186/s40317-025-00407-3.

Lampert, W. (1989). The adaptive significance of diel vertical migration of zooplankton. *Functional ecology*, 21-27. https://doi.org/10.2307/2389671.

Last, K. S., Hobbs, L., Berge, J., Brierley, A. S., & Cottier, F. (2016). Moonlight drives ocean-scale mass vertical migration of zooplankton during the Arctic winter. Current Biology, 26(2), 244-251. http://dx.doi.org/10.1016/j.cub.2015.11.038.

Lipscombe, R. S., Spaet, J. L., Scott, A., Lam, C. H., Brand, C. P., & Butcher, P. A. (2020). Habitat use and movement patterns of tiger sharks (Galeocerdo cuvier) in eastern Australian waters. ICES Journal of Marine Science, 77(7-8), 3127-3137. https://doi.org/10.1093/icesjms/fsaa212.

Liu, K. M., Sibagariang, R. D. R., Joung, S. J., & Wang, S. B. (2018). Age and growth of the shortfin mako shark in the Southern Indian Ocean. Marine and Coastal Fisheries, 10(6), 577-589. https://doi.org/10.1002/mcf2.10054.

Liu, H., Duan, Y., Yan, X., & Pang, C. (2022). Interannual variability of the thermocline depth in the south-central Indian Ocean: Respective influences of IOD and ENSO. International Journal of Climatology, 42(10), 5111-5120. https://doi.org/10.1002/joc.7522.

Loefer, J. K., Sedberry, G. R., & McGovern, J. C. (2005). Vertical movements of a shortfin mako in the western North Atlantic as determined by pop-off satellite tagging.

Southeastern Naturalist, 4(2), 237-246. https://doi.org/10.1656/1528-7092(2005)004[0237:VMOASM]2.0.CO;2.

MacNeil, M. A., Graham, N. A., Cinner, J. E., Dulvy, N. K., Loring, P. A., Jennings, S., ... & McClanahan, T. R. (2010). Transitional states in marine fisheries: adapting to predicted global change. *Philosophical Transactions of the Royal Society B: Biological Sciences*, *365*(1558), 3753-3763. https://doi.org/10.1098/rstb.2010.0289.

Madigan, D. J., Richardson, A. J., Carlisle, A. B., Weber, S. B., Brown, J., & Hussey, N. E. (2021). Water column structure defines vertical habitat of twelve pelagic predators in the South Atlantic. *ICES Journal of Marine Science*, *78*(3), 867-883. https://doi.org/10.1093/icesjms/fsaa222.

Maia, A., Queiroz, N., Correia, J. P., & Cabral, H. (2006). Food habits of the shortfin mako, *Isurus oxyrinchus*, off the southwest coast of Portugal. Environmental Biology of Fishes, 77(2), 157-167. https://doi.org/10.1007/s10641-006-9067-7.

Maia, A., Queiroz, N., Cabral, H. N., Santos, A. M., & Correia, J. P. (2007). Reproductive biology and population dynamics of the shortfin mako, *Isurus oxyrinchus* Rafinesque, 1810, off the southwest Portuguese coast, eastern North Atlantic. Journal of Applied Ichthyology, 23(3), 246-251. https://doi.org/10.1111/j.1439-0426.2007.00849.x.

Mas, F., Cortés, E., Coelho, R., Defeo, O., Miller, P., Carlson, J., ... & Domingo, A. (2024). Blue shark (Prionace glauca) movements, habitat use, and vertical overlap with longline fishing gears in the southwestern Atlantic Ocean. Marine Biology, 171(5), 106. https://doi.org/10.1007/s00227-024-04421-6.

Matich, P., Plumlee, J. D., Bubley, W., Curtis, T. H., Drymon, J. M., Mullins, L. L., ... & Fisher, M. R. (2024). Long-term effects of climate change on juvenile bull shark migratory patterns. *Journal of Animal Ecology*. https://doi.org/10.1111/1365-2656.14140.

Matsumoto, T., Saito, H., & Miyabe, N. (2005). Swimming behavior of adult bigeye tuna using pop-up tags in the central Atlantic Ocean. Collect. Vol. Sci. Pap. ICCAT, 57(1), 151-170.

Mejuto, J., García-Cortés, B., Ramos-Cartelle, A., De la Serna, J. M., González-González, I., & Fernández-Costa, L. (2009). Standardized catch rates for the blue shark (Prionace glauca) and shortfin mako (*Isurus oxyrinchus*) caught by the Spanish surface longline fleet in the Atlantic Ocean during the period 1990-2007. *Collect. Vol. Sci. Pap. ICCAT*, *64*(5), 1509-1521.

Mollet, H. F., Testi, A. D., Compagno, L. J., & Francis, M. P. (2002). Re-identification of a lamnid shark embryo. FISHERY BULLETIN-NATIONAL OCEANIC AND ATMOSPHERIC ADMINISTRATION, 100(4), 865-875.

Morrison, P. R., Bernal, D., Sepulveda, C. A., Wegner, N. C., & Brauner, C. J. (2022). Temperature independence of haemoglobin–oxygen affinity in smalleye Pacific opah (Lampris incognitus) and swordfish (Xiphias gladius). Journal of Experimental Biology, 225(19), jeb243820. https://doi.org/10.1242/jeb.243820.

Musyl, M. K., Brill, R. W., Curran, D. S., Gunn, J. S., Hartog, J. R., Hill, R. D., ... & Brainard, R. E. (2001). Ability of archival tags to provide estimates of geographical position based on light intensity. In Electronic Tagging and Tracking in Marine Fisheries: Proceedings of the Symposium on Tagging and Tracking Marine Fish with Electronic Devices, February 7–11, 2000, East-West Center, University of Hawaii (pp. 343-367). Dordrecht: Springer Netherlands. https://doi.org/10.1007/978-94-017-1402-0_19.

Musyl, M. K., Brill, R. W., Boggs, C. H., Curran, D. S., Kazama, T. K., & Seki, M. P. (2003). Vertical movements of bigeye tuna (Thunnus obesus) associated with islands, buoys, and seamounts near the main Hawaiian Islands from archival tagging data. Fisheries Oceanography, 12(3), 152-169. https://doi.org/10.1046/j.1365-2419.2003.00229.x.

Musyl, M. K., Moyes, C. D., Brill, R. W., & Fragoso, N. M. (2009). Factors influencing mortality estimates in post-release survival studies. *Marine Ecology Progress Series*, *396*, 157-159. https://doi.org/10.3354/meps08432.

Musyl, M. K., Brill, R., Curran, D. S., Fragoso, N. M., McNaughton, L., Nielsen, A., ... & Moyes, C. D. (2011). Postrelease survival, vertical and horizontal movements, and thermal habitats of five species of pelagic sharks in the central Pacific Ocean. Fishery Bulletin, 109(4), 341. https://scholarworks.wm.edu/handle/internal/18668.

Nagelkerken, I., & Munday, P. L. (2016). Animal behaviour shapes the ecological effects of ocean acidification and warming: moving from individual to community-level responses. Global Change Biology, 22(3), 974-989. https://doi.org/10.1111/gcb.13167.

Nakamura, I., Watanabe, Y. Y., Papastamatiou, Y. P., Sato, K., & Meyer, C. G. (2011). Yo-yo vertical movements suggest a foraging strategy for tiger sharks Galeocerdo cuvier. *Marine Ecology Progress Series*, *424*, 237-246. https://doi.org/10.3354/meps08980.

Nasby-Lucas, N., Dewar, H., Sosa-Nishizaki, O., Wilson, C., Hyde, J. R., Vetter, R. D., ... & Kohin, S. (2019). Movements of electronically tagged shortfin mako sharks (*Isurus oxyrinchus*) in the eastern North Pacific Ocean. Animal Biotelemetry, 7(1), 1-26. https://doi.org/10.1186/s40317-019-0174-6.

Natanson, L. J., Kohler, N. E., Ardizzone, D., Cailliet, G. M., Wintner, S. P., & Mollet, H. F. (2006). Validated age and growth estimates for the shortfin mako, *Isurus oxyrinchus*, in the North Atlantic Ocean. In Special Issue: Age and Growth of Chondrichthyan Fishes: New Methods, Techniques and Analysis (pp. 367-383). Dordrecht: Springer Netherlands. https://doi.org/10.1007/978-1-4020-5570-6_16.

Nathan, R., Getz, W. M., Revilla, E., Holyoak, M., Kadmon, R., Saltz, D., & Smouse, P. E. (2008). A movement ecology paradigm for unifying organismal movement research. Proceedings of the National Academy of Sciences, 105(49), 19052-19059. https://doi.org/10.1073/pnas.0800375105.

Nosal, A. P., Cartamil, D. P., Wegner, N. C., Lam, C. H., & Hastings, P. A. (2019). Movement ecology of young-of-the-year blue sharks Prionace glauca and shortfin makos *Isurus oxyrinchus* within a putative binational nursery area. Marine Ecology Progress Series, 623, 99-115. https://doi.org/10.3354/meps13021.

Osgood, G. J., White, E. R., & Baum, J. K. (2021). Effects of climate-change-driven gradual and acute temperature changes on shark and ray species. Journal of Animal Ecology, 90(11), 2547-2559. https://doi.org/10.1111/1365-2656.13560.

Otero, J., Jensen, A. J., L'Abée-Lund, J. H., Stenseth, N. C., Storvik, G. O., & Vøllestad, L. A. (2012). Contemporary ocean warming and freshwater conditions are related to later sea age at maturity in Atlantic salmon spawning in Norwegian rivers. *Ecology and Evolution*, *2*(9), 2192-2203. https://doi.org/10.1002/ece3.337.

Pacoureau, N., Rigby, C. L., Kyne, P. M., Sherley, R. B., Winker, H., Carlson, J. K., ... & Dulvy, N. K. (2021). Half a century of global decline in oceanic sharks and rays. *Nature*, *589*(7843), 567-571. https://doi.org/10.1038/s41586-020-03173-9.

Pade, N. G., Queiroz, N., Humphries, N. E., Witt, M. J., Jones, C. S., Noble, L. R., & Sims, D. W. (2009). First results from satellite-linked archival tagging of porbeagle shark, Lamna nasus: area fidelity, wider-scale movements and plasticity in diel depth changes. Journal of Experimental Marine Biology and Ecology, 370(1-2), 64-74. https://doi.org/10.1016/j.jembe.2008.12.002.

Pandolfi, J. M., Connolly, S. R., Marshall, D. J., & Cohen, A. L. (2011). Projecting coral reef futures under global warming and ocean acidification. *science*, *333*(6041), 418-422. DOI: 10.1126/ciência.1204794.

Pedersen, T. (2024). patchwork: The composer of plots (R package version 1.3.0). https://CRAN.R-project.org/package=patchwork.

Perry, A. L., Low, P. J., Ellis, J. R., & Reynolds, J. D. (2005). Climate change and distribution shifts in marine fishes. *science*, *308*(5730), 1912-1915. DOI: 10.1126/ciência.1111322.

Peter Klimley, A., Beavers, S. C., Curtis, T. H., & Jorgensen, S. J. (2002). Movements and swimming behaviour of three species of sharks in La Jolla Canyon, California. Environmental biology of fishes, 63(2), 117-135. https://doi.org/10.1023/A:1014200301213.

Posit team (2024). RStudio: Integrated Development Environment for R. Posit Software, PBC, Boston, MA. URL http://www.posit.co/.

Preti, A., Soykan, C. U., Dewar, H., Wells, R. D., Spear, N., & Kohin, S. (2012). Comparative feeding ecology of shortfin mako, blue and thresher sharks in the California Current.

Environmental Biology of Fishes, 95(1), 127-146. https://doi.org/10.1007/s10641-012-9980-x.

Queiroz, N., Humphries, N. E., Noble, L. R., Santos, A. M., & Sims, D. W. (2010). Short-term movements and diving behaviour of satellite-tracked blue sharks Prionace glauca in the northeastern Atlantic Ocean. *Marine Ecology Progress Series*, *406*, 265-279. https://doi.org/10.3354/meps08500.

Queiroz, N., Humphries, N. E., Noble, L. R., Santos, A. M., & Sims, D. W. (2012). Spatial dynamics and expanded vertical niche of blue sharks in oceanographic fronts reveal habitat targets for conservation. PloS one, 7(2), e32374. https://doi.org/10.1371/journal.pone.0032374.

Queiroz, N., Humphries, N. E., Mucientes, G., Hammerschlag, N., Lima, F. P., Scales, K. L., ... & Sims, D. W. (2016). Ocean-wide tracking of pelagic sharks reveals extent of overlap with longline fishing hotspots. Proceedings of the National Academy of Sciences, 113(6), 1582-1587. https://doi.org/10.1073/pnas.1510090113.

Queiroz, N., Humphries, N. E., Couto, A., Vedor, M., Da Costa, I., Sequeira, A. M., ... & Sousa, L. L. (2019). Global spatial risk assessment of sharks under the footprint of fisheries. Nature, 572(7770), 461-466. https://doi.org/10.1038/s41586-019-1444-4.

Rafinesque, C. S. (1810). *Caratteri di alcuni nuovi generi e nuove specie di animali e piante della Sicilia*.

Ribot-Carballal, M. C., Galván-Magaña, F., & Quiñónez-Velázquez, C. (2005). Age and growth of the shortfin mako shark, *Isurus oxyrinchus*, from the western coast of Baja California Sur, Mexico. Fisheries Research, 76(1), 14-21. https://doi.org/10.1016/j.fishres.2005.05.004.

Richardson, A. J., & Schoeman, D. S. (2004). Climate impact on plankton ecosystems in the Northeast Atlantic. *Science*, *305*(5690), 1609-1612. DOI: 10.1126/science.1100958

Rigby, C. L., Barreto, R., Carlson, J., Fernando, D., Fordham, S., Francis, M. P., *et al*. (2019). *Isurus oxyrinchus*. *The IUCN Red List of Threatened Species 2019:e.T39341A2903170*. Available online

at: http://dx.doi.org/10.2305/IUCN.UK.2019-1.RLTS.T39341A2903170.en (accessed September , 2025).

Roff, G., Brown, C. J., Priest, M. A., & Mumby, P. J. (2018). Decline of coastal apex shark populations over the past half century. *Communications Biology*, *1*(1), 223. https://doi.org/10.1038/s42003-018-0233-1.

Rogers, P. J., Huveneers, C., Page, B., Goldsworthy, S. D., Coyne, M., Lowther, A. D., ... & Seuront, L. (2015). Living on the continental shelf edge: habitat use of juvenile shortfin makos *Isurus oxyrinchus* in the Great Australian Bight, southern Australia. Fisheries Oceanography, 24(3), 205-218. https://doi.org/10.1111/fog.12103.

Rombouts, I., Beaugrand, G., Ibañez, F., Gasparini, S., Chiba, S., & Legendre, L. (2009). Global latitudinal variations in marine copepod diversity and environmental factors. *Proceedings of the Royal Society B: Biological Sciences*, *276*(1670), 3053-3062. https://doi.org/10.1098/rspb.2009.0742.

Rosa, R., Pimentel, M. S., Boavida-Portugal, J., Teixeira, T., Truebenbach, K., & Diniz, M. (2012). Ocean warming enhances malformations, premature hatching, metabolic suppression and oxidative stress in the early life stages of a keystone squid. *PLoS One*, *7*(6), e38282. https://doi.org/10.1371/journal.pone.0038282.

Rosa, R., Baptista, M., Lopes, V. M., Pegado, M. R., Ricardo Paula, J., Trübenbach, K., ... & Repolho, T. (2014). Early-life exposure to climate change impairs tropical shark survival. *Proceedings of the Royal Society B: Biological Sciences*, *281*(1793), 20141738. https://doi.org/10.1098/rspb.2014.1738.

Royer, F., Fromentin, J. M., & Gaspar, P. (2005). A state–space model to derive bluefin tuna movement and habitat from archival tags. Oikos, 109(3), 473-484. https://doi.org/10.1111/j.0030-1299.2005.13777.x.

Santos, C. C., Domingo, A., Carlson, J., Natanson, L., Travassos, P., Macias, D., ... & Coelho, R. (2020). Updates on the habitat use and migrations of shortfin mako in the Atlantic using satellite telemetry. *Collect. Vol. Sci. Pap. ICCAT*, *76*(10), 235-246.

Santos, C. C., Domingo, A., Carlson, J., Natanson, L. J., Travassos, P., Macías, D., ... & Coelho, R. (2021). Movements, habitat use, and diving behaviour of shortfin mako in

the Atlantic Ocean. Frontiers in Marine Science, 8, 686343. https://doi.org/10.3389/fmars.2021.686343.

Sayol, J. M., Marcos, M., Garcia-Garcia, D., & Vigo, I. (2023). Seasonal and interannual variability of Mediterranean Sea overturning circulation. Deep Sea Research Part I: Oceanographic Research Papers, 198, 104081. https://doi.org/10.1016/j.dsr.2023.104081.

Schaefer, K. M., & Fuller, D. W. (2002). Movements, behavior, and habitat selection of bigeye tuna (Thunnus obesus) in the eastern equatorial Pacific, ascertained through archival tags. Fishery Bulletin, 100(4), 765-789. https://link.gale.com/apps/doc/A95205122/AONE?u=anon~fc6d75b6&sid=googleScholar&xid=5dacd624.

Schaefer, K. M., Fuller, D. W., & Block, B. A. (2009). Vertical movements and habitat utilization of skipjack (Katsuwonus pelamis), yellowfin (Thunnus albacares), and bigeye (Thunnus obesus) tunas in the equatorial eastern Pacific Ocean, ascertained through archival tag data. In *Tagging and tracking of marine animals with electronic devices* (pp. 121-144). Dordrecht: Springer Netherlands. https://doi.org/10.1007/978-1-4020-9640-2_8.

Semba, Y., Aoki, I., & Yokawa, K. (2011). Size at maturity and reproductive traits of shortfin mako, *Isurus oxyrinchus*, in the western and central North Pacific. Marine and Freshwater Research, 62(1), 20-29. https://doi.org/10.1071/MF10123.

Sepulveda, C. A., Kohin, S., Chan, C., Vetter, R., & Graham, J. B. (2004). Movement patterns, depth preferences, and stomach temperatures of free-swimming juvenile mako sharks, *Isurus oxyrinchus*, in the Southern California Bight. Marine Biology, 145(1), 191-199. https://doi.org/10.1007/s00227-004-1356-0.

Sepulveda, C. A., Aalbers, S. A., Heberer, C., Kohin, S., & Dewar, H. (2018). Movements and behaviors of swordfish Xiphias gladius in the United States pacific leatherback conservation area. *Fisheries Oceanography*, *27*(4), 381-394. https://doi.org/10.1111/fog.12261.

Sibert, J. R., Musyl, M. K., & Brill, R. W. (2003). Horizontal movements of bigeye tuna (Thunnus obesus) near Hawaii determined by Kalman filter analysis of archival tagging data. Fisheries Oceanography, 12(3), 141-151. https://doi.org/10.1046/j.1365-2419.2003.00228.x.

Simpfendorfer, C., Cortés, E., Heupel, M., Brooks, E., Babcock, E., Baum, J., ... & Soldo, A. (2008). *An integrated approach to determining the risk of overexploitation for data-poor pelagic Atlantic sharks* (p. 15). ICCAT SCRS/2008/140.

Simpfendorfer, C. A., Heithaus, M. R., Heupel, M. R., MacNeil, M. A., Meekan, M., Harvey, E., ... & Wirsing, A. J. (2023). Widespread diversity deficits of coral reef sharks and rays. Science, 380(6650), 1155-1160. DOI: 10.1126/science.ade4884.

Simpson, S. D., Jennings, S., Johnson, M. P., Blanchard, J. L., Schön, P. J., Sims, D. W., & Genner, M. J. (2011). Continental shelf-wide response of a fish assemblage to rapid warming of the sea. *Current Biology*, *21*(18), 1565-1570. DOI: 10.1016/j.cub.2011.08.016.

Sims, D. W., Southall, E. J., Richardson, A. J., Reid, P. C., & Metcalfe, J. D. (2003). Seasonal movements and behaviour of basking sharks from archival tagging: no evidence of winter hibernation. Marine Ecology Progress Series, 248, 187-196. https://doi.org/10.3354/meps248187.

Skubel, R. A., Wilson, K., Papastamatiou, Y. P., Verkamp, H. J., Sulikowski, J. A., Benetti, D., & Hammerschlag, N. (2020). A scalable, satellite-transmitted data product for monitoring high-activity events in mobile aquatic animals. *Animal Biotelemetry*, *8*(1), 34. https://doi.org/10.1186/s40317-020-00220-0.

Stevens, J. D. (2008). The biology and ecology of the shortfin mako shark, *Isurus oxyrinchus*. *Sharks of the open ocean: biology, fisheries and conservation*, 87-94. DOI: 10.1002/9781444302516.

Stevens, J. D., Bradford, R. W., & West, G. J. (2010). Satellite tagging of blue sharks (Prionace glauca) and other pelagic sharks off eastern Australia: depth behaviour, temperature experience and movements. *Marine biology*, *157*(3), 575-591. https://doi.org/10.1007/s00227-009-1343-6.

Stewart, J. S., Field, J. C., Markaida, U., & Gilly, W. F. (2013). Behavioral ecology of jumbo squid (Dosidicus gigas) in relation to oxygen minimum zones. *Deep Sea Research Part II: Topical Studies in Oceanography*, *95*, 197-208. https://doi.org/10.1016/j.dsr2.2012.06.005.

Stramma, L., Schmidtko, S., Levin, L. A., & Johnson, G. C. (2010). Ocean oxygen minima expansions and their biological impacts. *Deep Sea Research Part I: Oceanographic Research Papers*, *57*(4), 587-595. https://doi.org/10.1016/j.dsr.2010.01.005.

Thieurmel, B., & Elmarhraoui, A. (2022). suncalc: Compute sun position, sunlight phases, moon position and lunar phase (R package version 0.5.1). CRAN. https://CRAN.R-project.org/package=suncalc.

Tukey, J. W. (1977). *Exploratory data analysis* (Vol. 2, pp. 131-160). Reading, MA: Addison-wesley.

Vandeperre, F., Aires-da-Silva, A., Fontes, J., Santos, M., Serrão Santos, R., & Afonso, P. (2014). Movements of blue sharks (Prionace glauca) across their life history. PloS one, 9(8), e103538. https://doi.org/10.1371/journal.pone.0103538.

Vaudo, J. J., Wetherbee, B. M., Wood, A. D., Weng, K., Howey-Jordan, L. A., Harvey, G. M., & Shivji, M. S. (2016). Vertical movements of shortfin mako sharks *Isurus oxyrinchus* in the western North Atlantic Ocean are strongly influenced by temperature. Marine Ecology Progress Series, 547, 163-175. https://doi.org/10.3354/meps11646.

Vaudo, J. J., Byrne, M. E., Wetherbee, B. M., Harvey, G. M., & Shivji, M. S. (2017). Long-term satellite tracking reveals region-specific movements of a large pelagic predator, the shortfin mako shark, in the western North Atlantic Ocean. Journal of applied ecology, 54(6), 1765-1775. https://doi.org/10.1111/1365-2664.12852.

Vaudo, J. J., Dewar, H., Byrne, M. E., Wetherbee, B. M., & Shivji, M. S. (2024). Integrating vertical and horizontal movements of shortfin mako sharks *Isurus oxyrinchus* in the eastern North Pacific Ocean. Marine Ecology Progress Series, 732, 85-99. https://doi.org/10.3354/meps14542.

Vedor, M., Mucientes, G., Hernández-Chan, S., Rosa, R., Humphries, N., Sims, D. W., & Queiroz, N. (2021a). Oceanic diel vertical movement patterns of blue sharks vary

with water temperature and productivity to change vulnerability to fishing. Frontiers in Marine Science, 8, 688076. https://doi.org/10.3389/fmars.2021.688076.

Vedor, M., Queiroz, N., Mucientes, G., Couto, A., Costa, I. D., Santos, A. D., ... & Sims, D. W. (2021b). Climate-driven deoxygenation elevates fishing vulnerability for the ocean's widest ranging shark. Elife, 10, e62508. https://doi.org/10.7554/eLife.62508.

Vera-Mera, S., Mejía, D., Mera, C., Vélez-Soledispa, M., Briones-Mendoza, J., Galván-Magaña, F., & Tamayo-Vega, S. (2025). Age and Growth of the Shortfin Mako Shark, *Isurus oxyrinchus* (Rafinesque, 1810), in the Ecuadorian Pacific Ocean. Fisheries Management and Ecology, e12795. https://doi.org/10.1111/fme.12795.

Vetter, R., Kohin, S., Preti, A., Mcclatchie, S. A. M., & Dewar, H. (2008). Predatory interactions and niche overlap between mako shark, *Isurus oxyrinchus*, and jumbo squid, Dosidicus gigas, in the California Current. *Reports/California Cooperative Oceanic Fisheries Investigations*, *49*, 142-156.

Weng, K. C., & Block, B. A. (2004). Diel vertical migration of the bigeye thresher shark (Alopias superciliosus), a species possessing orbital retia mirabilia. *Fishery Bulletin-National Oceanic and Atmospheric Administration*, *102*(1), 221-229.

Weng, K. C., Castilho, P. C., Morrissette, J. M., Landeira-Fernandez, A. M., Holts, D. B., Schallert, R. J., ... & Block, B. A. (2005). Satellite tagging and cardiac physiology reveal niche expansion in salmon sharks. Science, 310(5745), 104-106. DOI: 10.1126/ciência.1114616.

Weng, K. C., Foley, D. G., Ganong, J. E., Perle, C., Shillinger, G. L., & Block, B. A. (2008). Migration of an upper trophic level predator, the salmon shark Lamna ditropis, between distant ecoregions. *Marine Ecology Progress Series*, *372*, 253-264. https://doi.org/10.3354/meps07706.

Wernberg, T., Russell, B. D., Thomsen, M. S., Gurgel, C. F. D., Bradshaw, C. J., Poloczanska, E. S., & Connell, S. D. (2011). Seaweed communities in retreat from ocean warming. Current biology, 21(21), 1828-1832. DOI: 10.1016/j.cub.2011.09.028.

Wildlife Computers. (2024). *MiniPAT Tag User Manual*. Seattle, WA: Wildlife Computers. https://www.wildlifecomputers.com.

Wilson, K. L., Tittensor, D. P., Worm, B., & Lotze, H. K. (2020). Incorporating climate change adaptation into marine protected area planning. Global Change Biology, 26(6), 3251-3267. https://doi.org/10.1111/gcb.15094.

Worm, B., & Lotze, H. K. (2021). Marine biodiversity and climate change. In Climate change (pp. 445-464). Elsevier. https://doi.org/10.1016/B978-0-12-821575-3.00021-9.

Yao, C. L., & Somero, G. N. (2014). The impact of ocean warming on marine organisms. Chinese Science Bulletin, 59(5), 468-479. https://doi.org/10.1007/s11434-014-0113-0.

Zeileis, A., & Grothendieck, G. (2005). zoo: S3 infrastructure for regular and irregular time series. Journal of Statistical Software, 14(6), 1–27. https://doi.org/10.18637/jss.v014.i06.

Zhai, F., Yu, B., Dong, Y., Gu, Y., Liu, Z., & Li, P. (2025). Three-dimensional structure of interannual-to-decadal variations in water temperature in the Yellow sea during 1998–2021. Climate Dynamics, 63(1), 61. https://doi.org/10.1007/s00382-024-07537-z.

7.Annexes

(A)

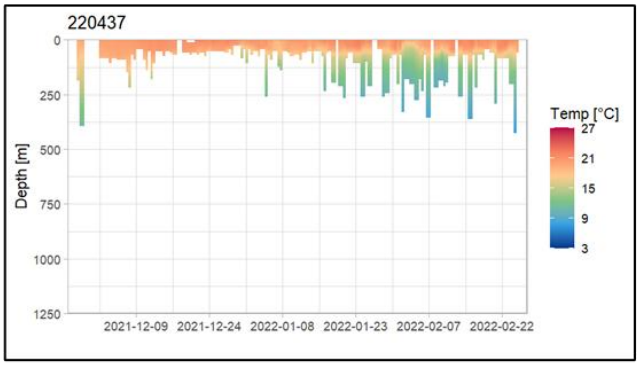

(B)

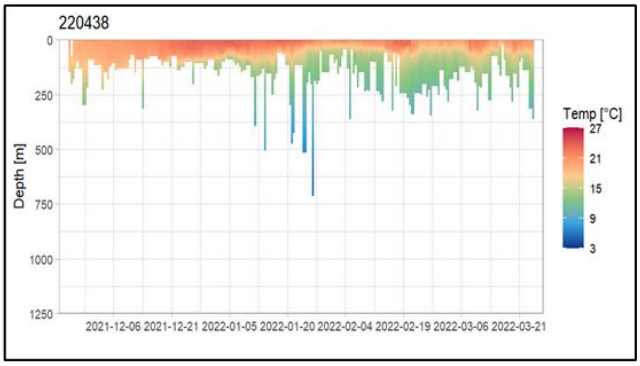

(C)

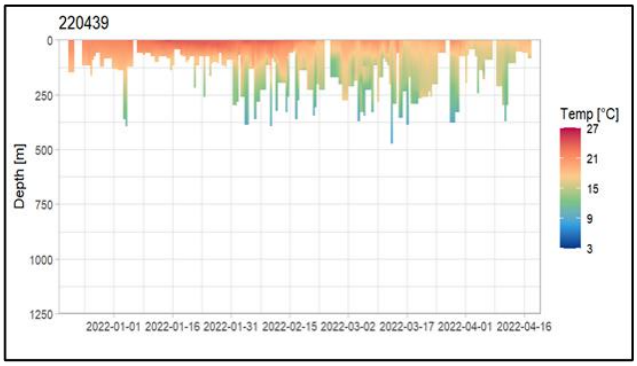

(D)

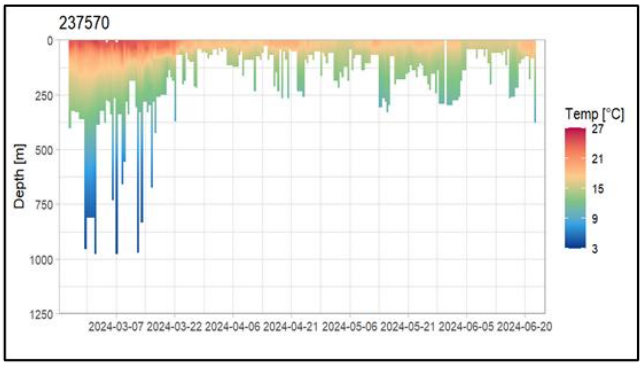

(E)

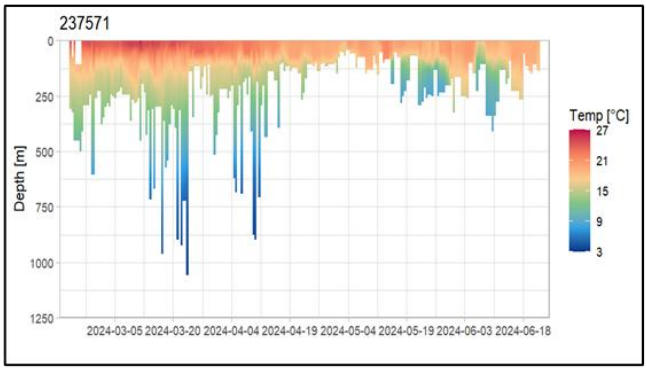

(F)

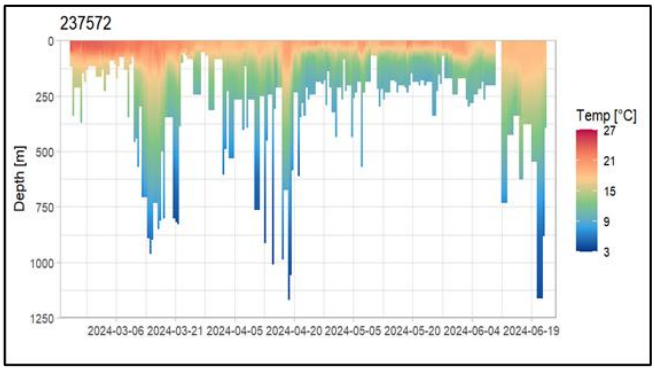

(G)

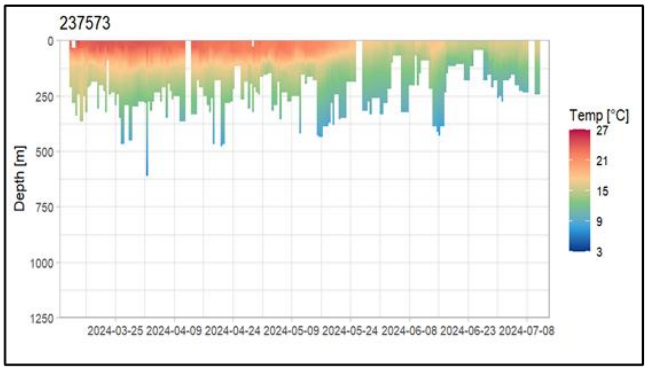

(H)

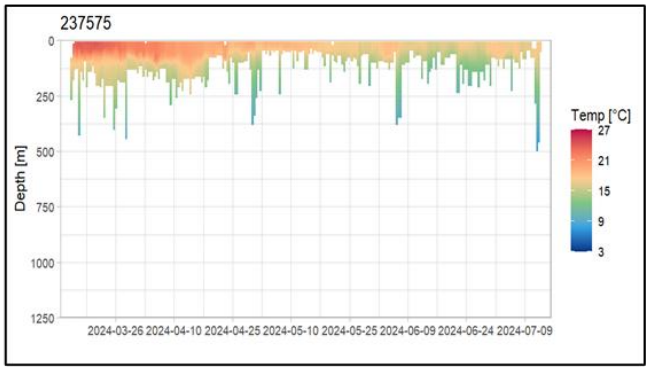

Figure A 1: Depth and Temperature Profile Analysis recorded by *Isurus oxyrinchus* individuals during the tagging period. (A) S1; (B) S2; (C) S3; (D) S4; (E) S5; (F) S6;(G) S7. Lines represent depth over time, while colour shading indicates water temperature.

(A)

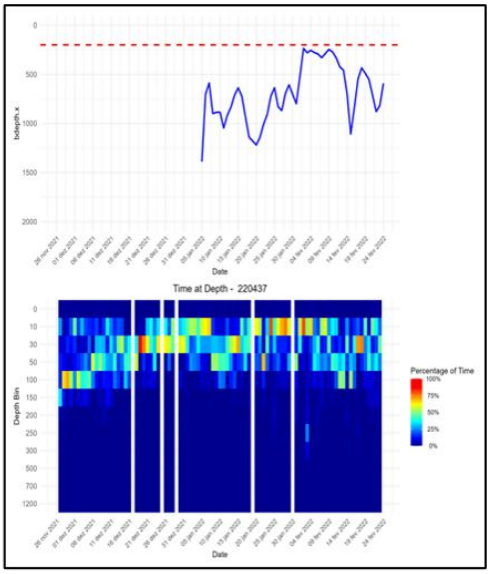
bdepth.x
Date
Time at Depth - 220437
Depth Bin
Percentage of Time
100%
75%
50%
25%
0%

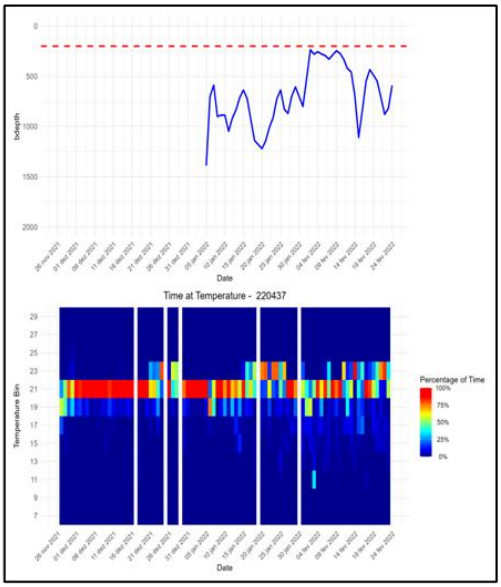
bdepth
Date
Time at Temperature - 220437
Temperature Bin
Percentage of Time
100%
75%
50%
25%
0%

(B)

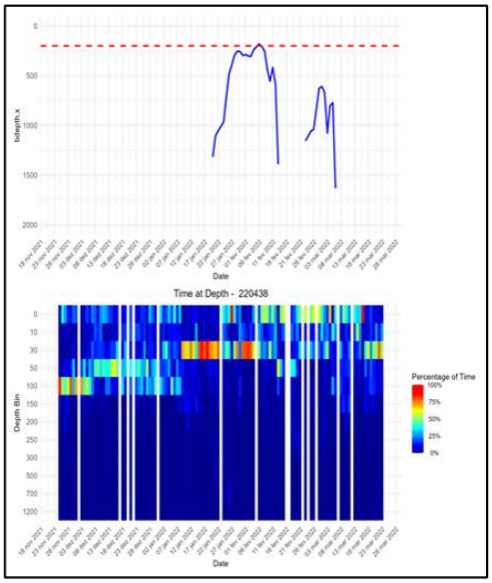
bdepth.x
Date
Time at Depth - 220438
Depth Bin
Percentage of Time
100%
75%
50%
25%
0%

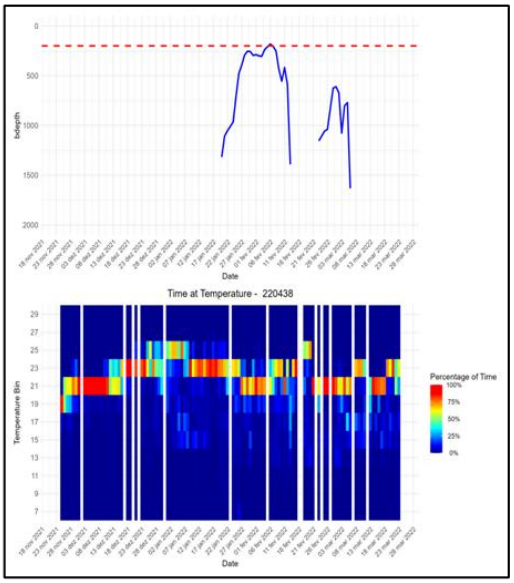
bdepth
Date
Time at Temperature - 220438
Temperature Bin
Percentage of Time
100%
75%
50%
25%
0%

(C)

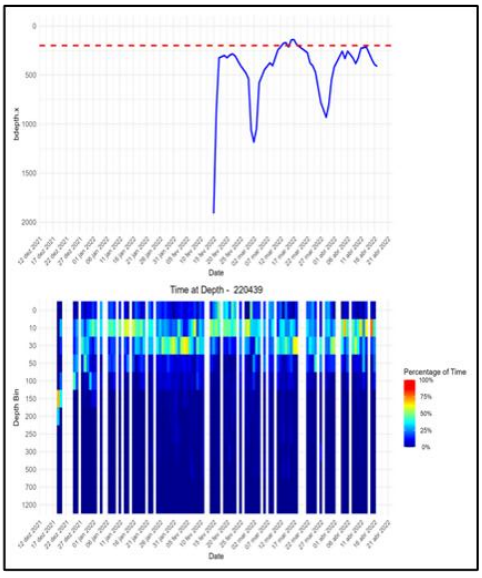
bdepth.x
Date
Time at Depth - 220439
Depth Bin
Percentage of Time
100%
75%
50%
25%
0%

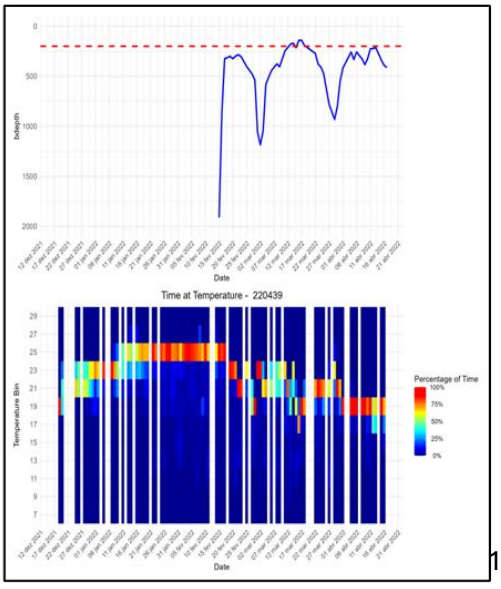
bdepth
Date
Time at Temperature - 220439
Temperature Bin
Percentage of Time
100%
75%
50%
25%
0%

(D)

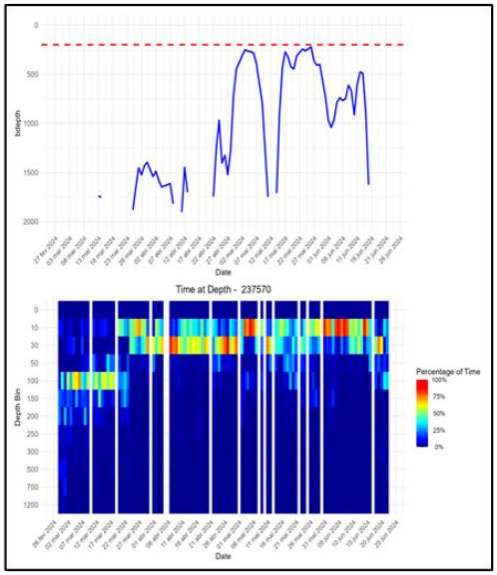
bdepth
Date
Time at Depth - 237570
Depth Bin
Percentage of Time
100%
75%
50%
25%
0%

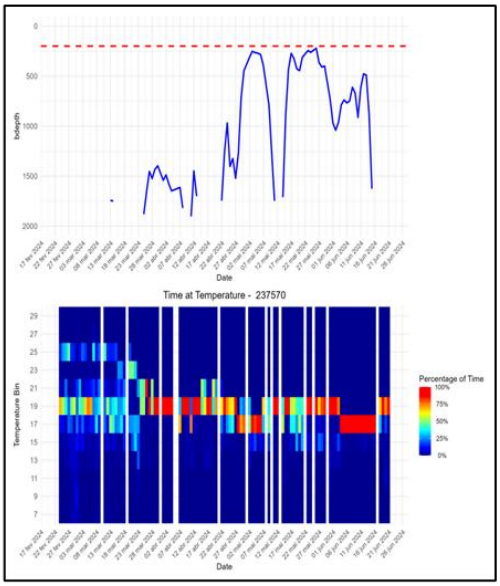
bdepth
Date
Time at Temperature - 237570
Temperature Bin
Percentage of Time
100%
75%
50%
25%
0%

(E)

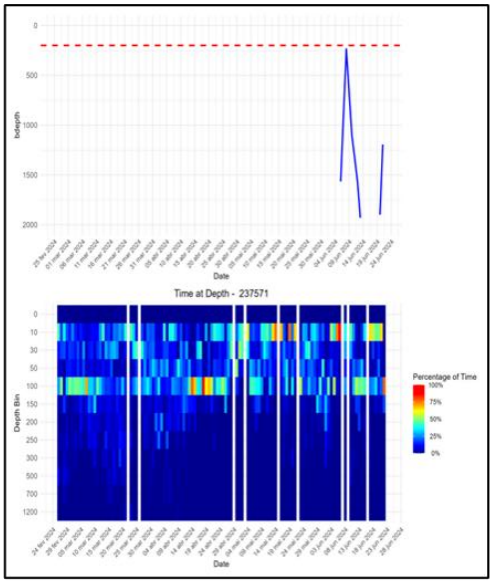
bdepth
Date
Time at Depth - 237571
Depth Bin
Percentage of Time
100%
75%
50%
25%
0%

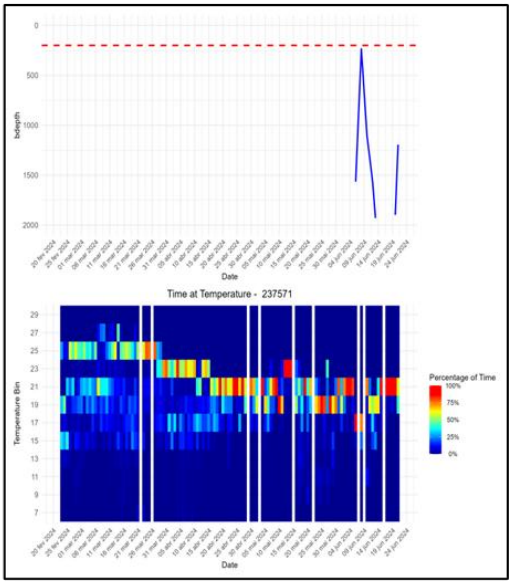
bdepth
Date
Time at Temperature - 237571
Temperature Bin
Percentage of Time
100%
75%
50%
25%
0%

(F)

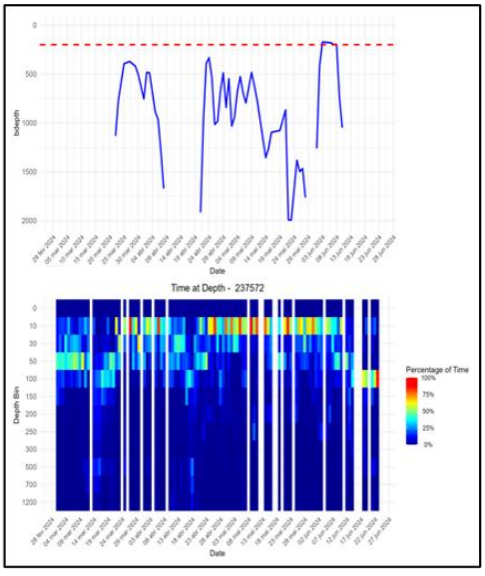
bdepth
Date
Time at Depth - 237572
Depth Bin
Percentage of Time
100%
75%
50%
25%
0%

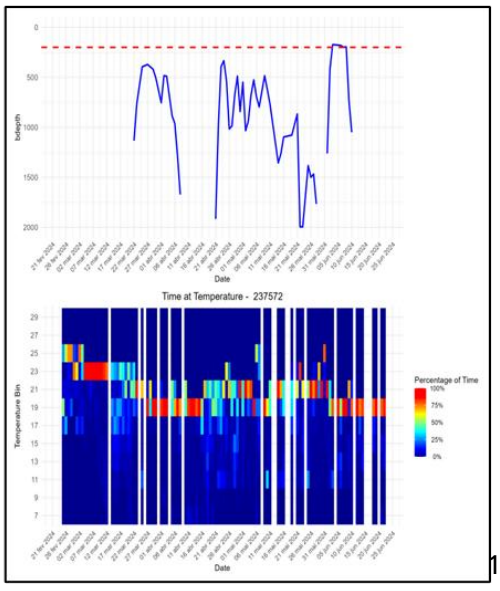
bdepth
Date
Time at Temperature - 237572
Temperature Bin
Percentage of Time
100%
75%
50%
25%
0%

(G)

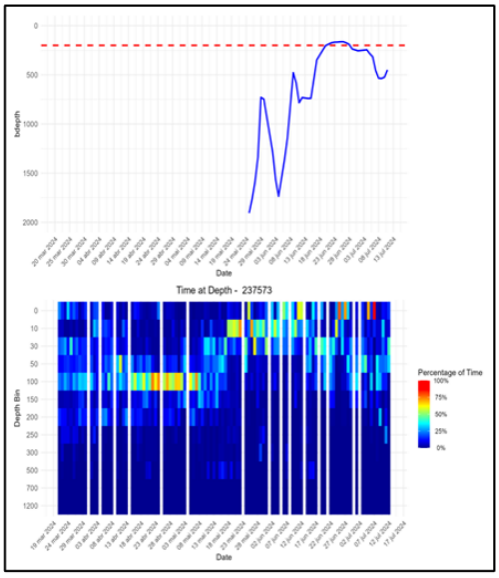
bdepth
Date
Time at Depth - 237573
Depth Bin
Percentage of Time
100%
75%
50%
25%
0%

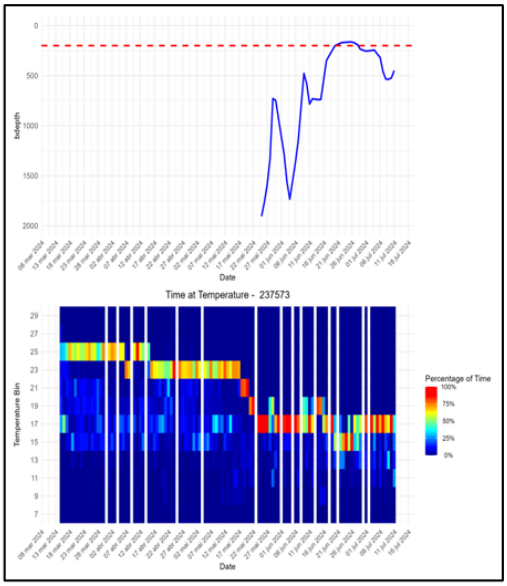
bdepth
Date
Time at Temperature - 237573
Temperature Bin
Percentage of Time
100%
75%
50%
25%
0%

(H)

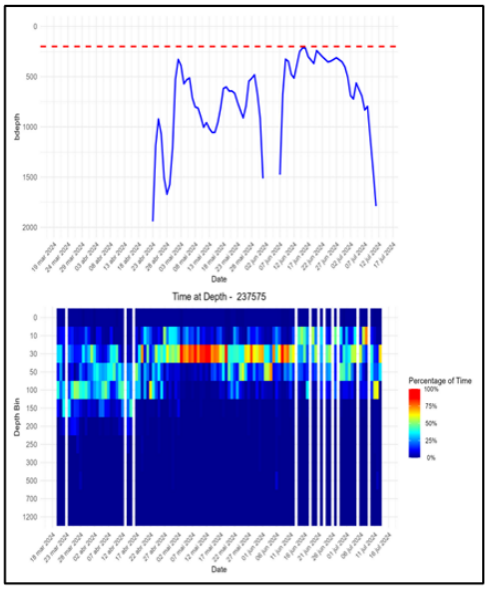
bdepth
Date
Time at Depth - 237575
Depth Bin
Percentage of Time
100%
75%
50%
25%
0%

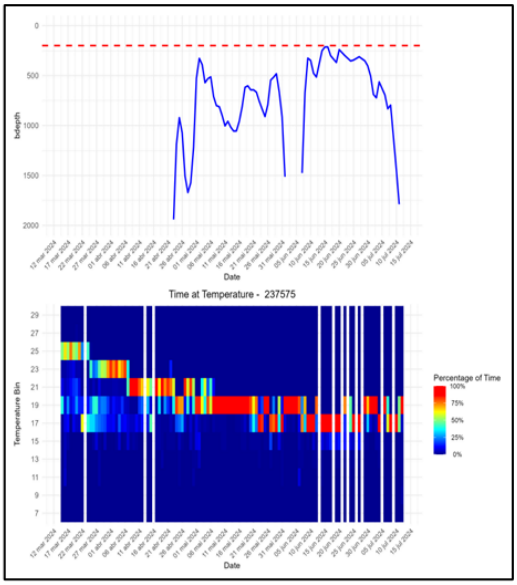
bdepth
Date
Time at Temperature - 237575
Temperature Bin
Percentage of Time
100%
75%
50%
25%
0%

(FI)

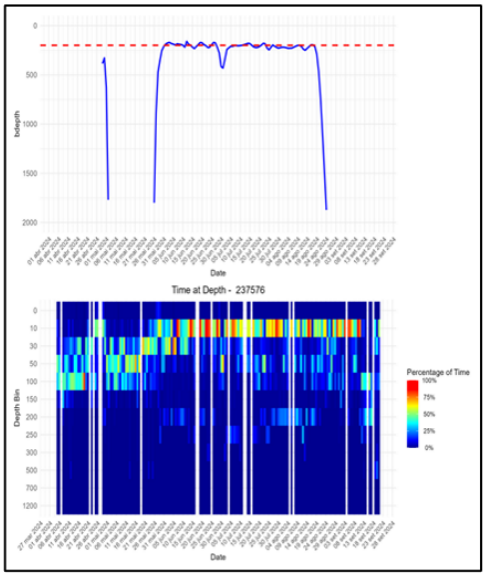
bdepth
Date
Time at Depth - 237576
Depth Bin
Percentage of Time
100%
75%
50%
25%
0%

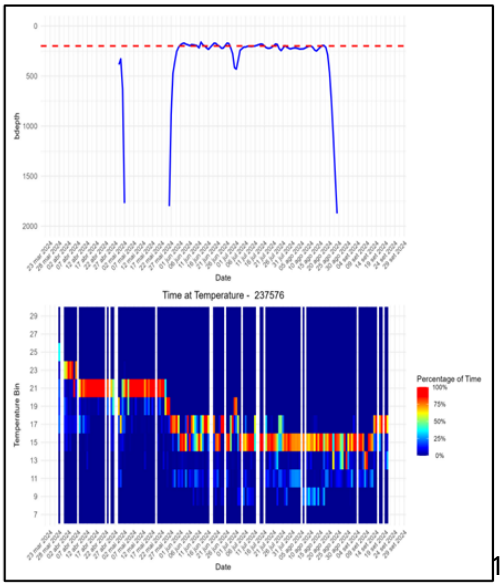
bdepth
Date
Time at Temperature - 237576
Temperature Bin
Percentage of Time
100%
75%
50%
25%
0%

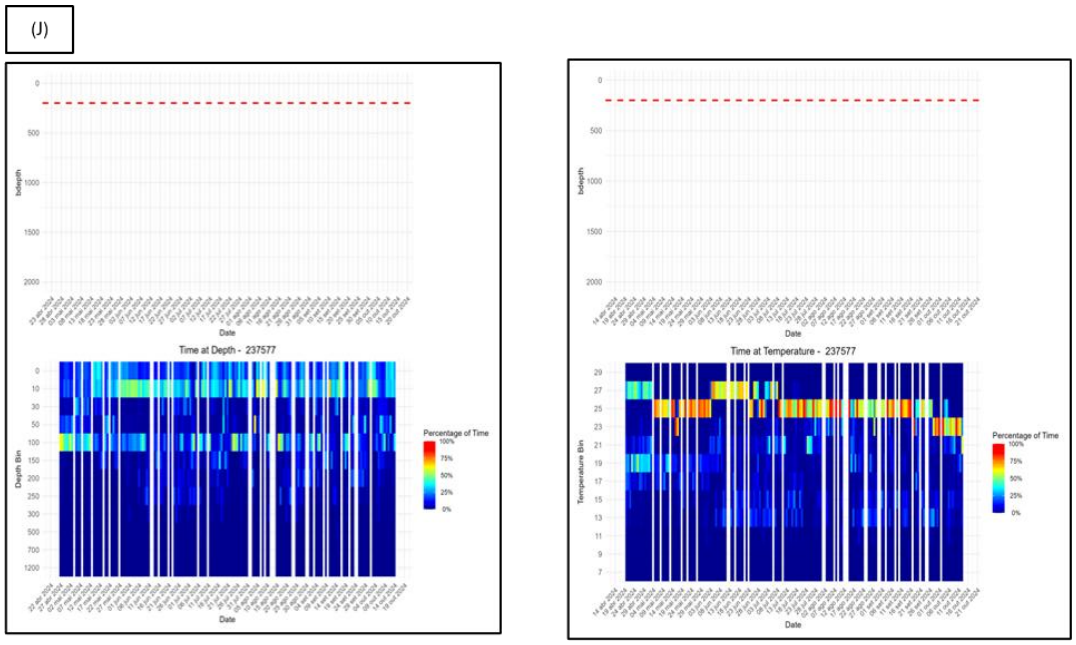

Figure A 2: Variation in the percentage of time spent by individuals (A) S1; (B) S2; (C) S3, (D)S4; (E) S5; (F)S6; (G) S7; (H) S8; (I) S9; (J) S10 at different depths and temperatures.

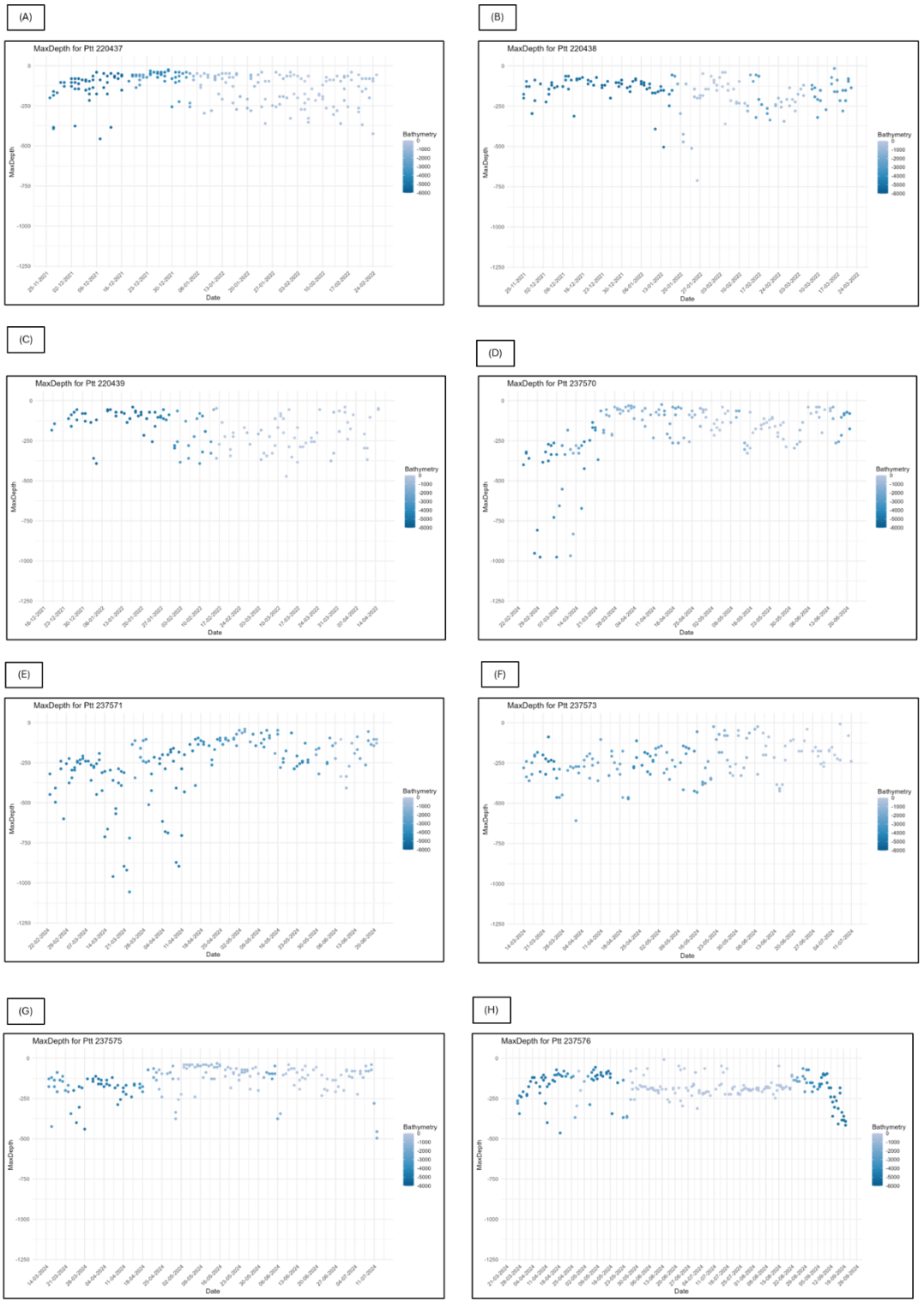

Figure A 3: Relationship between maximum depth and maximum (MaxTemp) and minimum (MinTemp) temperature for ID; (A) S1; (B) S2; (C) S3, (D)S4; (E) S5; (F)S7; (G) S8; (H) S9. Points are coloured according to local bathymetry at the time of recording.

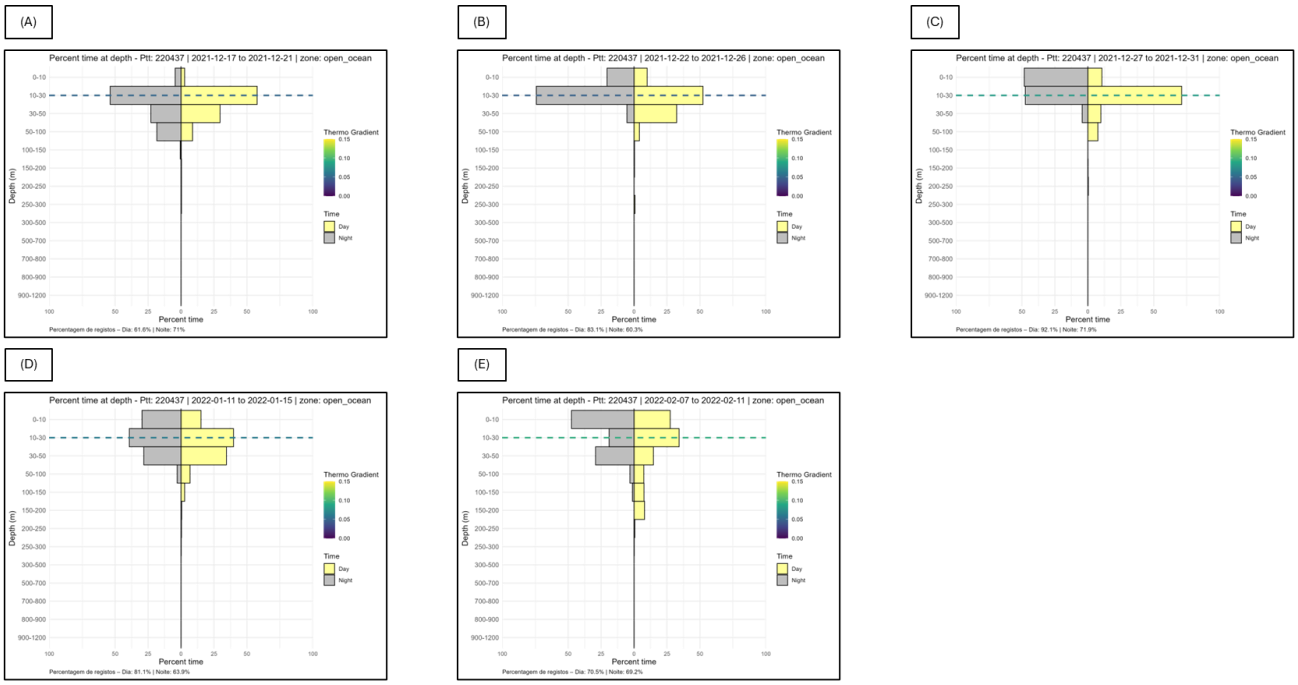

Figure A 4: Distribution of daytime and nighttime occurrence percentages by depth stratum for individual S1 during all block of days.

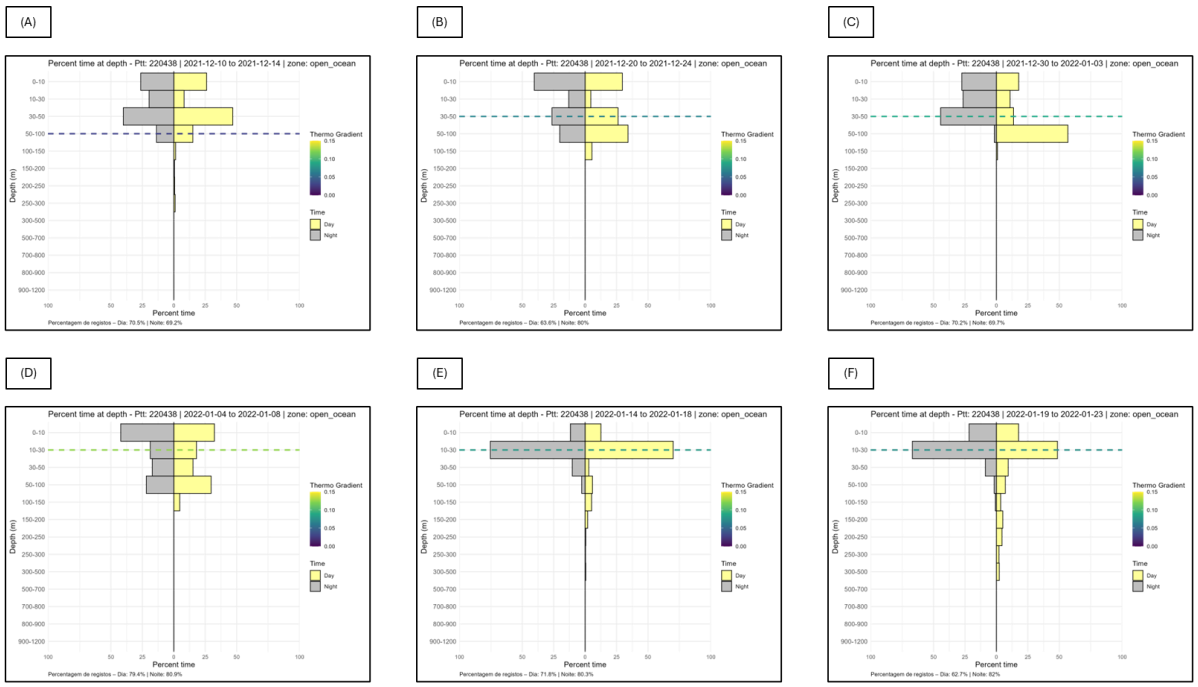

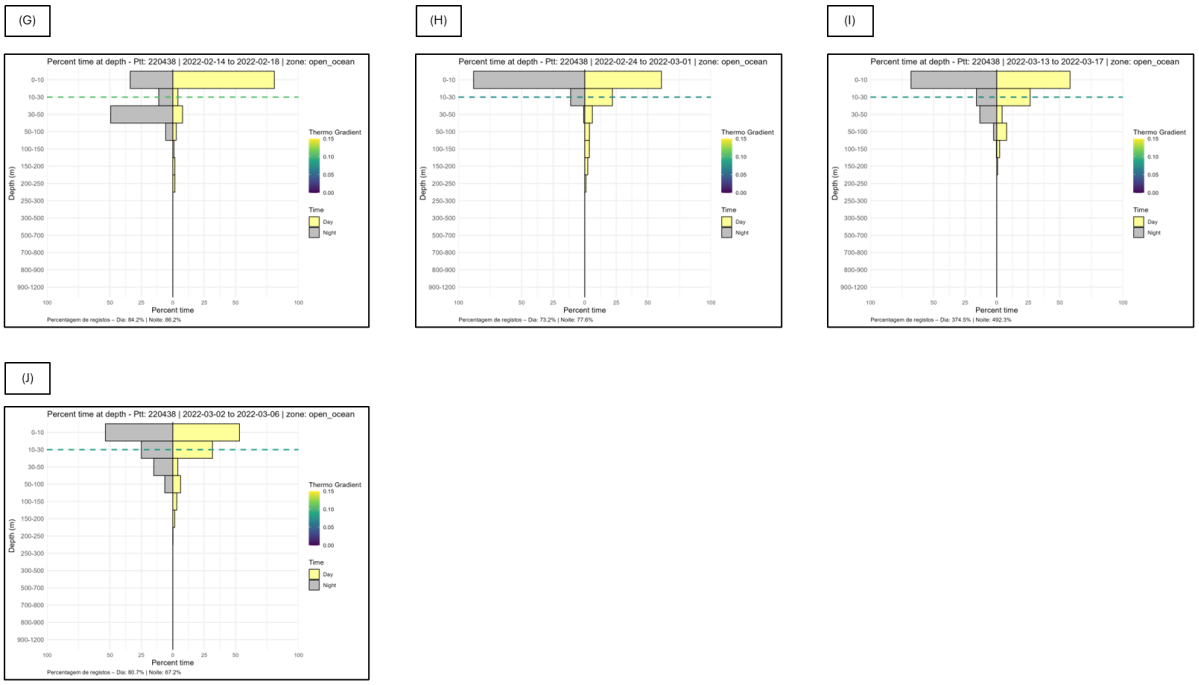

Figure A 5: Distribution of daytime and nighttime occurrence percentages by depth stratum for individual S2 during all block of days; (A) block 1; (B) block 2; (C) block 3, (D) block 4; (E) block 5; (F) block 6; (G) block 7; (H) block 8; (I) block 9 and (J) block 10.

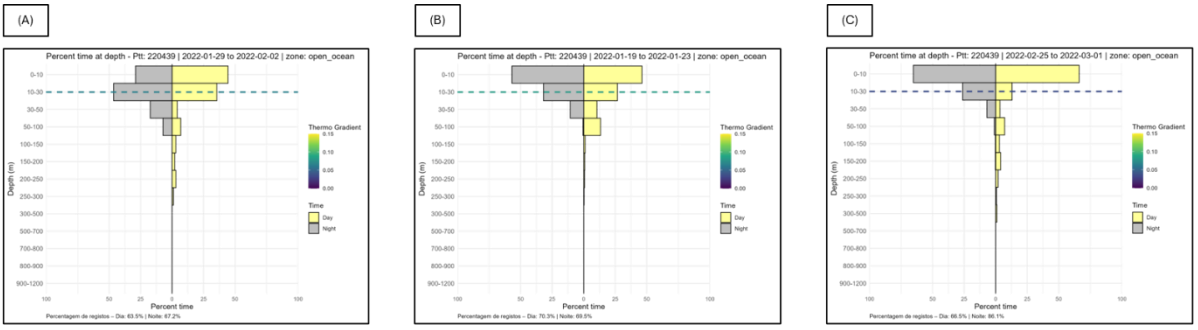

Figure A 6: Distribution of daytime and nighttime occurrence percentages by depth stratum for individual S3 during all block of day 1 (A); 2(B); 3(C).

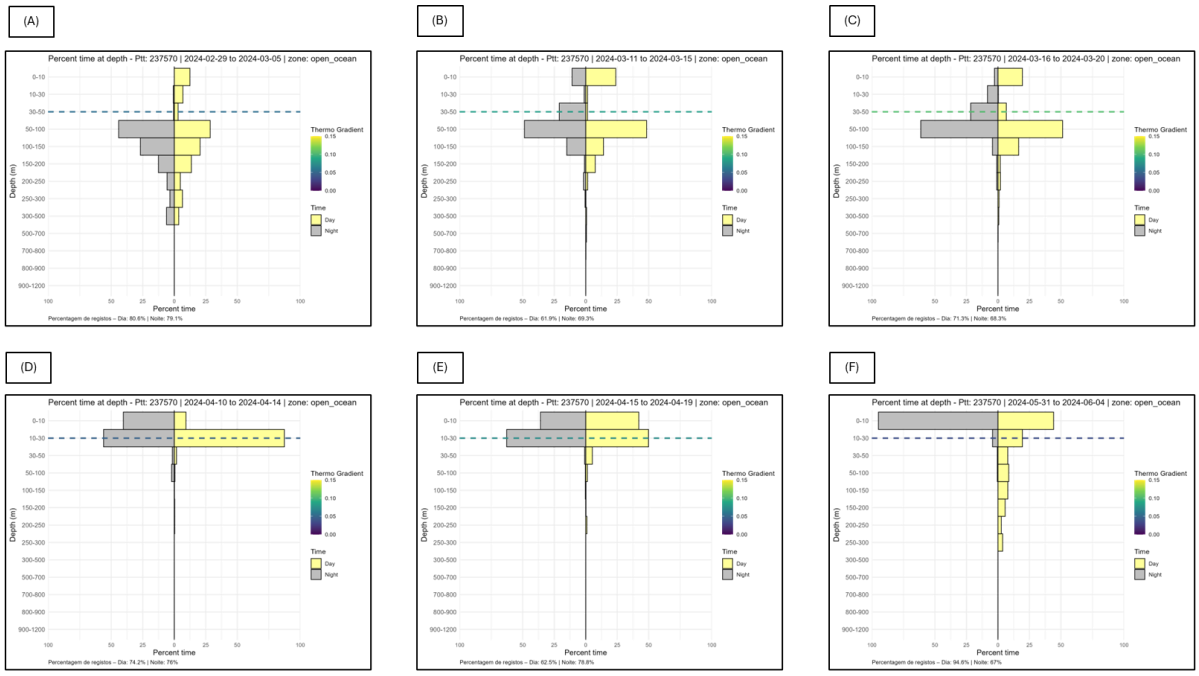

Figure A 7: Distribution of daytime and nighttime occurrence percentages by depth stratum for individual S4 during all block of days (A) block 1; (B) block 2; (C) block 3, (D) block 4; (E) block 5; (F) block 6.

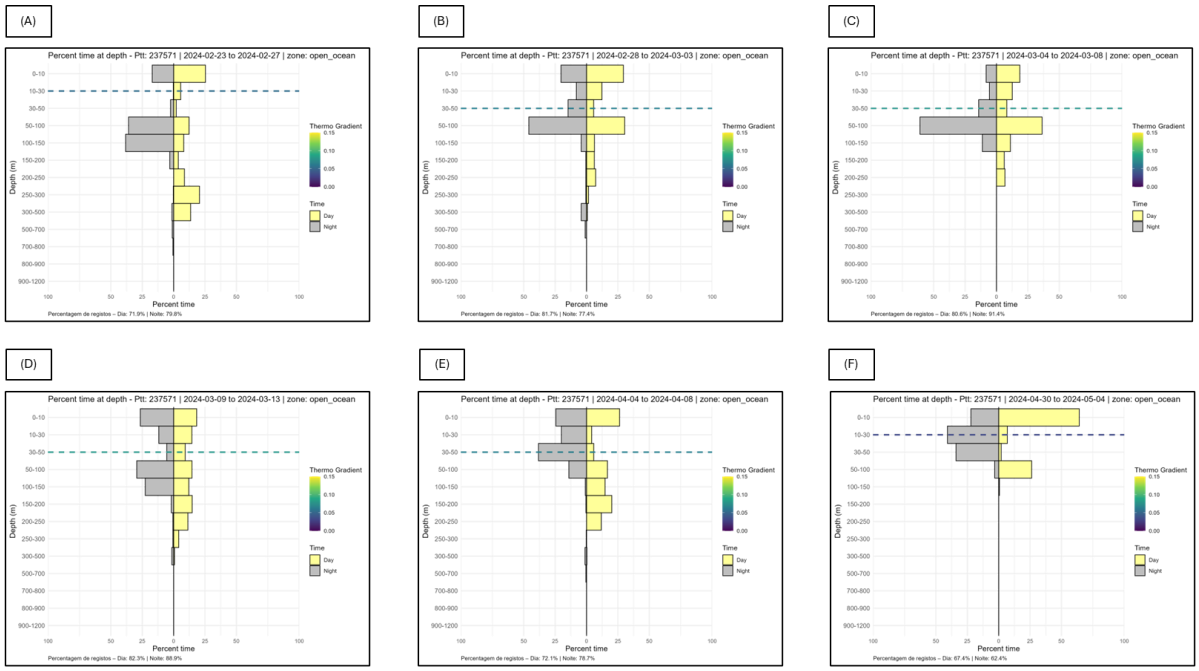

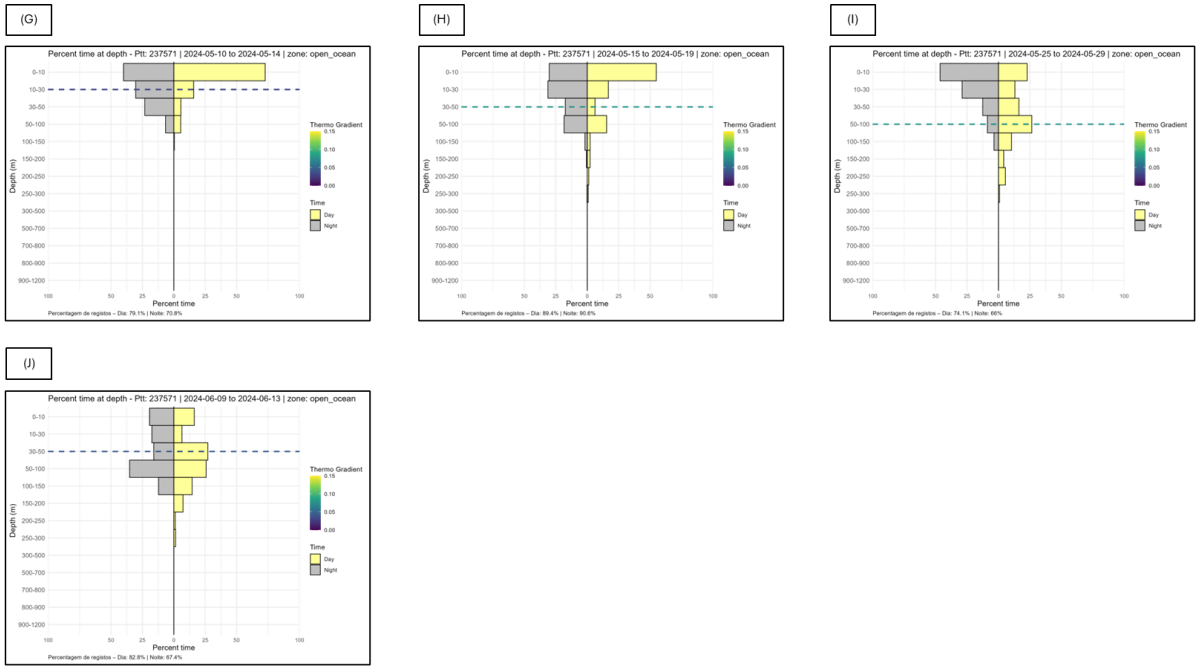

Figure A 8: Distribution of daytime and nighttime occurrence percentages by depth stratum for individual S5 during the block 1 (A); 2 (B); 3 (C); 4 (D); 7 (E); 8 (F); 9(G); 10 (H); 11 (I) and 12 (J).

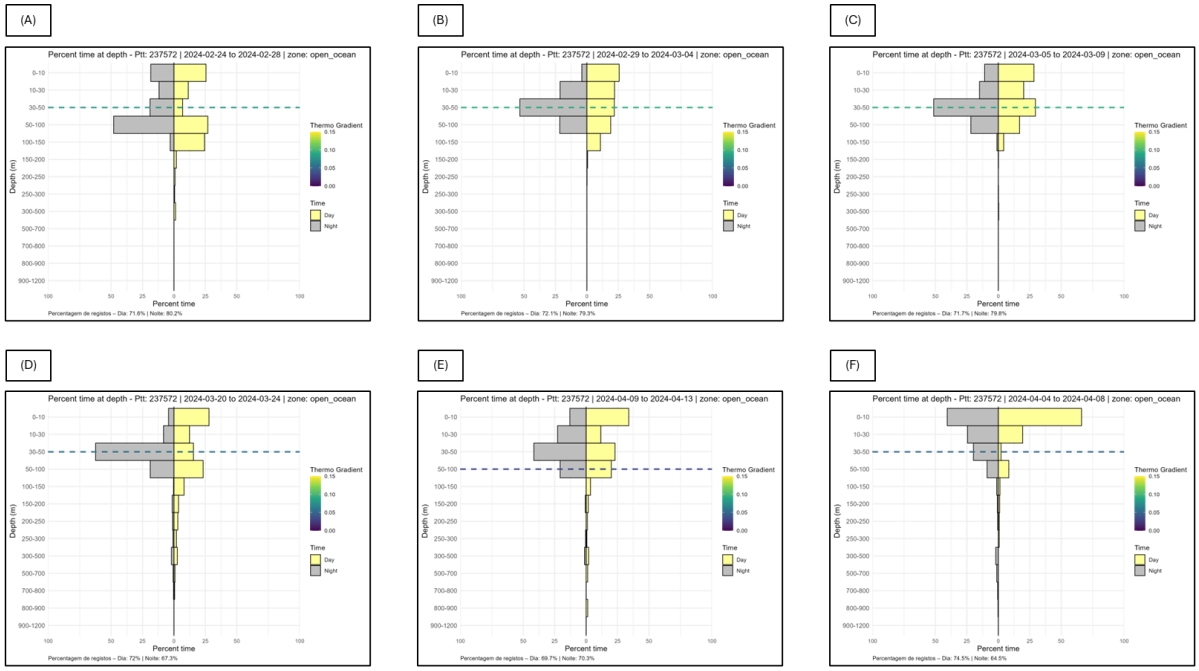

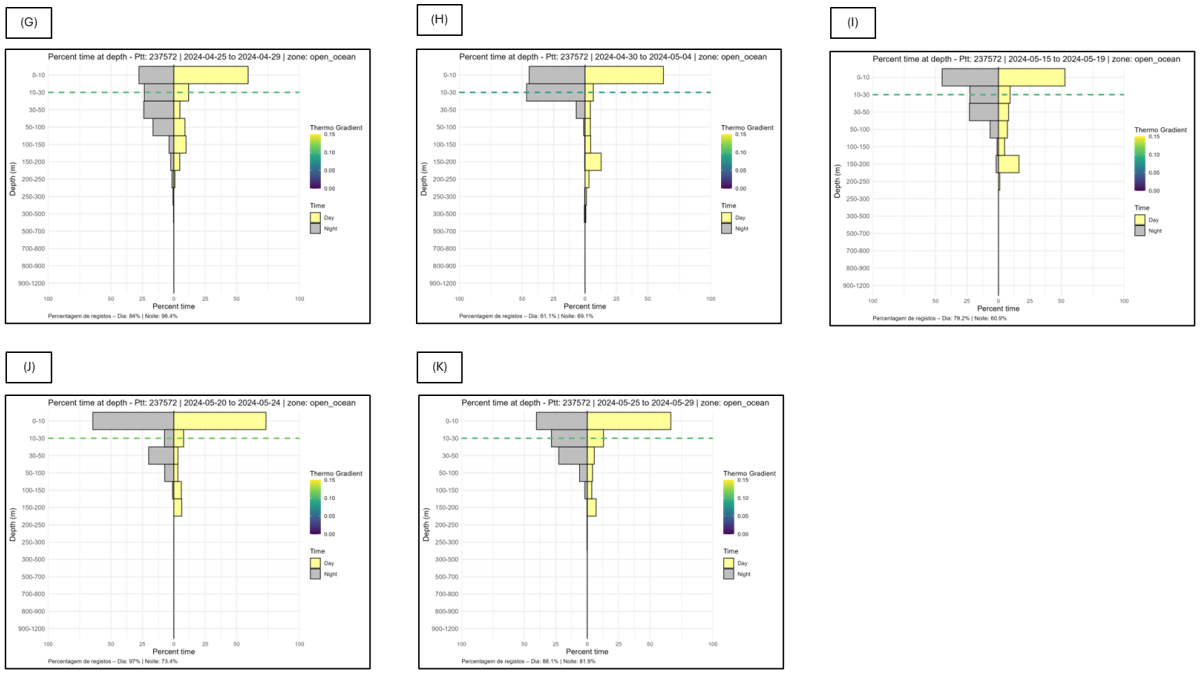

Figure A 9: Distribution of daytime and nighttime occurrence percentages by depth stratum for individual S6 during the block of days 1 (A); 2 (B) ; 3 (C); 6(D); 7 (E); 8 (F); 9(G); 10(H); 11(I); 12 (J); 13(K).

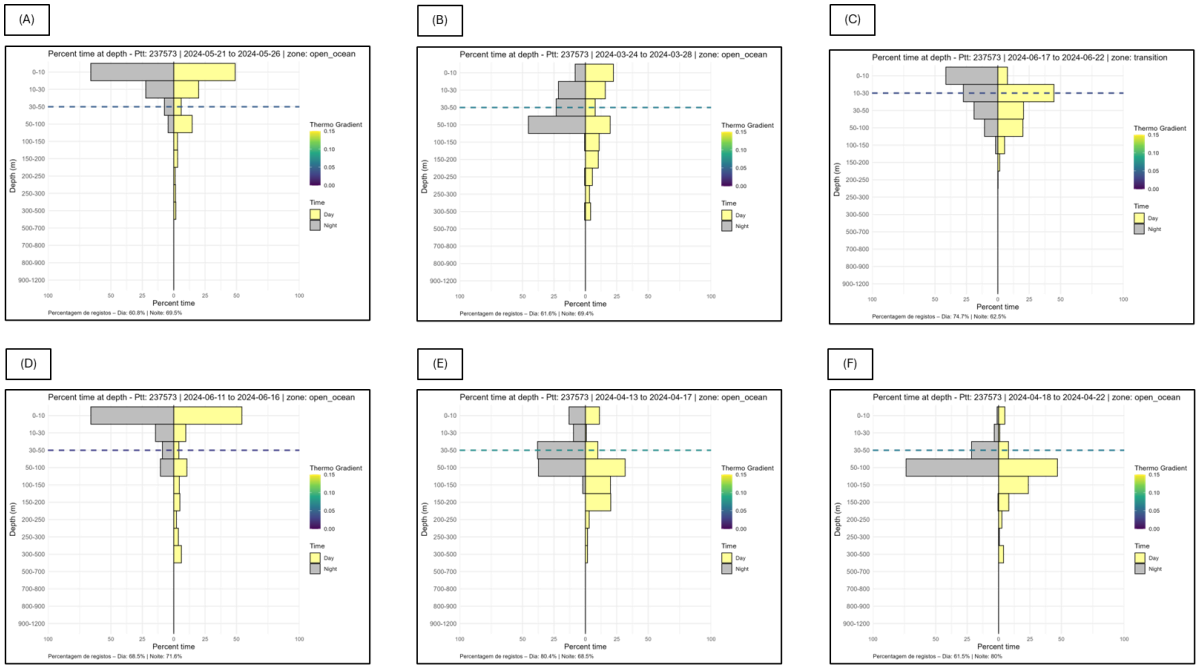

Figure A 10: Distribution of daytime and nighttime occurrence percentages by depth stratum for individual S7 during the block of days 1 (A); 2 (B); 3 (C); 4(D); 5 (E) and 6 (F).

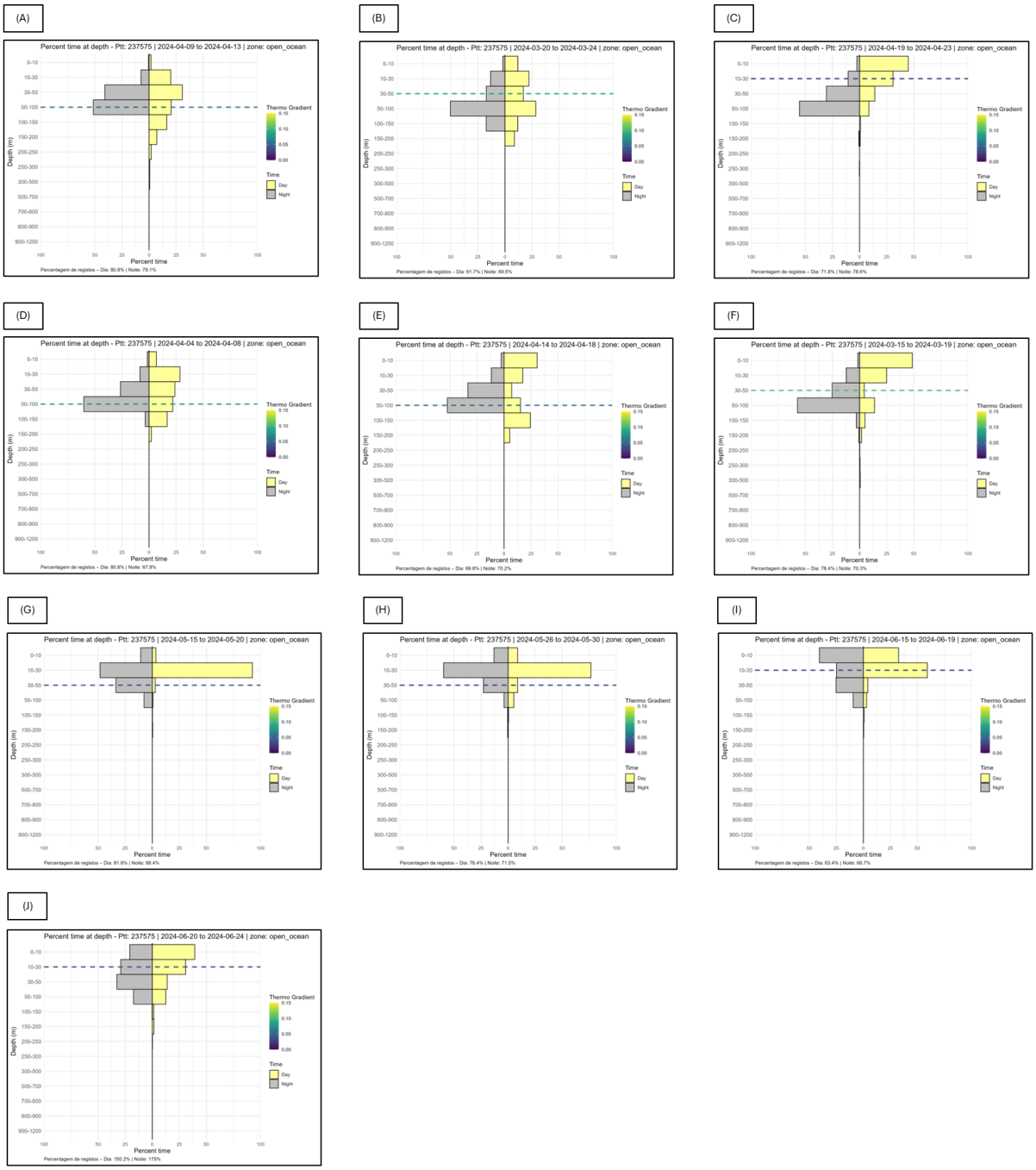

Figure A 11: Distribution of daytime and nighttime occurrence percentages by depth stratum for individual S8 during 1 (A); 2 (B) ; 3 (C); 4(D); 5 (E); 6 (F); 7 (G); 8 (H); 9 (I); 10 (J).

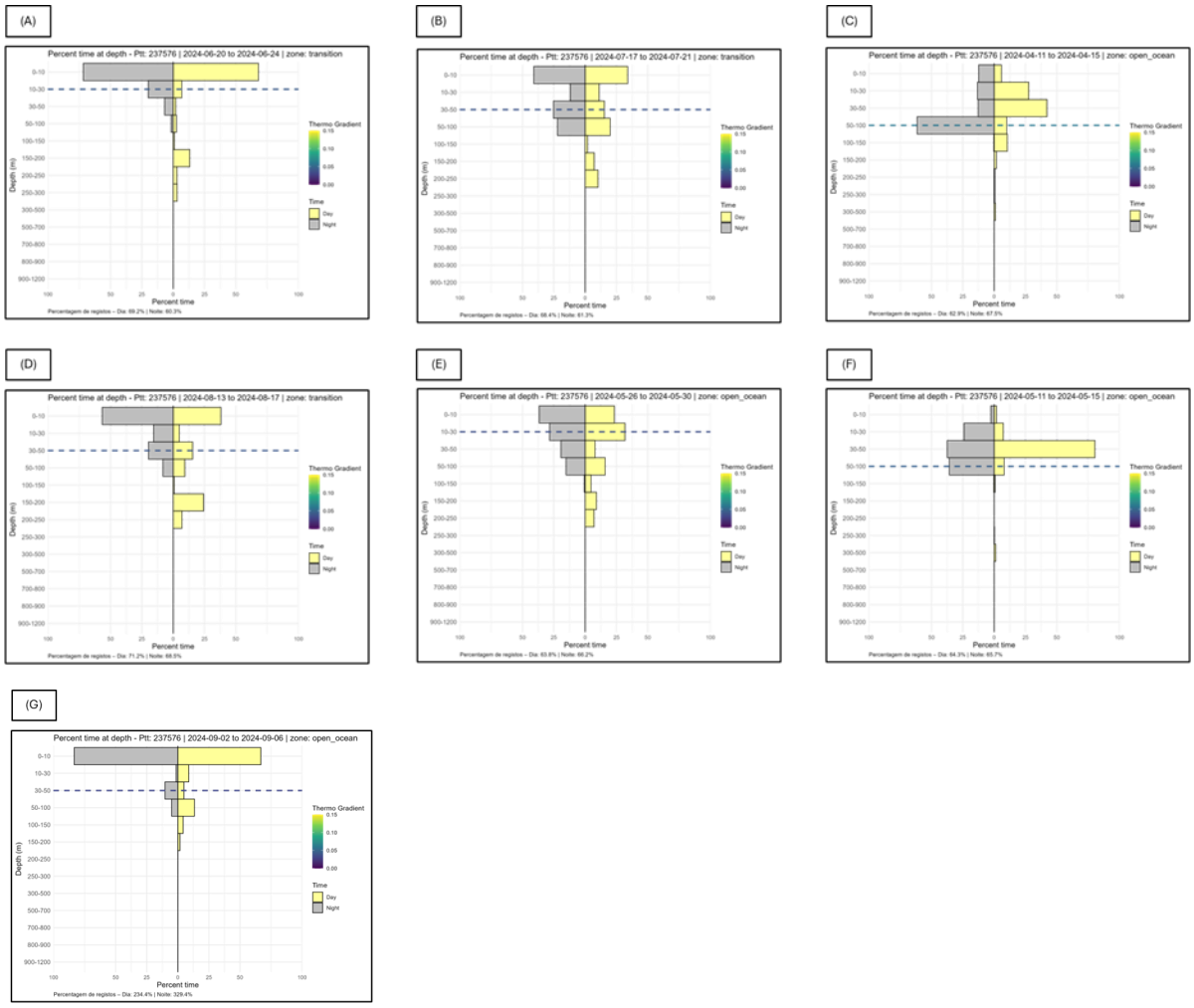

Figure A 12: Distribution of daytime and nighttime occurrence percentages by depth stratum for individual S9 during block of days 1 (A); 2 (B) ; 3 (C); 4(D); 5 (E); 6 (F); 7 (G).

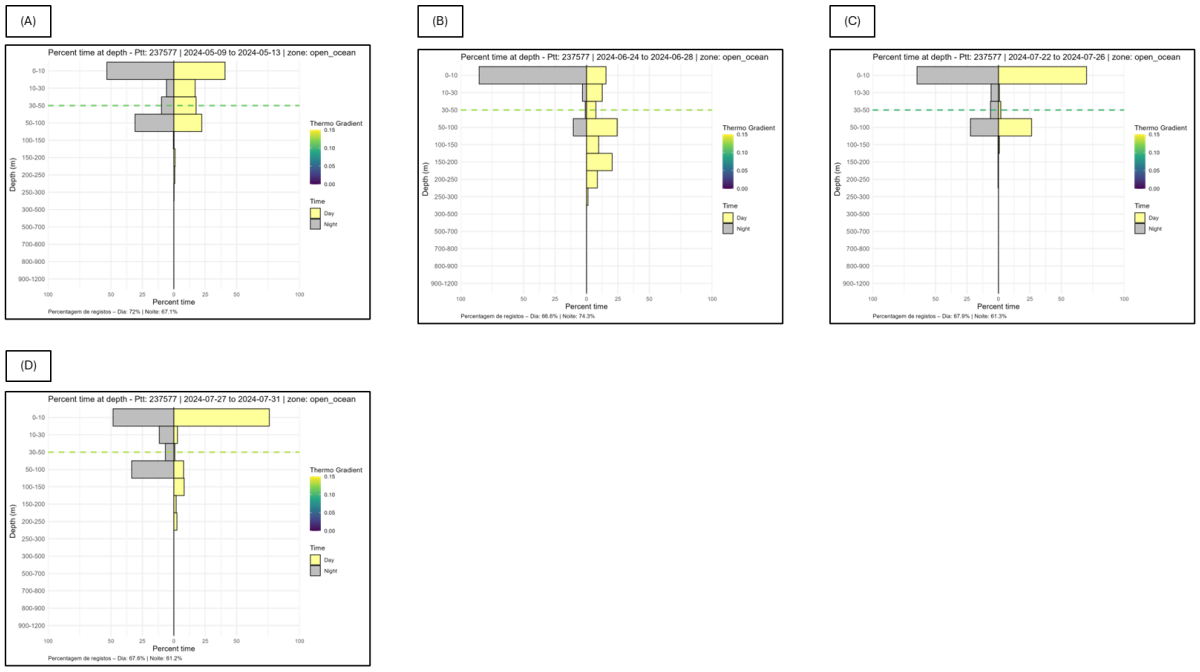

Figure A 13: Distribution of daytime and nighttime occurrence percentages by depth stratum for individual S10 during block of days 1 (A); 2 (B); 3 (C); 4(D).

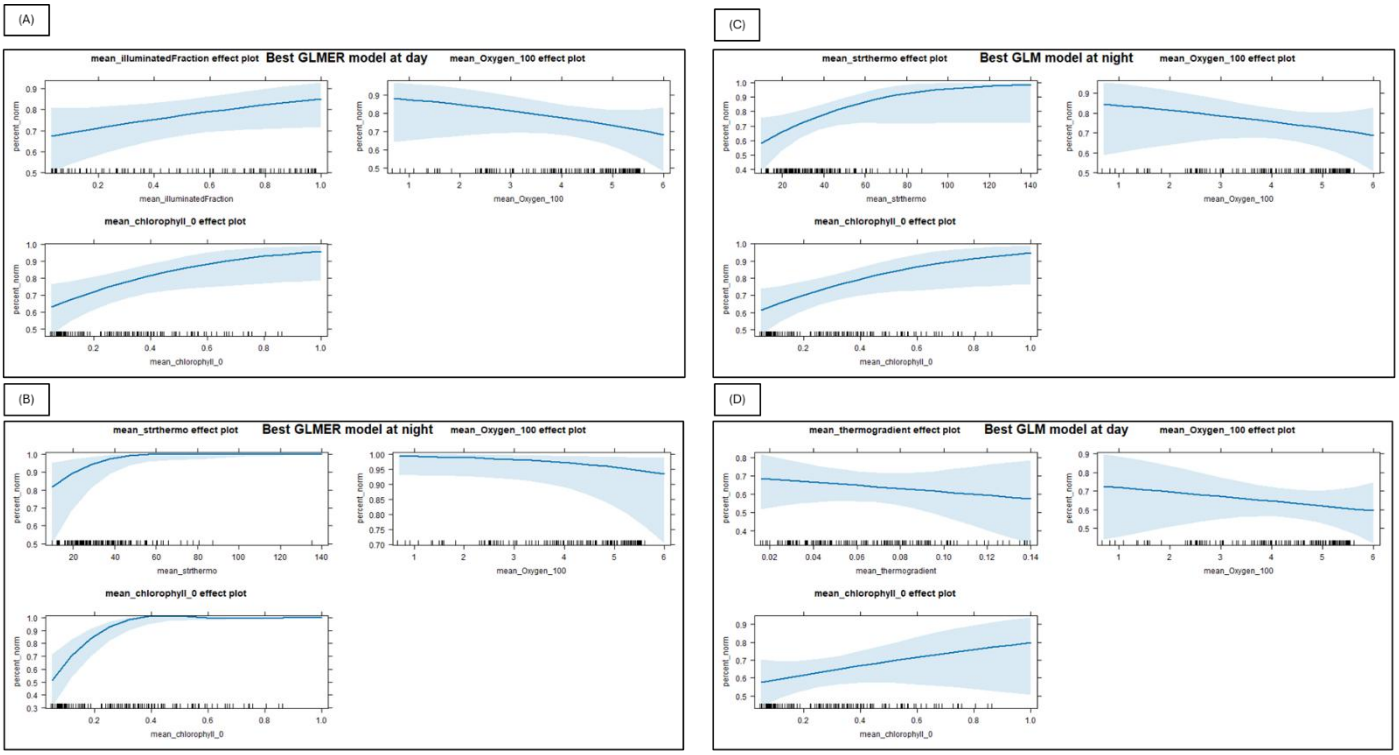

Figure A 14: Graphical analysis of the GLM and GLMM models. (A) Best model GLMM at day; (B) Best model GLMM at night; (C) Best model GLM at night; (D) Best model GLM at day.